DEVELOPMENTAL DYNAMICS 203:253–310 (1995)

Stages of Embryonic Development of the Zebrafish

CHARLES B. KIMMEL, WILLIAM W. BALLARD, SETH R. KIMMEL, BONNIE ULLMANN, AND THOMAS F. SCHILLING

Institute of Neuroscience, University of Oregon, Eugene, Oregon 97403-1254 (C.B.K., S.R.K., B.U., T.F.S.); Department of Biology, Dartmouth College, Hanover, NH 03755 (W.W.B.)

ABSTRACT **We describe a series of stages for development of the embryo of the zebrafish, *Danio (Brachydanio) rerio*. We define seven broad periods of embryogenesis—the zygote, cleavage, blastula, gastrula, segmentation, pharyngula, and hatching periods. These divisions highlight the changing spectrum of major developmental processes that occur during the first 3 days after fertilization, and we review some of what is known about morphogenesis and other significant events that occur during each of the periods. Stages subdivide the periods. Stages are named, not numbered as in most other series, providing for flexibility and continued evolution of the staging series as we learn more about development in this species. The stages, and their names, are based on morphological features, generally readily identified by examination of the live embryo with the dissecting stereomicroscope. The descriptions also fully utilize the optical transparancy of the live embryo, which provides for visibility of even very deep structures when the embryo is examined with the compound microscope and Nomarski interference contrast illumination. Photomicrographs and composite camera lucida line drawings characterize the stages pictorially. Other figures chart the development of distinctive characters used as staging aid signposts.**

© 1995 Wiley-Liss, Inc.

Key words: *Danio rerio*, Morphogenesis, Embryogenesis, Zygote, Cleavage, Blastula, Gastrula, Segmentation, Pharyngula, Hatching

CONTENTS

© 1995 WILEY-LISS, INC.

INTRODUCTION

A staging series is a tool that provides accuracy in developmental studies. This is because different embryos, even together within a single clutch, develop at slightly different rates. We have seen asynchrony appearing in the development of zebrafish, *Danio (Brachydanio) rerio*, embryos fertilized simultaneously in vitro (C. Walker and G. Streisinger, in Westerfield, 1994) and incubated at an optimal temperature without crowding (28.5°C, 5–10 embryos/ml). Asynchrony arises at the earliest stages, and it becomes more pronounced as time passes. Comparisons reveal more of this variability among embryos from different clutches than from within a single clutch. Genetic uniformity may alleviate but does not eliminate this problem; even embryos of a clonal strain of zebrafish (Streisinger et al., 1981) develop asynchronously.

As for other kinds of embryos, staging by morphological criteria partly resolves this problem. For example, primary trigeminal sensory neurons in the head (Metcalfe et al., 1990) and primary motoneurons in the trunk (Eisen et al., 1986) both initiate axogenesis during stages when somites appear successively along the body axis. Staging by somite number more accurately predicts where these neurons will be in their development than does staging by elapsed time after fertilization (personal communications from W.K. Metcalfe and J.S. Eisen). Recording one's experiments with reference to a staging series provides a good way to ensure reproducibility and to allow subsequent incorporation

Received August 22, 1994; accepted January 4, 1995.

Address reprint requests/correspondence to Charles B. Kimmel, Institute of Neuroscience, 1254 University of Oregon, Eugene, OR 97403-1254.

Thomas F. Schilling is now at the Department of Molecular Embryology, Imperial Cancer Research Fund, Lincoln's Inn Fields, London WCZA 3PX, UK.

of new observations and details. A series based on morphology can also facilitate communication; the descriptor "18-somite embryo" has more meaning than "18-hour-old embryo," particularly in cross-species comparisons.

An earlier staging series for zebrafish, although less complete than the present one, fairly accurately portrays the first third (or 1st day) of embryonic development, and includes useful sets of photographs (Hisaoka and Battle, 1958; Hisaoka and Firlit, 1960). Warga and Kimmel (1990) briefly described stages of the blastula and gastrula. Preliminary versions of this series were circulated and published in *The Zebrafish Book* (Westerfield, 1994). The present version substantially revises, corrects, and expands the earlier ones. An up-to-date version is available in electronic form on the Internet World Wide Web server: "http:/zfish.uoregon.edu.

ORGANIZATION

We have named the stages rather than numbering them as in most other series, because named stages are more flexible and easier to remember or recognize than numbered ones. A stage defines more than an instant in time, it is merely a device for approximately locating a part of the continuum of development. With named stages one can easily add detail as it is learned, and intercalate new stages into the series as necessary for a particular study without resorting to cumbersome devices like decimal numbers, minuses, and pluses. For example, here we describe a five-somite stage, and next a 14-somite stage, but a particular study might use eight stages in between (six-somite, seven-somite, and so on), and one will immediately understand their meaning. We emphasize that we do not mean to exclude these extra stages, wherever they are in the series, by ignoring them.

As an aid to communicating a broader perspective toward development, we group the stages into larger time-blocks called periods (Table 1), and summarize in the text the principal events during these periods. Specialized terms are defined in the glossary, and boldface type in the text highlights terms important for staging. Table 2 collects brief descriptions of all the stages, and Figure 1 shows corresponding sketches. One can use these two sources to approximately locate a stage of interest, and then find additional detail as necessary in the text and other figures.

TABLE 1. Periods of Early Development

Period	h	Description
Zygote	0	The newly fertilized egg through the completion of the first zygotic cell cycle
Cleavage	¾	Cell cycles 2 through 7 occur rapidly and synchronously
Blastula	2¼	Rapid, metasynchronous cell cycles (8, 9) give way to lengthened, asynchronous ones at the midblastula transition; epiboly then begins
Gastrula	5¼	Morphogenetic movements of involution, convergence, and extension form the epiblast, hypoblast, and embryonic axis; through the end of epiboly
Segmentation	10	Somites, pharyngeal arch primordia, and neuromeres develop; primary organogenesis; earliest movements; the tail appears
Pharyngula	24	Phylotypic-stage embryo; body axis straightens from its early curvature about the yolk sac; circulation, pigmentation, and fins begin development
Hatching	48	Completion of rapid morphogenesis of primary organ systems; cartilage development in head and pectoral fin; hatching occurs asynchronously
Early larva	72	Swim bladder inflates; food-seeking and active avoidance behaviors

PROCEDURES

Staging

One can determine the approximate developmental stage of a living embryo by examining it with a dissecting stereo-microscope, generally with transmitted (not epi- or incident) illumination and high magnification (about 50×). During the segmentation period the tail elongates, and if the embryo is left within its chorion, the tail eventually curves over the trunk and head so as to obscure the view. When this has happened, one must remove the embryo from its chorion to stage it, either manually with #5 watchmaker's forceps, or by treatment with a proteolytic enzyme (Westerfield, 1994). Late in the pharyngula period the embryo, if removed from the chorion, swims away in response to touch; this can be prevented by anesthesia in 0.003% tricaine (3-amino benzoic acid ethyl ester; Sigma Chemical Co.) at pH 7 (Westerfield, 1994). Repeated anesthesia and rinsing appears to slightly but significantly retard subsequent development (see legend to Fig. 2).

Nomarski Optics

A compound microscope equipped with Nomarski differential interference contrast optics and objectives in the range of 25× to 40× reveals details otherwise not visible in the live preparation and permits the most critical staging. For instance, Nomarski optics permits the most accurate counts of cells in the blastula and of somites during segmentation. Moreover, "prim" stages refer to the position of a structure, the *prim*ordium of the posterior lateral line, that one must use Nomarski optics to see for the sharpest determination of stages during much of the pharyngula period. The embryo is anesthetized, removed from the chorion, and mounted between bridged coverslips (Westerfield, 1994), for observation and later recovery.

It is always better to stage embryos while they are alive rather than after killing and fixation. For example, staging during the straightening and hatching periods calls for a comparison of sizes of the head and the

TABLE 2. Stages of Embryonic Development[a]

Stage	h	HB	Description
Zygote period			
1-cell	0	1,2	Cytoplasm streams toward animal pole to form the blastodisc
Cleavage period			
2-cell	¾	3	Partial cleavage
4-cell	1	4	2 × 2 array of blastomeres
8-cell	1¼	5	2 × 4 array of blastomeres
16-cell	1½	6	4 × 4 array of blastomeres
32-cell	1¾	7	2 regular tiers (horizontal rows) of blastomeres, sometimes in 4 × 8 array
64-cell	2	8	3 regular tiers of blastomeres
Blastula period			
128-cell	2¼	9	5 blastomere tiers; cleavage planes irregular
256-cell	2½		7 blastomere tiers
512-cell	2¾		9 tiers of blastomeres; NO: YSL forms
1k-cell	3	10	11 tiers of blastomeres; NO: single row of YSL nuclei; slight blastodisc cell cycle asynchrony
High	3⅓		>11 tiers of blastomeres; beginning of blastodisc flattening; NO: YSL nuclei in two rows; substantial division asynchrony
Oblong	3⅔	11	Flattening produces an elliptical shape; NO: multiple rows of YSL nuclei
Sphere	4	12	Spherical shape; flat border between blastodisc and yolk
Dome	4⅓	13	Shape remains spherical; yolk cell bulging (doming) toward animal pole as epiboly begins
30%-epiboly	4⅔	14	Blastoderm an inverted cup of uniform thickness; margin reaches 30% of distance between the animal and vegetal poles
Gastrula period			
50%-epiboly	5¼		Blastoderm remains uniform in thickness
Germ-ring	5⅔		Germ ring visible from animal pole; 50%-epiboly
Shield	6	15	Embryonic shield visible from animal pole, 50%-epiboly
75%-epiboly	8	16	Dorsal side distinctly thicker; epiblast, hypoblast, evacuation zone visible
90%-epiboly	9		Brain rudiment thickened; notochord rudiment distinct from segmental plate
Bud	10	17	Tail bud prominent; notochord rudiment distinct from neural keel; early polster; midsagittal groove in anterior neural keel; 100%-epiboly
Segmentation period			
1-somite	10⅓		First somite furrow
5-somite	11⅔	18	Polster prominent; optic vesicle, Kupffer's vesicle
14-somite	16	19	EL = 0.9 mm; otic placode; brain neuromeres, v-shaped trunk somites; YE barely forming; NO: pronephric duct
20-somite	19	20	EL = 1.4 mm; YE/YB > 0.5 and < 1; muscular twitches; lens, otic vesicle, rhombic flexure; hindbrain neuromeres prominent; tail well extended
26-somite	22		EL = 1.6 mm; HTA = 125°; side-to-side flexures; otoliths; Prim-3
Pharyngula period			
Prim-5	24		EL = 1.9 mm; HTA = 120°; OVL = 5; YE/YB = 1; early pigmentation in retina and skin; median fin fold; red blood cells on yolk, heartbeat
Prim-15	30		EL = 2.5 mm; HTA = 95°; OVL = 3; YE/YB > 1; YB/HD = 2; early touch reflex and reduced spontaneous movements; retina pigmented; dorsal stripe to somite 12; weak circulation; caudal artery halfway to end of tail; caudal vein braided; shallow pectoral fin buds; straight tail; NO: cellular degeneration at end of tail; circulation in aortic arch 1
Prim-25	36		EL = 2.7 mm; HTA = 75°; OVL = 1; PF(H/W) = ¾; early motility; tail pigmentation and ventral stripe filling out; strong circulation; single aortic arch pair; caudal artery is ¾ of the way to the end of tail; pericardium not swollen; NO: PF apical ectodermal ridge
High-pec	42		EL = 2.9 mm; HTA = 55°; OVL < 1 and > ½; YE/YB = 1.5; YB/HD < 1.3; PF(H/W) = 1; dechorionated embryos rest on side after swimming; YE remaining cylindrical; PF apical ridge prominent; early lateral stripe; complete dorsal stripe; xanthophores in head only; iridophores in retina only; pericardium prominent; NO: heart chambers; segmental blood vessels; mandibular and hyoid arches; foregut developments; olfactory cilia; thickened otic vesicle walls
Hatching period			
Long-pec	48		EL = 3.1 mm; HTA = 45°; OVL = ½; PF(H/W) = 2; resting dorsal up; YE beginning to taper; PF pointed; dorsal and ventral stripes meet at tail; ca. 6 melanophores in lateral stripe; iridophores plentiful on retina; distinct yellow cast to head; NO: circulation in 2–4 aortic arches and in segmental vessels; olfactory cilia beating; semicircular canals; neuromasts
Pec-fin	60		EL = 3.3 mm; HTA = 35°; movements too rapid to resolve; YB tapering into YE; up to 10 melanophores in lateral stripe; PF flattened into fin shape with prominent circulation; iridophore retinal ring fills out; iridophores in dorsal stripe; NO: PF cartilage and actinotrichia; gut tract; 2 chambers in otic vesicle; early jaw cartilages; circulation in 5–6 aortic arches; mouth remaining small and open at ventral location midway between eyes
Protruding-mouth	72		EL = 3.5 mm; HTA = 25°; wide open mouth protruding anterior to eye; iridophores in yolk stripe; eye half covered by iridophores; dorsal body as yellow as head; NO: gill slits and filament buds; cartilage in branchial arch 1 and 5; operculum covers the branchial arch 1 or 2; clerithrum

[a]EL, embryo length; PF, pectoral fin; h, hours of development at 28.5°C; HB, approximate stage no. in the Hisaoka and Battle (1958) zebrafish staging series (reasonably accurate through HB stage 20); HD, head diameter in dorsal view; NO, Nomarski optics; H/W, height/width; Prim, Prim stages refer to the no. of the myotome to which the leading end of the posterior lateral line *primordium* has advanced; YB, yolk ball; YE, yolk extension; YSL, yolk syncytial layer; HTA, head-trunk angle; OVL, otic vesicle length.

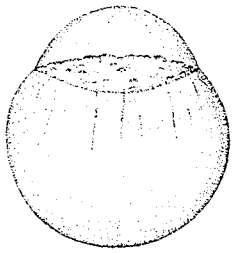

1-cell
0.2 h

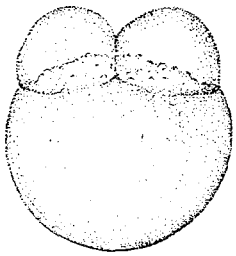

2-cell
0.75 h

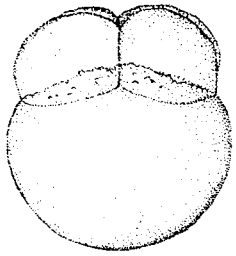

4-cell
1 h

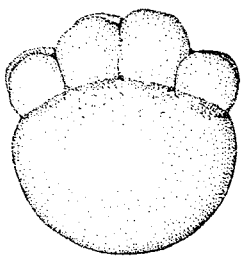

8-cell
1.25 h

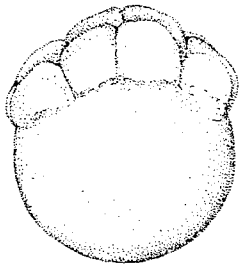

16-cell
1.5 h

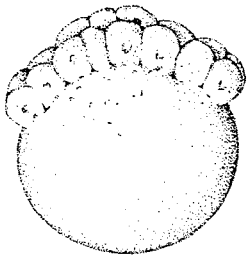

32-cell
1.75 h

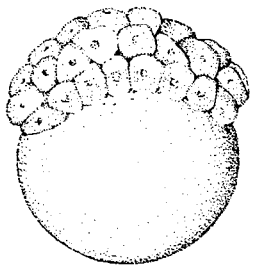

64-cell
2 h

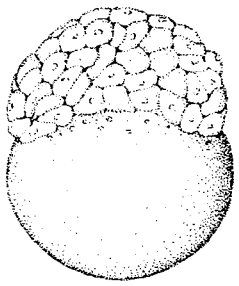

128-cell
2.25 h

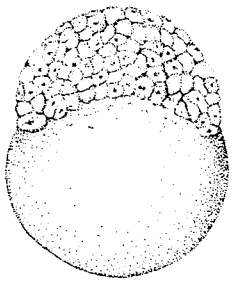

256-cell
2.5 h

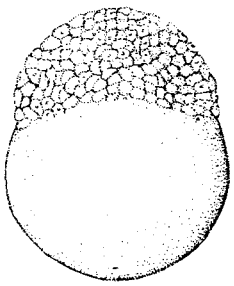

512-cell
2.75 h

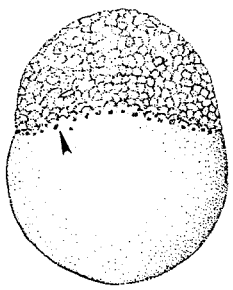

1k-cell
3 h

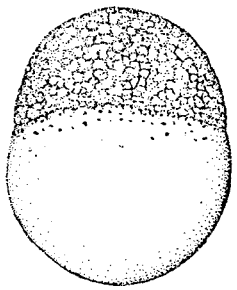

high
3.3 h

Fig. 1 (Legend to Fig. 1 appears on page 259).

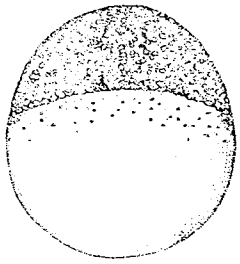

oblong
3.7 h

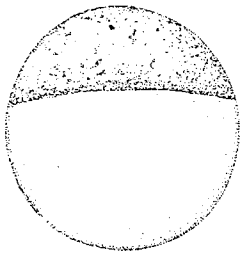

sphere
4 h

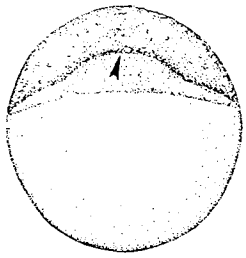

dome
4.3 h

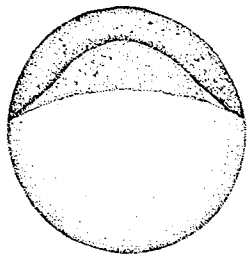

30%-epiboly
4.7 h

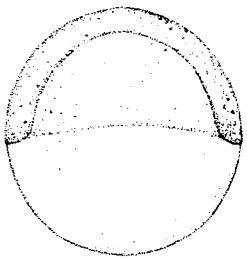

50%-epiboly
5.3 h

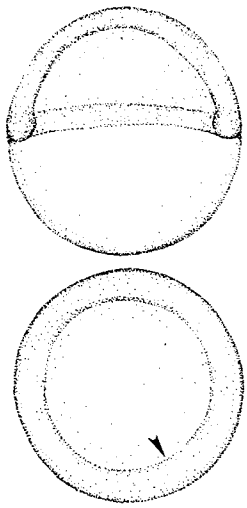

germ ring
5.7 h

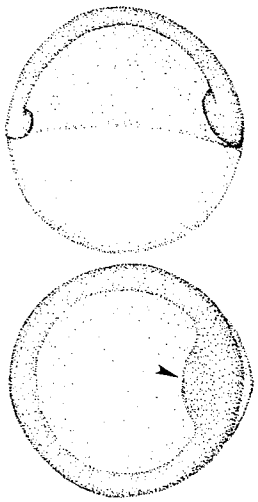

shield
6 h

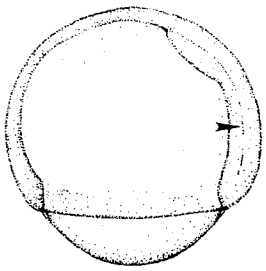

75%-epiboly
8 h

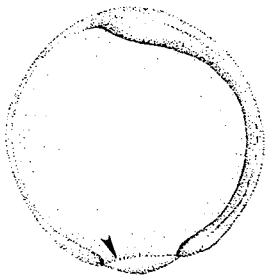

90%-epiboly
9 h

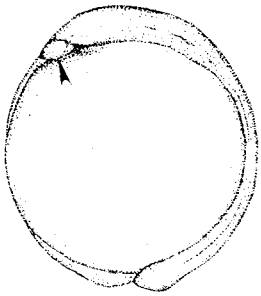

bud
10 h

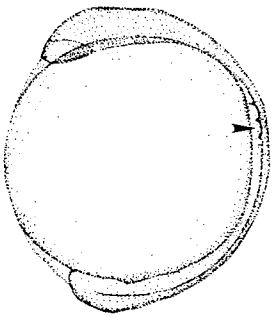

3-somite
11 h

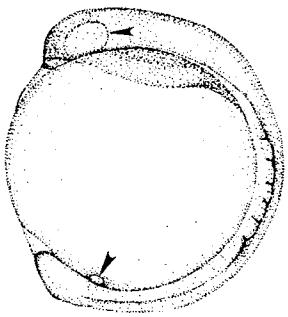

6-somite
12 h

Fig. 1 (*continued*).

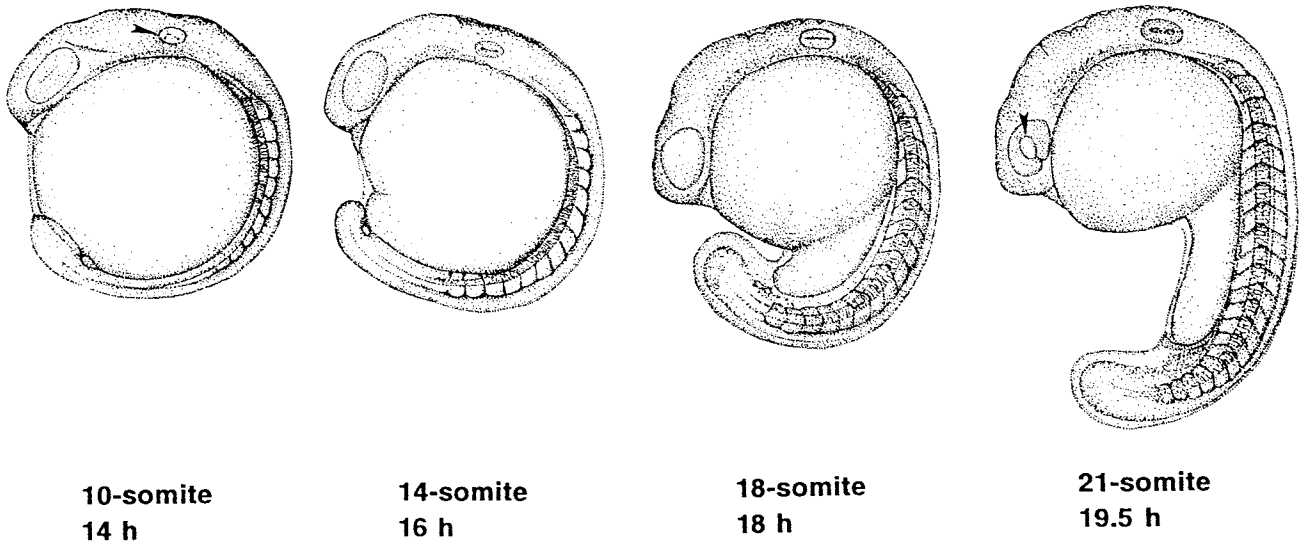

10-somite
14 h

14-somite
16 h

18-somite
18 h

21-somite
19.5 h

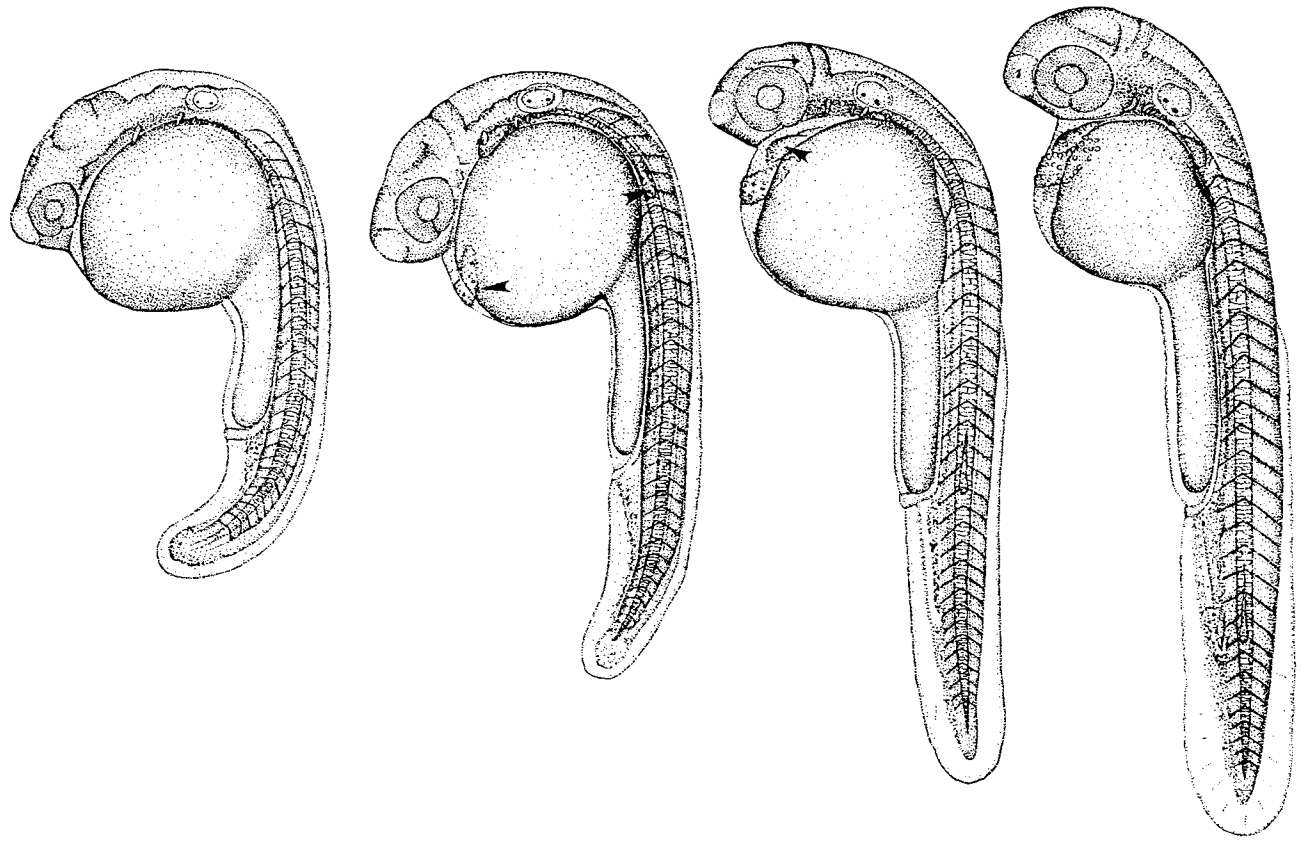

26-somite
22 h

prim-6
25 h

prim-16
31 h

prim-22
35 h

Fig. 1 (*continued*).

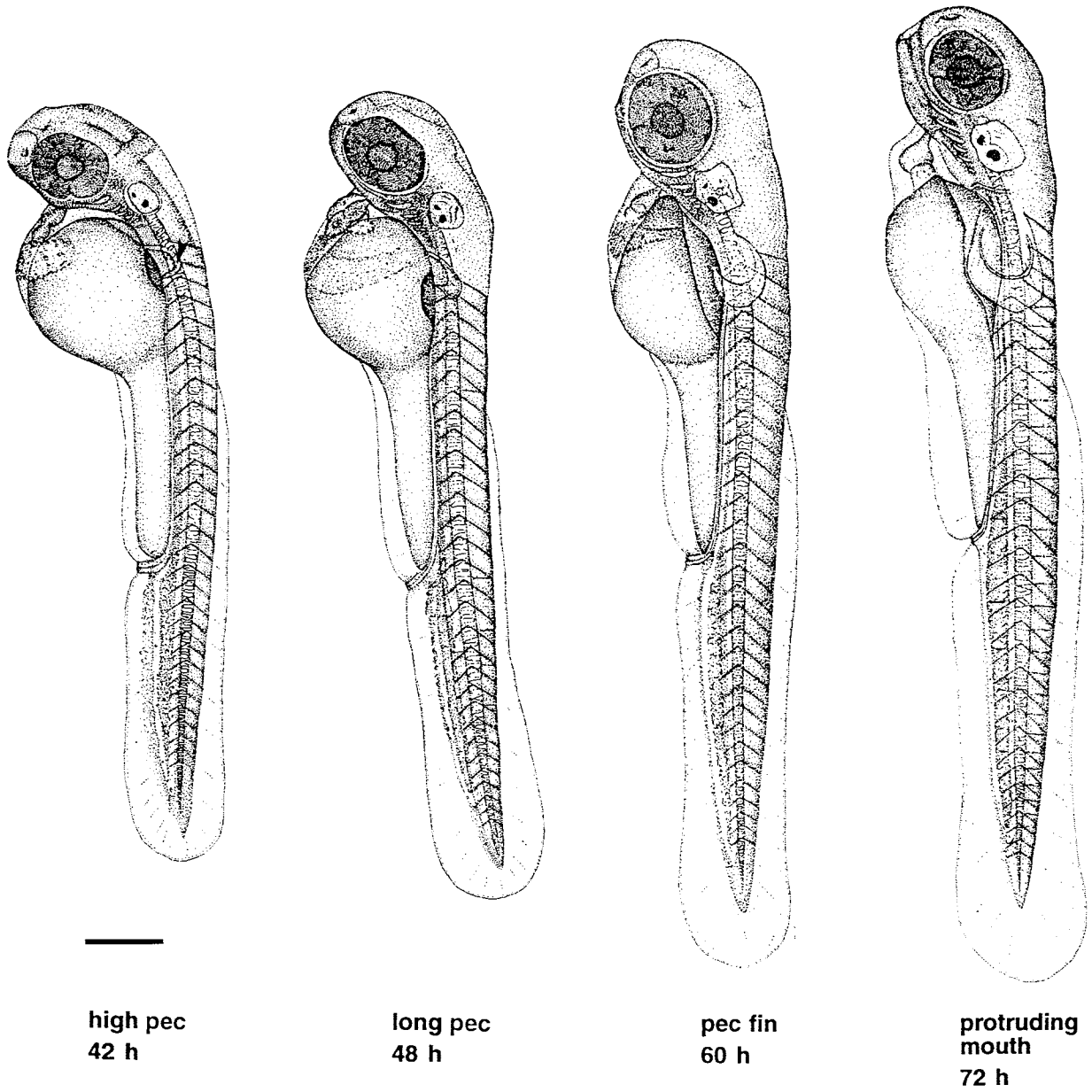

Fig. 1. Camera lucida sketches of the embryo at selected stages. The animal pole is to the top for the early stages, and anterior is to the top later, except for the two animal polar (AP) views shown below their side view counterparts for germ-ring and shield gastrulas. Face views are shown during cleavage and blastula stages. After shield stage, the views are of the embryo's left side, but before the shield arises one cannot reliably ascertain which side is which. Pigmentation is omitted. Arrowheads indicate the early appearance of some key diagnostic features at the following stages: 1k-cell: YSL nuclei. Dome: the doming yolk syncytium. Germ ring: germ ring. Shield: embryonic shield. 75%-epiboly: Brachet's cleft. 90%-epiboly: blastoderm margin closing over the yolk plug. Bud: polster. 3-somite: third somite. 6-somite: eye primordium (upper arrow), Kupffer's vesicle (lower). 10-somite: otic placode. 21-somite: lens primordium. Prim-6: primordium of the posterior lateral line (on the dorsal side), hatching gland (on the yolk ball). Prim-16: heart. High-pec: pectoral fin bud. Scale bar = 250 μm.

yolk mass, and differential shrinkage during fixation distorts the normal relationship. Nevertheless, if preservation is good enough, one can fairly reliably stage fixed and whole-mounted embryos (e.g., immunolabeled ones) using other criteria. One cannot easily stage an embryo after it is sectioned.

Photographs

The accompanying photographs are of living embryos, anesthetized for the later stages. The original photographs were made as color slides (Kodak Ektachrome 160T DX), and the black and whites plates are reproduced from internegatives. Sets of copies of the

original color slides are available at cost from the authors. The lower-magnification views, showing the entire embryo, were made using a Zeiss STEMI stereo dissecting microscope: The embryo is mounted on a depression slide, without an overlying coverslip, in standard embryo medium (Westerfield, 1994) containing 1.5–3% methyl cellulose to allow positioning as desired. The higher-magnification views, showing parts of embryos, were taken with Nomarski optics (generally a Zeiss 40× water-immersion objective) using a Zeiss UEM compound microscope. The embryo was mounted between coverslips, sometimes in 1% agar, for positioning.

TEMPERATURE AND STANDARD DEVELOPMENTAL TIME

We convert staging information to "standard developmental time," as designated by the letter "h," and defined as normalized *h*ours after fertilization at 28.5°C, an optimal temperature of incubation (G. Streisinger, unpublished experiments). Incubation at another temperature will change developmental rate, as may be useful in particular studies, e.g., to bring embryos to two different stages at the same time for heterochronic transplantation. Comparisons of embryos raised at different temperatures should be made with caution, because there is no assurance that all features of the embryo coordinately change their rates of development when the temperature is changed. Nevertheless, embryos appear to develop normally if they are kept within an eight degree range, between 25°C (perhaps a few degrees lower; see Schirone and Gross, 1968) and 33°C. Incubating them for long periods above or below these extremes may produce abnormalities. Figure 2 shows the rates of development at the extremes, and the legend to this figure provides a simple formula permitting one to estimate when an embryo developing at any temperature within this range will reach a given stage.

ZYGOTE PERIOD (0–¾ h)

The newly fertilized egg is in the zygote period until the first cleavage occurs (Fig. 3), about 40 minutes after fertilization. The zygote is about 0.7 mm in diameter at the time of fertilization. We include only a single stage; however many changes are occurring, and one

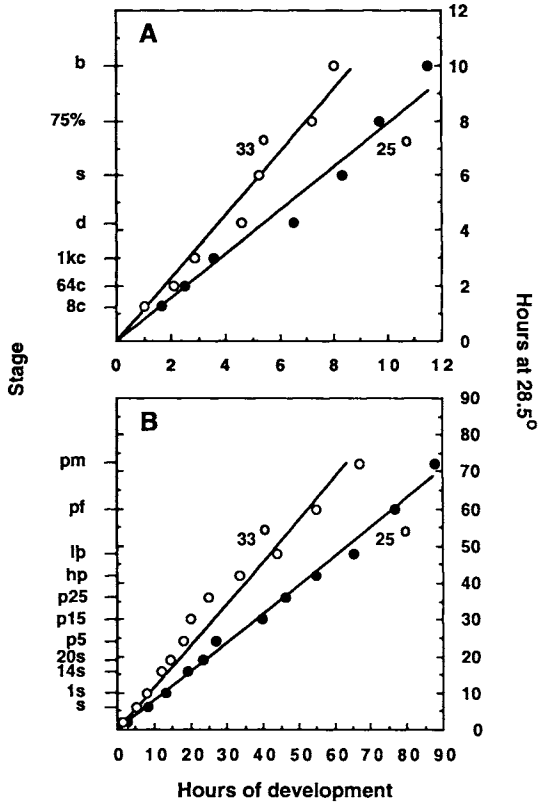

Fig. 2. Rates of development for embryos incubated at 25°C (solid circles) and 33°C (open circles). **A:** Development showing selected stages through the bud stage (occurring at 10 h at the standard temperature of 28.5°C). **B:** Development through the end of embryogenesis, the protruding-mouth stage (occurring at 72 h at the standard temperature). The stages (8c through b for A, and s through pm for B) are positioned along the ordinate according to when they occur at 28.5°C, the standard incubation temperature. Because of this presentation, a plot of development at 28.5°C would be expected to yield a straight line passing through the origin, and with a slope of 1.0. We determined this to be the case, in fact, by watching sets of control embryos developing at 28.5° during collection of the data for this experiment (not shown). Notice in the figures that developmental rates at both 25°C and 33°C are also approximately linear, and that the slopes of the lines at each temperature are the same in A and B. Hence developmental rate varies as a linear function of incubation temperature, and a simple calculation allows one to determine approximately when embryos developing at any temperature between the extremes will reach a desired stage of interest: $H_T = h/(0.055T - 0.57)$, where H_T = hours of development at temperature T, and h = hours of development to reach the stage at 28.5°, as set out in Table 1. For example, computation of development to the 20-somite stage (occurring at 19 h at the standard temperature) yields 23.6 hours at 25°C, and 15 hours at 33°C. These times do not differ significantly from those observed (23.5 hours and 14.5 hours). **Stage abbreviations** (and hours of development to reach the stage at 28.5° in parentheses): 8c, 8-cell (1.25 h); 64c, 64 cell (2 h); 1kc, 1k-cell (3 h); d, dome (4.3 h); s, shield (6 h); 75%, 75%-epiboly (8 h); b, bud (10 h); 1s, 1-somite (10.3 h); 14s, 14-somite (16 h); 20s, 20-somite (19 h); p5, prim-5 (24 h); p15, prim-15 (30 h); p25, prim-25 (36 h); hp, high-pec (42 h); lp, long-pec (48 h); pf, pec-fin (60 h); pm, protruding-mouth (72 h). **Method:** Observations were made on embryos developing from several natural spawnings, separated in each case into groups at each of the temperatures (25.0°C, 28.5°C, and 33.0°C) ± 0.2°C. Each group generally included 20–30 embryos, never less than 6. They were incubated in covered 150-ml beakers, in water baths regulated so that the temperatures within the beakers themselves were as desired. We assigned a time point for a particular stage when we judged that the majority of embryos in a given group had reached that stage. We used several defining characteristics for the stage, not just the most obvious one, and discarded malformed embryos. Further, we took care to assure that embryos taken at intervals from the beakers for staging were not developing differently from control embryos kept separately without being disturbed. This is because staging, particularly at the later time points, necessarily involves some handling of the embryos that could retard development (e.g., pipetting, dechorionation, tricaine anesthesia, mounting in observation chambers), particularly if done repeatedly. In fact during these studies we observed that repeated anesthesia and rinsing (3 times over the period between 20 h and 48 h) significantly retard development: Treated embryos looked 2–6 h younger than control embryos at the long-pec stage.

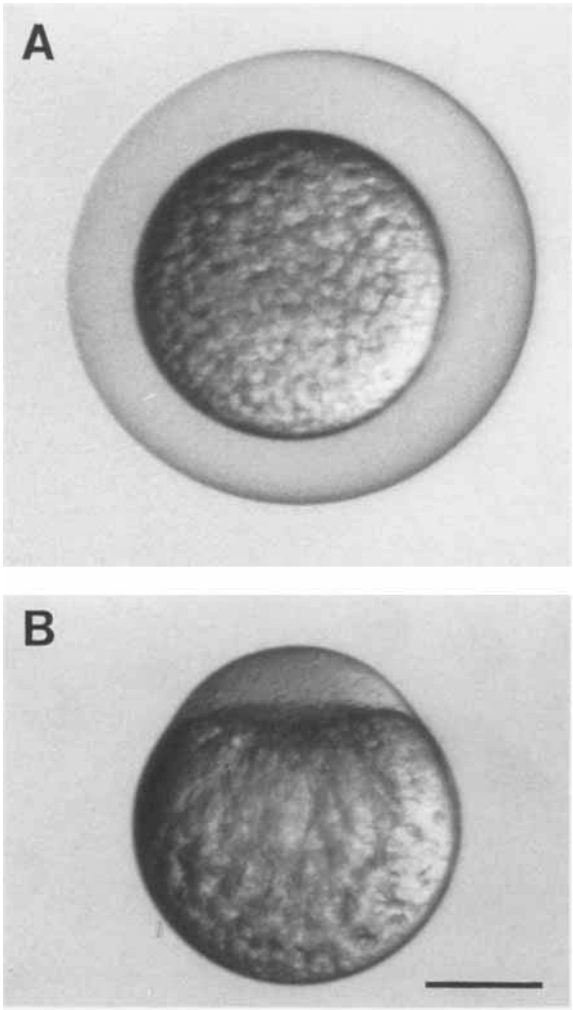

Fig. 3. The zygote period. **A:** The zygote within its uplifted chorion, a few minutes after fertilization. **B:** The dechorionated zygote with the animal pole to the top, about 10 min after fertilization. Yolk-free cytoplasm has begun to segregate to the animal pole. Scale bar = 250 μm.

could easily subdivide the period (see Hisaoka and Battle, 1958).

Stages During the Zygote Period

One-cell stage (0 h). The chorion swells and lifts away from the newly fertilized egg (Fig. 3A). Fertilization also activates cytoplasmic movements, easily evident within about 10 minutes. Nonyolky cytoplasm begins to stream toward the animal pole, segregating the blastodisc from the clearer yolk granule-rich vegetal cytoplasm (Fig. 3B). This segregation continues during early cleavage stages.

CLEAVAGE PERIOD (¾–2¼ h)

After the first cleavage the cells, or blastomeres, divide at about 15-minute intervals (Figs. 4, 5). The cytoplasmic divisions are meroblastic; they only incompletely undercut the blastodisc, and the blastomeres, or a specific subset of them according to the stage (Kimmel and Law, 1985a), remain interconnected by cytoplasmic bridges. The six cleavages that comprise this period frequently occur at regular orientations (Figs. 6, 7) so that one can see how many blastomeres are present are by their arrangement; counting them is unneccessary.

One can be quite accurate about staging during this period, as well as the early part of the next one, by using Nomarski optics to subdivide each cell cycle. All the cells of the blastodisc procede through their cell cycles synchronously, or nearly so. Nuclei are present and visible during about the first half of each cycle, i.e., during interphase, and the nuclear shapes change systematically (see below, Fig. 10). The nuclei are globular during very early interphase, become spherical by late interphase, and then, as the cells enter mitosis, their nuclei take on an ellipsoidal shape shortly before disappearing during prophase. The long axis of the ellipsoid predicts the orientation of the following cleavage. Mitotic chromosomes, present during the other half of the cleavage cell cycle, are more difficult to visualize. Near the end of mitosis, and heralding the cytoplasmic division, the blastomeres become more rounded in shape.

Stages During the Cleavage Period

Two-cell stage (¾ h). The first cleavage furrow, ending the first zygotic cell cycle, is vertically oriented, as is usual until the 32-cell stage. The furrow arises near the animal pole and progresses rapidly toward the vegetal pole, passing through only the blastodisc and not the yolky region of the egg (Fig. 4A). Near the bottom of the blastodisc the furrow changes to a horizontal orientation to undercut the blastodisc in the fashion described originally by Wilson (1889) for the sea bass, but still leaves the cells only partly cleaved from the underlying yolky region. The two blastomeres are of equal size and appear otherwise undistinguished from one another.

The following several cleavages are strictly oriented relative to the first one. However, the eventual axes of body symmetry (i.e., the dorsal-ventral and anterior-posterior axes) apparently cannot be predicted with any certainty from the orientation of the cleavage (Kimmel and Warga, 1987; Abdelilah et al., 1994; Helde et al., 1994), despite some reports to the contrary (Strehlow and Gilbert, 1993; Strehlow et al., 1994).

Four-cell stage (1 h). The two blastomeres cleave incompletely (Fig. 4B) and in a single plane that passes through the animal pole at right angles to the plane of the first cleavage. Hence, cycle 3 begins with four blastomeres in a 2 × 2 array. A view from the animal pole ("animal polar view," cartooned in Fig. 6) reveals that the blastodisc is ellipsoidal in shape. The second cleavage plane is oriented along the longer axis.

Eight-cell stage (1¼ h). Cleavages ending cycle 3, still incomplete, occur in two separate planes, parallel to the first one, and on either side of it. They cut the blastodisc into a 2 × 4 array of blastomeres. As the

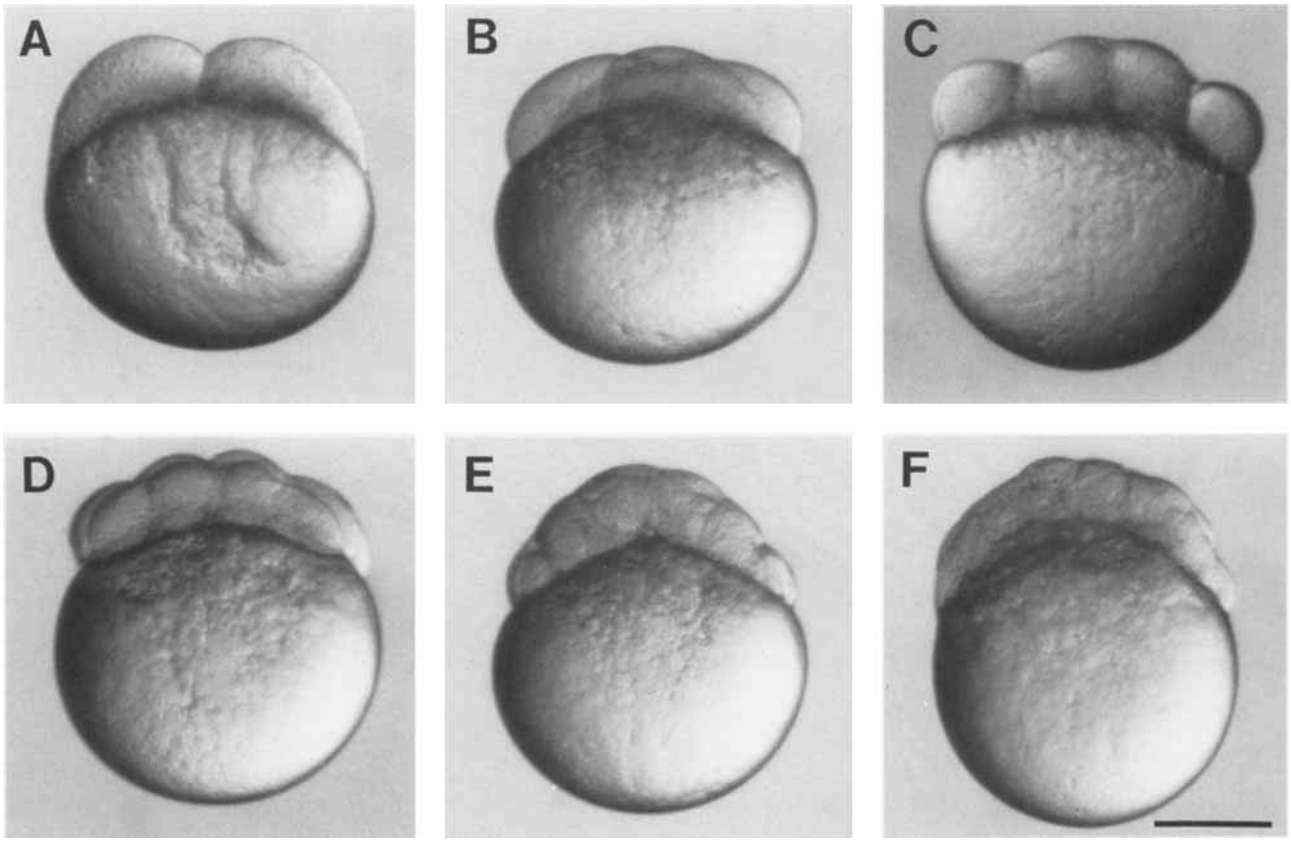

Fig. 4. Embryos during the cleavage period. Face views, except for B, which shows the embryo twisted about the animal-vegetal axis, roughly 45° from the face view. **A:** Two-cell stage (0.75 h). **B:** Four-cell stage (1 h). **C:** Eight-cell stage (1.25 h). **D:** Sixteen-cell stage (1.5 h). **E:** Thirty-two cell stage (1.75 h). **F:** Sixty-four cell stage (2 h). Scale bar = 250 μm.

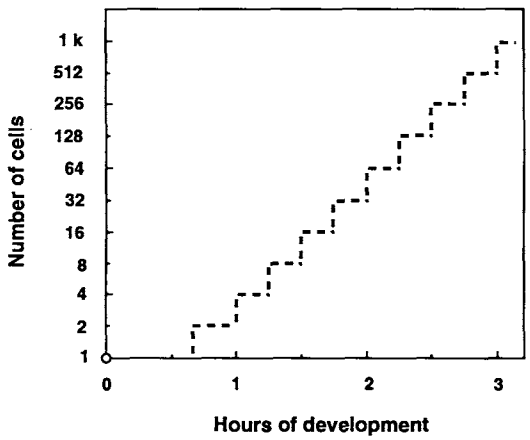

Fig. 5. Idealized blastomere number as a function of time after fertilization (at 28.5°C), for the time when divisions occur fairly synchronously, before the midblastula transition at the tenth cycle.

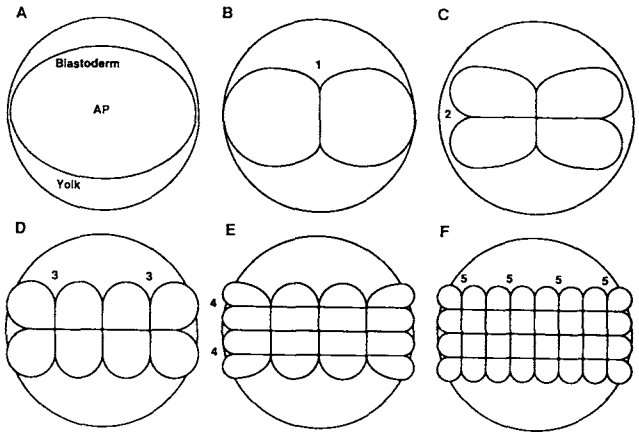

Fig. 6. Diagrammatic animal polar views of the planes of the first five cleavages. The outer circle is the yolk, and the inner ellipse in **A** is the uncleaved blastodisc. **B–F** show successive cleavages, with odd numbered cleavages cutting the short axis of the blastodisc and even-numbered ones cutting the long axis. Reprinted from Kimmel et al. (1991) with permission of Wiley-Liss, a division of John Wiley & Sons, Inc.

dechorionated embryo usually lies in a dish, the four-cell aspect, rather than the two-cell aspect, faces the observer. This "face" view (Kimmel and Law, 1985a) is along the odd-numbered cleavage planes (furrows 1 and 3 are visible; Fig. 7). The dechorionated embryo tends to lie in the same orientation through late blas-

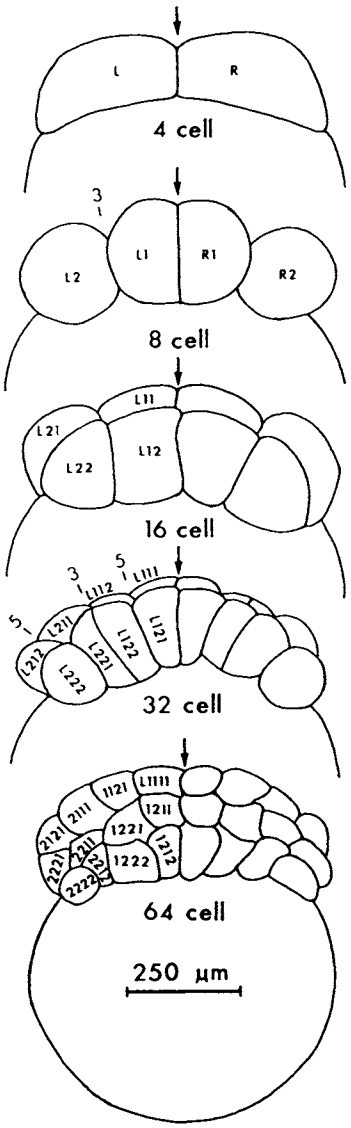

Fig. 7. Camera lucida drawings of face views during cleavage, showing lineal relationships of the blastomeres from the four-cell stage through the 64-cell stage. Blastomere names are according to cell lineage, and also indicate cell positions. Each name represents two cells in the embryo, one visible in the figure and one that would be visible by rotating the embryo through 180° about the animal-vegetal axis (i.e., only two cells are shown here at the four-cell stage). Cell L is to the left of the first cleavage plane, and cell R is to the right at the four-cell stage. (Hence the designations L and R are not with reference to the future left and right sides of the embryo; see text.) Cell L divides to generate L1, by convention the sister closer to the animal pole, and L2. L1 divides to generate L11 (closer to the animal pole) and L12, and so on. The deep cells are not in the drawing for the 64-cell stage. Reproduced with permission from Academic Press from Kimmel and Law (1985a).

tula stages, and this view is the one shown in the first part of Figure 1 (through the high stage), Figure 4 (except for Fig. 4B), and Figure 7.

16-cell stage (1½ h). The fourth set of cleavages also occur along two planes, parallel to and on either side of the second one, and produces a 4 × 4 array of cells. Use care to distinguish this stage from the eight-cell stage, because they look similar in face view (Fig. 4C,D).

For the first time some of the cells now become completely cleaved from the others. These "complete" cells are the four most central blastomeres, the quartet that is entirely surrounded by other cells in Figure 6E. Their complete cleavage occurs near the end of the 16-cell stage because of the way the cleavage furrows undercut the blastodisc from the center, going outward toward the blastodisc margin. Indeed, the undercutting furrows still do not reach the margin, and the 12 cells surrounding these four central ones, the so-called marginal blastomeres, remain connected to the yolk cell by cytoplasmic bridges (Kimmel and Law, 1985a). From this stage onward until the midblastula period the cleavages completely partition most or all of the nonmarginal blastomeres, but still incompletely partition the marginal ones.

32-cell stage (1¾ h). The cleavages ending cycle 5 often occur along four parallel planes, rather than two, lying between those of the first and third cycles. However, oblique orientations of the furrows are now common. Frequently the 32 blastomeres of this stage are present in a 4 × 8 array, but other regular patterns, as well as irregular ones involving one or more of the blastomeres, also occur (Kimmel and Law, 1985b). In a side view one usually sees two *tiers,* or horizontal rows, of blastomeres between the margin and the animal pole (Figs. 4E, 7). This is because the plane of the blastodisc is curved; marginal cells are more vegetal, and they lie partly in front of the nonmarginal ones positioned closer to the animal pole.

64-cell stage (2 h). Cleavages ending the sixth cycle pass horizontally, so that in an animal polar view the blastomere array may look similar to the 32-cell stage, although the cells entering cycle 7 are smaller. From the side the cell mound looks distinctly higher (Figs. 1, 4F, 7). For the first time some of the blastomeres completely cover other ones. The buried cells, or deep cells, each arise as one of the two daughters of the four central blastomeres that were present at the 32-cell stage. The other daughter remains superficial, in the topmost tier of what is now the enveloping layer (EVL) of the blastodisc. During the same cleavage the horizontal divisions of marginal blastomeres present at cycle 6 produce two EVL sister cells, and in a face view of the 64-cell stage one sees three tiers of EVL cells (Fig. 7).

BLASTULA PERIOD (2¼–5¼ h)

We use the term blastula to refer to the period when the blastodisc begins to look ball-like, at the 128-cell stage, or eighth zygotic cell cycle, and until the time of onset of gastrulation, ca. cycle 14. Important processes occur during this blastula period; the embryo enters midblastula transition (MBT), the yolk syncytial layer (YSL) forms, and epiboly begins. Epiboly continues during the gastrulation period.

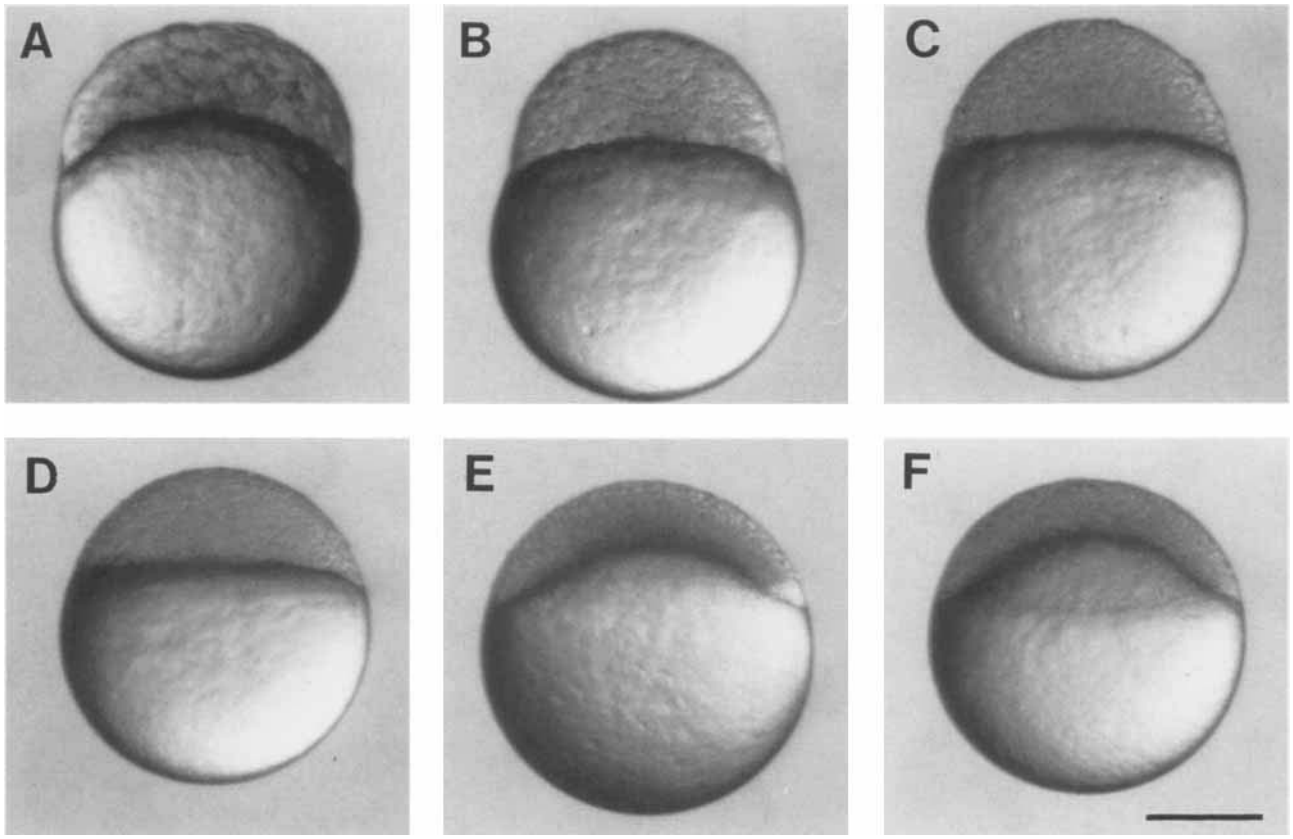

Fig. 8. Face views of embryos during the blastula period. **A:** 256-cell stage (2.5 h). **B:** High stage (3.3 h). **C:** Transition between the high and oblong stages (3.5 h). **D:** Transition between the oblong and sphere stages (3.8 h). **E:** Dome stage (4.3 h). **F:** 30%-epiboly stage (4.7 h). Scale bar = 250 μm.

"Stereoblastula" would be a more appropriate term than blastula to describe the period, for it means no blastocoele is present, which is the case (Fig. 8). Only small irregular extracellular spaces exist between the deep cells of the blastodisc. The orientation of the cleavage planes is indeterminate, and they are much less regularly arranged than they were during the cleavage period. The daughter cells from these later cleavages slip out of what have been rather neat rows, in either side or top views, so that blastomere size is more useful than blastomere position in determining the stage during this period. The blastodisc looks slightly ellipsoidal in animal polar view (particularly during the early part of the period).

Early on, the cells of the blastula continue to divide synchronously, at the same rhythm as before (Figs. 5, 9). More accurately, the cleavages during the early blastula period are "metasynchronous" because the mitoses do not all occur at quite the same time. Instead, a wave crosses the blastodisc at the end of each cell cycle. Cells near the animal pole enter the wave first, and the marginal cells enter the wave last. Generally the wave passes through the blastodisc obliquely, such that, from a face view, one can observe the wave pass across the field of cells along the long axis of the blastoderm, as it also passes from the animal pole to the margin.

Cell cycle lengthening marks the onset of the mid-blastula transition (MBT; Kane and Kimmel, 1993; Fig. 9A). Not all of the cycles begin to lengthen synchronously or to the same extent (Fig. 9B), and at any time point after MBT some cells are in interphase and have nuclei easily visualized with Nomarski optics (Fig. 10A,D), while other cells are in mitosis (and have no nuclei; Fig. 10C,E): Asynchrony among the blastomeres is thus immediately apparent from the morphology. The MBT begins during the tenth cell cycle (512-cell stage), two cycles earlier than in *Xenopus* (Newport and Kirshner, 1982a,b), but otherwise the essentials of the MBT, its features, and how its onset is controlled appear the same in the two species (Kane and Kimmel, 1993). As interphases lengthen, cells become motile, and RNA synthesis increases over background levels.

Time-lapse analysis reveals that after the onset of the MBT the deep cells are motile during their longer interphases (Kane and Kimmel, 1993). The deep cell

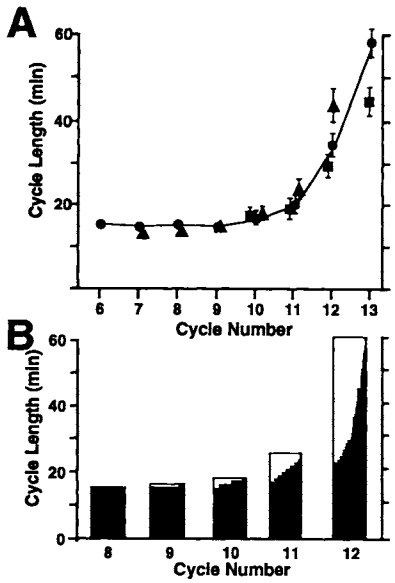

Fig. 9. Cell cycle lengthening and loss of synchrony at the midblastula transition, beginning at the tenth zygotic cell cycle (512-cell stage). The three different symbols in **A** represent data collected by following fields of cells in three different embryos. The distributions in **B** represent cycle lengths of individual cells followed in a field within a single embryo. Reproduced from Kane and Kimmel (1993) with permission from Company of Biologists Ltd.

movements appear to be unoriented, at least as seen from the surface.

The marginal tier of blastomeres in the early blastula have a unique fate. They lie against the yolk cell and remain cytoplasmically connected to it throughout cleavage. Beginning during cycle 10 (Kimmel and Law, 1985b), the marginal cells undergo a collapse, releasing their cytoplasm and nuclei together into the immediately adjoining cytoplasm of the yolk cell. Thus arises the **yolk syncytial layer (YSL)** a feature prominent with Nomarski optics, and important for staging (Fig. 10). After the YSL forms, the EVL cells that were in the second blastodisc tier now lie at the marginal position. They look like their former neighbors did, but with the important difference that these new marginal blastomeres are nonsyncytial: For the first time, none of the blastomeres have cytoplasmic bridges to other cells, except those present for a short time between newly divided sibling-cell pairs.

Although the YSL forms just at the time of the MBT, the regulatory control of these two events appears to be distinct; MBT alone depends on the nuclear-cytoplasmic ratio (Kane, 1991). The YSL nuclei continue to undergo mitotic divisions in the midblastula, but the nuclear divisions are unaccompanied by cytoplasmic ones, and the yolk cell remains uncleaved and syncytial. As in the blastodisc, the YSL division cycles lengthen during the midblastula period, but not as much, and the YSL nuclei continue to divide metasynchronously, not asynchronously. After about three cycles, and coinciding with the beginning of epiboly, the YSL divisions abruptly cease (Kane et al., 1992; see also Trinkaus, 1992). The YSL nuclei now begin to enlarge; possibly meaning that they are actively transcribing RNA.

The YSL, an organ unique to teleosts, may be extraembryonic, making no direct contribution to the body of the embryo. At first the YSL has the form of a narrow ring around the blastodisc edge (Fig. 10), but soon (within two division cycles) it spreads underneath the blastodisc, forming a complete "internal" syncytium (the I-YSL), that persists throughout embryogenesis. In this position, between the embryonic cells and their yolk stores, the I-YSL might be presumed to be playing a nutritive role. Another portion of it, the E-YSL, is transiently "external" to the blastodisc edge during epiboly. Indeed, work with the teleost *Fundulus* shows that this region, the E-YSL, appears to be a major motor for epiboly (Trinkaus, 1984).

Epiboly, beginning in the late blastula (Solnica-Krezel and Driever, 1994), is the thinning and spreading of both the YSL and the blastodisc over the yolk cell, as you might model by pulling a knitted ski cap over your head. Eventually, at the end of the gastrula period, the yolk cell becomes engulfed completely. During the early stages of this morphogenetic movement the blastodisc thins considerably, changing from a high-piled cell mound (Fig. 8B) to a cup-shaped cell multilayer of nearly uniform thickness (Fig. 8F). This is accomplished by the streaming outward, toward the surface, of the deepest blastomeres. As they move, they mix fairly indiscriminately among more superficial cells along their way (Wilson et al.,1993). Active cell repacking by these so-called radial intercalations (Keller, 1980) may be a part of the driving force of early epiboly. The intercalations do not drive deep cells into the EVL, which remains a compartmentalized monolayer (Kimmel et al., 1990b). Additionally, deep blastomeres at the margin mix together to a considerably lesser extent than do the central ones (Helde et al., 1994), where, as can be seen from Figure 8, the pile is much thicker before epiboly begins. This relative lack of mixing among marginal blastomeres may have significance with respect to how pattern is established during early development. This is because the mesoderm will arise from these nonmixing marginal deep cells (see the fate map below, Fig. 14). Presuming that events specifying mesoderm begin to occur before epiboly, as they seem to do in *Xenopus,* then lack of mixing in the marginal deep cell population during epiboly could be important to maintain regions with different cellular "specifications" (Kimmel et al., 1991) or identities.

The yolk cell prominently changes shape at the same time that the radial intercalations occur. The I-YSL surface bulges or "domes" toward the animal pole, this change in shape being the clearest sign that epiboly is beginning (Fig. 8E), and serving to substantially increase the area of contact between the I-YSL and the blastodisc's inner surface. As the yolk cell domes, it

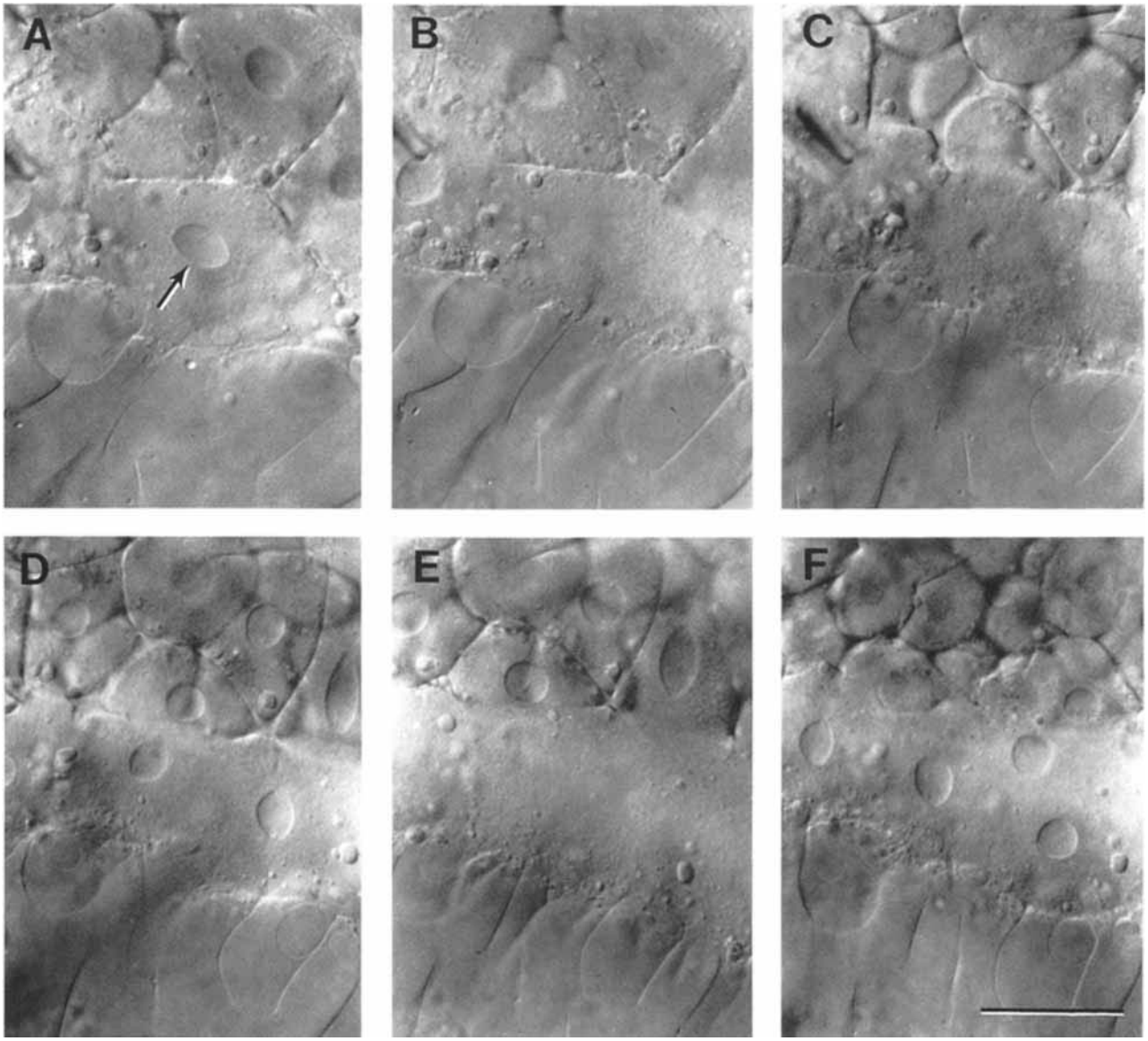

Fig. 10. Formation of the yolk syncytial layer (YSL), viewed with Nomarski optics. **A:** A marginal blastomere during the tenth interphase (512-cell stage; the arrow indicates its nucleus). **B:** The nucleus disappears as the cell enters the tenth mitosis, a special one because there is no cytokinesis. The daughter nuclei then reappear in a common cytoplasm during interphase 11. During very early interphase the nuclei are globular (**C**), and later, just before entering mitosis again they are large and football-shaped (**D**). The YSL nuclei continue to disappear during mitoses (**E;** mitosis 11; note that interphase nuclei are present just in the blastoderm cells and not the YSL, meaning that the blastoderm and YSL are no longer in synchrony), and reappear during interphases (**F;** interphase 12) for several mitotic cycles, always within a common syncytium. Reproduced with permission from Academic Press from Kimmel and Law (1985b). Scale bar = 50 μm.

occupies territory simultaneously vacated by the deep blastomeres during their radial intercalations; yolk cell doming could exert force that drives the deep cells outward. Whatever its cause, epiboly clearly involves the blastodisc and yolk cell alike, and begins quite rapidly. As epiboly continues during the next several hours, the E-YSL continues to advance across the yolk ahead of the cells that are riding upon it. In *Fundulus,* at least, desmosomes serve to attach the E-YSL to the EVL margin (Betchaku and Trinkaus, 1978), and the spreading YSL appears to pull the EVL along behind it.

Epiboly appears to depend on functional microtubules (Strähle and Jesuthasan, 1993) and might be under control of early-acting zygotic genes (Kane, 1991). The earliest-expressed genes identified so far code for regionally localized putative transcription factors, and begin expression in the late blastula (e.g., the gene *no tail,* Schulte-Merker et al., 1992; *goosecoid,* Stachel et al., 1993; *snail1,* Thisse et al., 1993).

Changes also occur in the EVL during the blastula period. At the end of the cleavage period there are more EVL cells than deep cells, but with successive divisions the EVL cells become vastly outnumbered. The EVL flattens, its cells thinning and stretching markedly to eventually form a tightly sealed (Bennett and Trinkaus, 1970) epithelial monolayer that becomes increasingly difficult to see. By the late blastula period, EVL cell cycles are longer and less synchronous than deep cell cycles (Kane et al., 1992). At the same time the EVL cells become lineage-restricted; their cell divisions generate daughters that are always within the EVL (Kimmel et al., 1990b). However, their developmental potential does not seem to be restricted during the late blastula period; if they are transplanted singly among the deep cells, their descendants acquire new fates (Ho, 1992a).

Stages During the Blastula Period

128-cell stage (2¼ h). The eighth cycle begins with 128 blastomeres arranged as a high mound of cells, a solid half ball perched on the yolk cell. In contrast to earlier cleavages, the cleavage furrows that bring the 64-cell stage to an end generally occur so irregularly that with few exceptions one cannot after this time deduce a blastomere's cellular ancestry from its position. One can, however, distinguish whether a view from the side corresponds to a view along the earlier odd-numbered cleavage planes (the face view, described above) or the even-numbered ones because of the oblong shape of the blastodisc, which remains as described for the four-cell stage. As seen from a face view, the EVL cells line up in about five irregular tiers between the animal pole and the margin.

256-cell stage (2½ h). A face view (Fig. 8A) at the end of the eighth set of cleavages reveals the EVL cells in about seven irregular tiers. The EVL cells thin out considerably during the interphase of this ninth cycle. The deep cells substantially outnumber those of the EVL. The ninth cleavage divisions are the last highly synchronous, or metasynchronous, ones to occur.

512-cell stage (2¾ h). Here begins midblastula transition; cell cycles lengthen gradually during the next several divisions (Fig. 9A). In face view, about nine somewhat irregular tiers of EVL blastomeres occur between the margin and animal pole. During the last part of this stage and particularly as they enter the tenth mitosis, the marginal blastomeres (the first-tier EVL cells) begin to lose their lower borders where they join the yolk cell (Fig. 10A,B). This morphogenetic change signals the beginning of formation of the YSL; the marginal cells specifically do not undergo cytokinesis following the tenth mitosis. This mitosis occurs with enough synchrony that one can still find a minute or so of time when all cells, including the yolk cell, are in mitosis (i.e., the cells have no interphase nuclei; Fig. 10C). The 512-cell stage is the last cycle when this is possible.

1k-cell stage (3 h). One can usually, but not always, see a YSL (Fig. 10D), irregular in form and containing a total of about 20 nuclei within a single ring around the blastodisc margin. There are fewer than 1,024 blastomeres after division 10 because the first-tier (marginal) EVL cells from the previous stage joined together in the YSL. Moreover, because of the manner of YSL formation, the cells making up the first EVL tier at this stage are descendants of those that were in the second tier a stage earlier.

In some embryos, the YSL forms over the course of two cycles, sometimes beginning a stage earlier and other times a stage later than the 1k stage.

About 11 tiers of cells occupy the EVL. The 11th set of mitoses occurs as a discernable wave passing through the blastodisc, and is the last one to do so. During this wave, for the first time, many of the cells can be seen to be out of phase with their neighbors; some have and some do not have interphase nuclei.

High stage (3⅓ h). This stage marks the end of the period during which the blastodisc perches "high" upon the yolk cell (Fig. 8B,C). There is still a pinched ring, a constriction, where the marginal cells meet the YSL. One distinguishes the high stage from earlier ones by the appearance and numbers of both blastodisc cells and YSL nuclei. In side view there are substantially more than 11 tiers of EVL cells visible between the margin and the animal pole. In any region of the blastodisc throughout this whole stage there are some cells in interphase and others in mitosis. Most blastodisc cells complete zygotic cell cycle 12, whereas a few complete cycle 13 during this stage.

The YSL still has the form of a thin ring, but its outer edge, i.e., the edge away from the blastodisc, is now much smoother in contour. The YSL nuclei reappear from their second division without cytokinesis (their 11th zygotic division) generally all still external to the blastodisc margin, and more tightly packed together (Fig. 10F).

Oblong stage (3⅔ h). The animal-vegetal axis of the blastula shortens, with the blastodisc compressing down upon the yolk cell, as one could imagine to result from a uniform increase in tension at the surface. The constriction at the blastodisc margin that has been present since the elevation of nonyolky cytoplasm during the one-cell stage diminishes (Fig. 8C) and then disappears. Eventually the blastula acquires a smoothly outlined ellipsoidal shape, as viewed from the side, and the stage is named for this oblong shape. The blastomeres are dividing highly asynchronously, many of them being in cycle 12 or 13. The EVL is by now extremely thin, and careful observation with Nomarski is needed to detect its presence.

The YSL is spreading deep underneath the blastodisc, and spreading away from it as well. During their interphases the YSL nuclei form several rows, some nuclei invariably in the I-YSL.

Sphere stage (4 h). Continued shortening along the animal-vegetal axis generates a late blastula of smooth and approximately spherical shape. The overall shape

then changes little the next several hours, well into the period of gastrulation, but cell rearrangements that begin now seem to occur more rapidly than at any other time in development. One distinguishes this stage from the dome stage that comes next by the appearance, at a very deep plane of focus, of the face between the lower part of the blastodisc and the upper part of the yolk cell, the I-YSL. At sphere stage specifically this interface is flat, or nearly flat (Fig. 8D).

Many of the cells of the blastodisc are in cycle 13, and in the EVL this cycle is often extremely long, such that mitoses occur very rarely in the EVL. The E-YSL is often noticeably thinner than earlier, and most YSL nuclei are internal. The last of the YSL nuclear divisions occur. Frequently, dechorionated embryos begin to be oriented animal pole-upward, rather than lying on their sides as earlier.

Dome stage (4⅓ h). Deep to the blastodisc the I-YSL surface begins to dome toward the animal pole (Fig. 8E). This prominent and rapidly occurring change in the interface between the yolk cell and the blastodisc represents the first sure sign that epiboly is beginning. EVL cells are in a long cycle 13, and many deep cells enter cycle 14. The E-YSL begins to narrow (Solnica-Krezel and Driever, 1994). The YSL nuclei are postmitotic; i.e., in contrast to when they were in mitotic cycles just preceding dome stage, the nuclei are now always visible. They begin to enlarge, and one can see them quite easily.

30%-epiboly stage (4⅔ h). Epiboly, including doming of the yolk cell, produces a **blastoderm,** as we may now call it, of nearly uniform thickness (Fig. 8F). It now consists of a highly flattened EVL monolayer (hard to see except by focusing exactly in the plane of the blastoderm surface with Nomarski optics), and a deep cell multilayer (DEL) about four cells thick.

The extent to which the blastoderm has spread over across the yolk cell provides an extremely useful staging index from this stage until epiboly ends. We define **percent-epiboly** to mean the fraction of the yolk cell that the blastoderm covers; percent-coverage would be a more precise term for what we mean to say, but percent-epiboly immediately focuses on the process and is in common usage. Hence, at 30%-epiboly the blastoderm margin is at 30% of the entire distance between the animal and vegetal poles, as one estimates along the animal-vegetal axis.

The blastoderm thickness is not exactly uniform in many embryos at this stage. Observing the marginal region from a side view, as the blastula is rotated about the animal-vegetal axis will reveal one region along the margin that is noticeably thinner and flatter than elsewhere. This particular region will become the dorsal side of the embryo (Schmitz and Campos-Ortega, 1994). We observe the asymmetry most easily using low-magification Nomarski optics. To distinguish the dorsal side with absolute confidence, however, one needs to await shield stage (6 h).

GASTRULA PERIOD (5¼–10 h)

Epiboly continues, and in addition, the morphogenetic cell movements of involution, convergence, and extension occur, producing the primary germ layers and the embryonic axis.

The beginning of involution defines the onset of gastrulation, and, so far as we have been able to tell, this occurs at 50%-epiboly (Fig. 11A). As a consequence, within minutes of reaching 50%-epiboly a thickened marginal region termed the **germ ring** appears, nearly simultaneously all around the the blastoderm rim (Fig. 11B, arrow in C). Convergence movements then, nearly as rapidly, produce a local accumulation of cells at one position along the germ ring, the so-called **embryonic shield** (Fig. 11D, arrow in E). During these events, epiboly temporarily arrests, but after the shield forms, epiboly continues; the margin of the blastoderm advances around the yolk cell to cover it completely (Fig. 11F–L). The advance occurs at a nearly constant rate, over an additional 15% of the yolk cell each hour, and providing a useful staging index during most of gastrulation (Fig. 12).

Just as there was no blastocoele during the blastula period, there is no archenteron in the gastrula. Neither is there a blastopore; DEL cells involute at the blastoderm margin, which thus plays the role of a blastopore. Involution produces the germ ring by folding the blastoderm back upon itself. Hence, within the germ ring there are two germ layers: The upper, the epiblast, continues to feed cells into the lower, the hypoblast, throughout gastrulation. Note that these terms, epiblast and hypoblast, are also used to describe layers of the avian embryonic blastoderm, but the layers so-named seem to be altogether different in these two kinds of vertebrate embryos.

As a morphogenetic movement, involution at the blastoderm margin seems particularly well docu-

Fig. 11. Development during the gastrula period. Left side views, except where noted, with anterior up and dorsal to the left. **A:** 50%-epiboly stage (5.25 h). **B:** Germ ring stage (5.7 h). **C:** Animal pole view of the germ ring stage; the arrow indicates the germ ring; the embryonic shield will probably develop from the flattened region of the ring at the lower right. **D:** Shield stage (6 h). The embryonic shield, marking the dorsal side, is visible as a thickening of the germ ring to the left. **E:** Animal pole view of the shield stage; the arrow indicates the embryonic shield. **F:** 70%-epiboly stage (7.7 h). The dorsal side of the blastoderm, to the left, is thicker than the ventral side, to the right. The anterior axial hypoblast, or prechordal plate (arrow), extends nearly to the animal pole. **G:** 70%-epiboly stage, ventral view, but tipped slightly forward anteriorly to reveal the now well-delineated axial hypoblast (arrow) of the prechordal plate. **H:** 75%-epiboly stage (8 h). The arrow indicates the thin evacuation zone on the ventral side. **I:** 80%-epiboly stage (8.4 h), dorsal view. The arrows indicate the boundaries between axial mesoderm in the midline, and the paraxial mesoderm flanking to either side. **J:** 90%-epiboly stage (9 h). The tail bud (arrow) becomes visible in some embryos at this stage. **K:** 90%-epiboly stage, ventral view. The anterior prechordal plate (compare with G) enlarges as the polster. **L:** Bud stage (10 h). The arrow shows the polster, and the arrowhead shows the tail bud. A distinctive region just ventral to the tail bud (i.e., just to the left in this view) shows where the yolk disappears as epiboly ends. Scale bar = 250 μm.

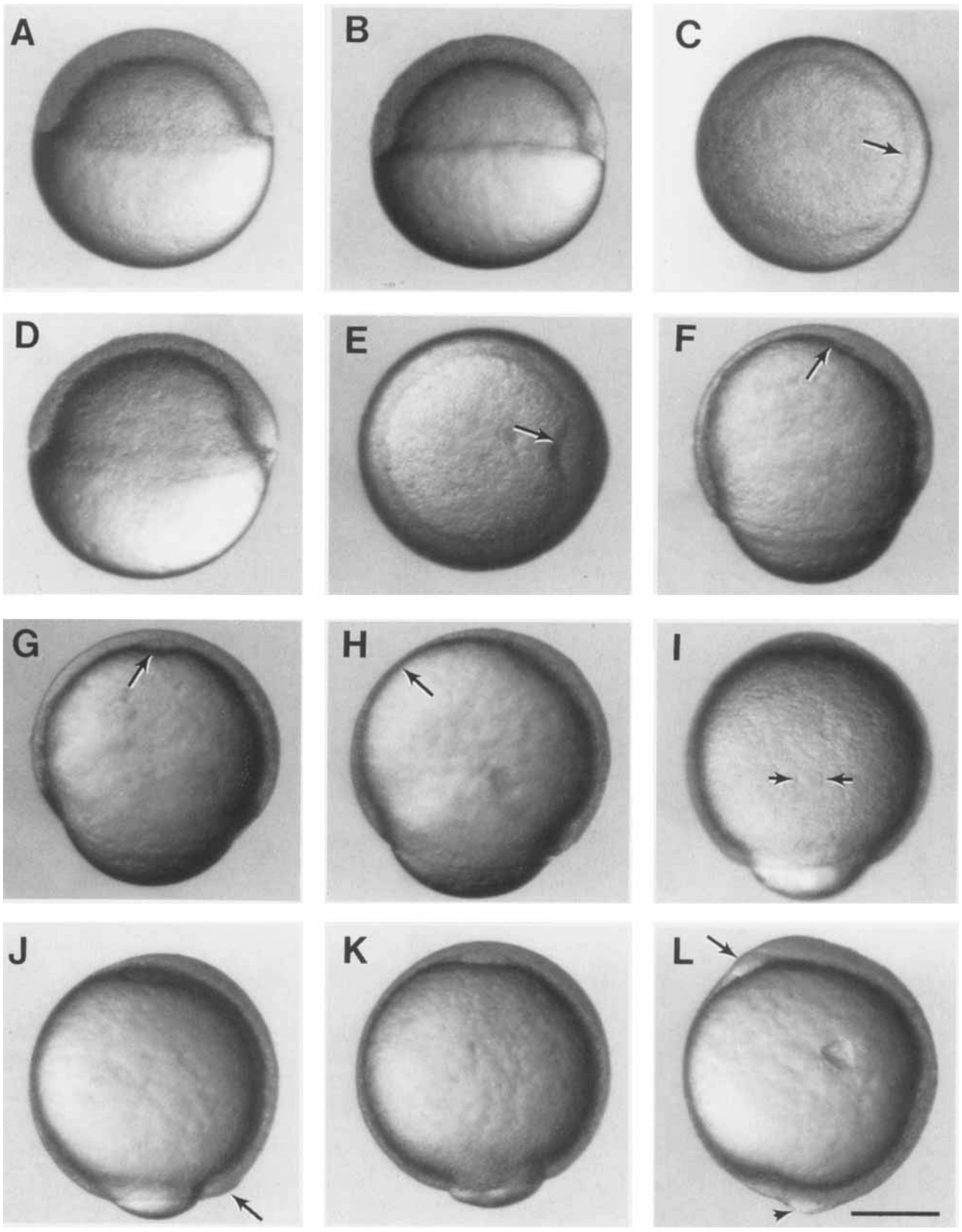

Fig. 11.

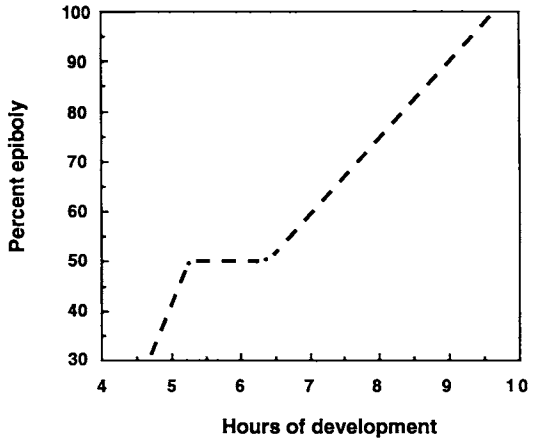

Fig. 12. Idealized rate of advance of the blastoderm margin over the yolk cell during epiboly (at 28.5°C). Percent epiboly refers to the fraction of the embryo (blastoderm plus yolk cell) that is covered by the blastoderm. After 6⅔ h the rate is fairly constant, at about 15% epiboly per hour. We observed groups of about a dozen embryos developing together to obtain the data, and here ignore variability among the embryos.

mented for the rosy barb (Wood and Timmermans, 1988), a small teleost that develops in many ways very similarly to the zebrafish. However, recently J.P. Trinkaus has obtained evidence (unpublished) that in *Fundulus,* a somewhat larger embryo, involution may not occur at all; rather, cells near but usually not just at the margin move from shallow to deeper positions as individuals, rather than in a rolling cell layer. This movement, termed ingression, could also happen in zebrafish (J. Shih and S.E. Fraser, unpublished observations), an issue for further study by high-resolution time-lapse analysis of whole cell fields of the sort done by Wood and Timmermans.

As a consequence of the inward movement, a fissure, Brachet's cleft (Ballard, 1980), becomes visible with Nomarski optics (Fig. 13), or in sectioned material, between the epiblast and hypoblast. We point out the location of the cleft in the drawing of the 75%-epiboly stage in Figure 1, although one cannot always locate it easily with the dissecting microscope (compare Figs. 11 and 13). Cells may not normally mix between the epiblast and hypoblast across Brachet's cleft (although they are able to so mix an experimental situation; see below). Cells in the two layers are streaming in different directions. Except for the dorsal region (see below), the epiblast cells generally stream toward the margin, and those reaching the margin move inward to enter the hypoblast. Then, as hypoblast cells, they stream away from the margin (Warga and Kimmel, 1990). The cells remaining in the epiblast when gastrulation ends correspond to the definitive ectoderm and will give rise to such tissues as epidermis, the central nervous system, neural crest, and sensory placodes. The hypoblast gives rise to derivatives classically ascribed to both the mesoderm and endoderm; Thisse et al. (1993) call the same layer "mesendoderm." Both names emphasize the absence of three separate germ layers at any stage during the gastrula period; only two are present. The hypoblast is only about one or two cells thick around most of the circumference of the embryo (Fig. 13), and it is presently unknown how this layer subdivides into endoderm and mesoderm.

In the manner of lineage restrictions to the EVL that occurred at sphere stage at 4 h, about an hour later many but not all DEL cells become lineage-restricted to one or another tissue or organ-specific fate. The restriction occurs about the time that gastrulation begins (Kimmel and Warga, 1987; Kimmel et al., 1990b, 1994), and as for the earlier EVL restriction, this restriction of DEL cells in the early gastrula seems unaccompanied by cell commitment (Ho and Kimmel, 1993): If DEL cells are transplanted, as single cells, from the marginal region that normally generates mesodermal or endodermal fates, to the animal pole region that normally forms ectodermal fates, they plastically regulate both their morphogenetic movements and their eventual fates, appearing indistinguishable from their new neighbors in both respects. The ability to developmentally regulate may involve dynamic regulation of the activities of zygotically expressed patterning genes: Marginal cells specifically express the gene *no tail (ntl),* the homologue of mouse *T/Brachyury,* that codes a nuclear protein (Schulte-Merker et al., 1992) essential for normal notochord development (Halpern et al., 1993; Schulte-Merker et al., 1994). Cells transplanted from the margin to the animal pole rapidly turn off *ntl* transcription, and cells transplanted in the opposite direction just as rapidly turn it on (Schulte-Merker et al., 1992). However, by the middle of gastrulation the ability of the cells to regulate so plastically seems to be lost, because single cells transplanted from the hypoblast to epiblast at this stage will rapidly leave their new positions, re-enter the hypoblast, and develop a hypoblast-derived fate appropriate for just where they end up. To exhibit this behavior, the transplanted cells have to cross Brachet's cleft, and time-lapse analysis reveals that they accomplish this unusual relocation apparently without impediment (Ho and Kimmel, 1993).

An organ- and tissue-level fate map is available for the onset of gastrulation (Fig. 14). The map is made by injecting single cells with lineage-tracer dye, and later ascertaining in what region of what organ the labeled descendants of the injected cell lie, and generally what differentiated type or types they have formed, as determined from the cell shapes, sizes, and positions. Topologically the fate map is broadly equivalent to fate maps of other chordates, notably amphibians (Keller, 1975; 1976; Dale and Slack, 1987), and also birds (Hatada and Stern, 1994) and mammals (Lawson et al., 1991). Within the DEL, primary germ layers are mapped according to latitude (position relative to the animal pole and the margin), and tissue rudiments can be located with reference to both cell latitude and longitude (the position relative to the dorsal midline). An-

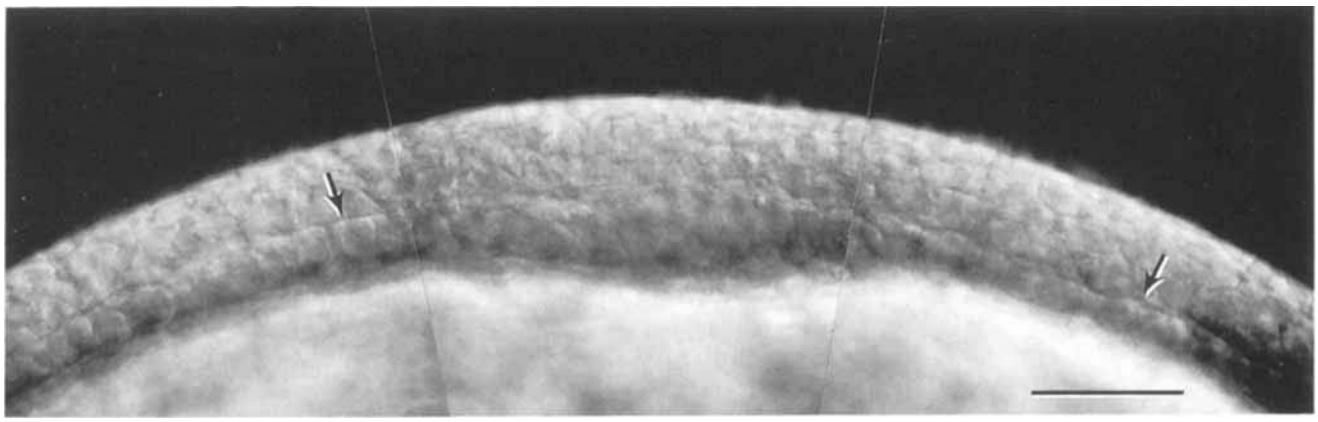

Fig. 13. The dorsal side of the blastoderm in a midgastrula embryo, at the 75%-epiboly stage. Nomarski optics. We positioned the embryo with its vegetal pole up, slightly flattened it between coverslips, and focused to obtain this optical section roughly midway between the animal and vegetal poles. Hence the view here is along the embryonic axis with midline structures at the center. The cellular blastoderm, above, covers the yolk cell, below. The EVL, vanishingly thin at this stage, is invisible (but easily visible in surface view). The arrows indicate Brachet's cleft, the distinctive boundary between the epiblast and hypoblast. The epiblast seems to be a multilayer of cells of nearly uniform thickness, but actually at this time it must be forming a single-cell layered pseudostratified epithelium (Papan and Campos-Ortega, 1994). The hypoblast is sandwiched between the epiblast and YSL. Away from the dorsal midline (e.g., in the region near the arrows) the paraxial hypoblast looks to be a monolayer of cuboidal cells. Specifically in the region of the midline Brachet's cleft is less distinct, the axial hypoblast is thickened, and it might consist of more than a single cell layer. Later, axial hypoblast will contribute to both the mesoderm (e.g., the notochord) and endoderm. Scale bar = 50 μm.

other notable feature, not apparent in the figure, is that position along the dorsal-ventral (DV) axis of the gastrula generally corresponds to later position along the anterior-posterior (AP) axis of the pharyngula. This is the case for all three germ layers; eventual AP cell positions in the spinal cord (ectoderm), muscle (mesoderm), and gut wall (endoderm) all correlate with DV cell position in the early gastrula. Morphogenesis to make this DV-AP transform is complicated and largely not understood. Consider the neurectodermal fate map: We see complexity in that not only do the more anterior neural fates map to the dorsal side of the gastrula, but also the more *ventral* cell types of the neural tube, the motoneurons and floor plate, map to the same region—the dorsal side of the gastrula (Kimmel et al., 1990b). We discuss later how dorsal cells in the gastrula eventually become ventral cells in the neural tube, but just how dorsal versus anterior fates sort out in this region of the fate map is simply unknown. Scattering of clonally related cells (and hence positionally related cells) during morphogenesis during and after gastrulation generally precludes very fine-grained mapping, but this is not always the case. For example, Stainier et al. (1993) have shown that single late blastula cells contribute progeny to either the heart's atrium or ventricle but do not scatter such that a single clone encompasses both chambers.

EVL cells neither divide (Kimmel et al., 1994) nor involute, nor do they appear to converge, at least very much, during gastrulation. They continue to flatten, and they relocate by epiboly toward the vegetal pole. Irrespective of their early positions, the EVL cells differentiate directly as periderm, an extremely flattened protective outer single-cell layer covering the entire embryo. The position of an EVL cell in the early gastrula fairly reliably predicts just where in the periderm of a later embryo a descendent clone will be located, which is useful for certain cell lineage and fate map analyses (Kimmel et al., 1990b).

Near the time that involution begins, other DEL cell movements and rearrangements occur both within the epiblast and hypoblast. During convergence, cells stream from all sectors of the blastoderm toward the dorsal side. Intercalations repack the cells in both layers. In the late blastula the intercalations were radial, and accompanied blastoderm thinning (epiboly). The new intercalations are mediolateral (Keller and Tibbetts, 1989); they effect convergent extension, a narrowing and elongation of the primary embryonic axis. As gastrulation proceeds the cells undergo many such directional intercalations, such that single-labeled clones descended from marked blastula founders become markedly spread apart. They form into long discontinuous strings of cells, oriented longitudinally (Warga and Kimmel, 1990b; Kimmel et al., 1994).

Formation of the embryonic shield visibly indicates that rapid convergence movements have begun. The shield is an accumulation and condensation of DEL cells along a local stretch of about 30° of longitude of the germ ring, and marks the future dorsal side of the embryo. Hence, when the shield forms one can reliably distinguish the orientation of the embryo's eventual DV axis. Cells involuting at the shield form the so-called axial hypoblast. Expression of the gene *goosecoid* is a reliable marker of where the shield will form, and appears to label the earliest cells to involute

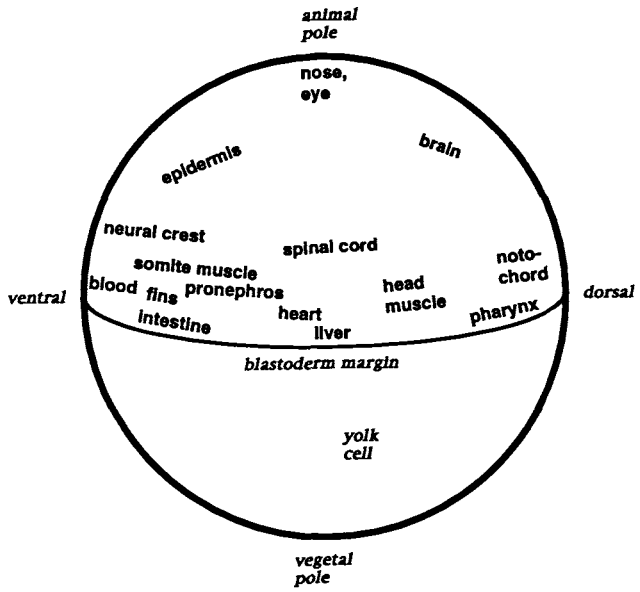

Fig. 14. Fate map of the deep cell layer (DEL) at gastrula onset, at the 50%-epiboly stage before formation of the germ ring and hypoblast. The blastoderm now has the shape of an inverted hemispherical cup overlying the yolk cell (see Figs. 1 and 11B). EVL cells contribute exclusively to the periderm, and no embryonic fates have been rigorously shown to derive from the yolk cell, including its YSL. Hence all known embryonic fates derive from the DEL, and we do not know if there is mapping at this stage according to cell depth within the DEL. Ectodermal fates map nearest the animal pole, mesoderm maps in a broad marginal ring, and endoderm overlaps this ring just at the blastoderm margin. Not all organ rudiments are shown for the sake of clarity; e.g., the hatching gland maps to a dorsal marginal position overlapping that of the pharynx. Muscle is widespread along the lateral and ventral blastoderm near the margin, and endothelium derives from a still wider mesodermal domain including all longitudes—dorsal, lateral, and ventral. Stomach, pancreas, and swim bladder map laterally, near the liver, and smooth muscle maps near the heart. The median and pectoral fins both map to or near the same ventral location. The basic outline of the map is reproduced from Kimmel et al. (1990b) with permission from Company of Biologists Ltd.; see also Kimmel and Warga (1987) for ectodermal fates and changes along the DV axis, and see Stainier et al. (1993) for the heart. R. Warga contributed unpublished fate map locations for all of the endodermal organs, smooth muscle, and the fins.

in the axial hypoblast (Stachel et al., 1993). These first cells, expressing *goosecoid,* stream anteriorward, and appear to correspond to precursors of the tetrapod prechordal plate. A principal derivative of the prechordal plate is the hatching gland, and the endodermal lining of the pharynx comes from the same region. Figure 14 does not show these fates; they lie at the margin just beneath the notochord region. Cells of the notochord rudiment, the chorda mesoderm, then begin to involute at the dorsal midline only shortly after these earliest prospective prechordal plate cells, as the embryonic shield becomes more easily visible.

Convergence and extension, involving cell mixing, and anteriorward cell migration are extreme within the embryonic shield and surrounding region. DEL cells in both layers of the early shield distribute along the entire length of the AP axis, from the pericardial region, ventral to the head, to the end of the tail. For example, axial cells in the shield epiblast can relocate anteriorward to form ventral forebrain (K. Hatta, unpublished observations), becoming new neighbors of cells originally located at the animal pole, for much of the forebrain fate maps to the animal pole of the early gastrula (Kimmel et al., 1990b). Anteriorward movement in the axial hypoblast of cells deriving from the shield is similarly remarkable: To form the hatching gland, located on the pericardium (on the yolk sac ventral to the head), prechordal plate cells must first move anteriorward along the dorsal midline. Then they move under and in front of the forebrain anlagen, where, as gastrulation ends, they form a prominent pile known as the polster (arrow at the bud stage in Figure 1 and upper arrow in Fig. 11L). Eventually the hatching gland forms on the pericardial membrane, ventral to the head (arrow at the prim-6 stage in Fig. 1). However, this last change, from a rostral to a ventral location, probably comes about with no real ventralward movement of these cells at all. Rather, head straightening that begins during the segmentation period (discussed in detail below), would serve to lift the head rudiment upward dorsally and away from the position of the hatching gland primordium, where these axial mesodermal cells might passively remain.

Axial mesoderm appears to have the potential to induce a second embryonic axis, as revealed in transplantation experiments involving cells of the embryonic shield of the early gastrula (Ho, 1992b). Hence, the embryonic shield, in terms of its inductive role demonstrated in these experiments, its dorsal marginal position in the embryo, and the fates it eventually generates, is broadly equivalent to the amphibian organizer region of Spemann.

As epiboly resumes (roughly 1½ hours after the beginning of gastrulation) and the shield extends toward the animal pole, one can clearly see that the blastoderm is prominently thicker on the dorsal side than on the ventral side (Fig. 11F–H,J). This seems to be due to the presence dorsally of axial hypoblast, for sections through the gastrula reveal that the epiblast does not appear regionally distinctive until late in the gastrula period (Schmitz et al., 1993) (R.M. Warga, unpublished observations). About midway through gastrulation, the axial hypoblast becomes clearly distinct from paraxial hypoblast, which flanks it on either side (Fig. 11I). Anterior paraxial hypoblast will generate muscles to move the eyes, jaws, and gills. More posteriorly, much of the paraxial hypoblast is present as the segmental plate that will form somites.

The dorsal epiblast begins to thicken rather abruptly near the end of gastrulation, the first morphological sign of development of the rudiment of the central nervous system rudiment, the neural plate. The thickening occurs anteriorly, and initially just at the midline, where the epiblast overlies axial mesoderm. The lateral borders of the neural plate remain morphologically indistinct at this time, in sectioned mate-

rial (Schmitz et al., 1993) as well as in the living embryo.

We define the gastrula period as ending when epiboly is complete and the tail bud has formed (Fig. 11L). However, this is purely operational, because gastrulation movements seem to continue in the tail bud after this time. DEL cells typically pass through cell cycle 15 and enter cycle 16 during gastrulation. The YSL is postmitotic, and the EVL cells typically are in a long interphase of cycle 14.

Stages During the Gastrula Period

50%-epiboly stage (5¼ h). Epiboly displaces the blastoderm margin to 50% of the distance between the animal and vegetal pole. The margin remains at about this same position for about 1 hour (Fig. 12), the duration of this stage and the next two. Hence, it is important to distinguish these early gastrula stages by examining the thickness at and along the marginal region of the blastoderm. At this 50%-epiboly stage radial intercalations have produced a blastoderm that is very uniform in thickness (Fig. 11A). In particular, an animal polar view with a dissecting microscope will reveal that the blastoderm rim is *not* yet distinctively thickened. Many DEL cells are in late cycle 14.

Germ-ring stage (5⅔ h). The germ ring forms as a thickened annulus at the blastoderm margin, as one can discern in an animal-polar view (Figs. 1, 11C; arrow). The germ ring appears nearly uniform in structure around the entire circumference of the blastoderm. Nomarski inspection, or sections of fixed embryos, reveal that within the germ ring the blastoderm consists of two layers, in addition to the EVL. The epiblast is uppermost, and is about three cells thick. The hypoblast lies beneath the epiblast, directly adjacent to the YSL. It is only about one to two cells thick. The yolk cell remains about half covered by the blastoderm (i.e., epiboly remains at 50%). Many DEL cells are completing cycle 14.

Shield stage (6 h). An animal polar view most easily reveals the embryonic shield, as well as the germ ring, if one is using a dissecting microscope (arrows in Figs. 1, 11E). A side view reveals that both the epiblast and hypoblast are locally thickened at the shield (Fig. 11D). Epiboly remains at 50% until late shield stage, when the yolk cell can be judged to be more than half covered by the blastoderm. Many DEL cells are beginning cycle 15.

Because the embryonic shield marks the eventual dorsal side of the embryo, and because cells at the animal pole will develop into head structures, one can reliably determine both the AP and DV axes for the first time. From this stage onward, because we can distinguish dorsal from ventral views, we use "side view" specifically with reference to the definitive embryonic axes.

75%-epiboly stage (8 h). Between about 60%- and 100%-epiboly we estimate the extent of epiboly for the staging index and determine the standard developmental age from the relationship in Figure 12. As epiboly continues the shape of the embryo itself becomes more along the animal-vegetal (approximately the AP) axis (Fig. 11F–J).

The embryonic shield becomes less distinctive, as compared to shield stage, as its cells repack to elongate the shield along the AP axis and narrow it mediolaterally. A ventral view reveals the anterior axial hypoblast that will develop as the prechordal plate reaches the animal pole (Fig. 11G; arrow). A side view shows that the blastoderm is thinner than elsewhere on the ventral side, above the margin (Fig. 11H; arrow). This region is the evacuation zone; cells leave it by both epiboly and convergence (Ballard, 1981). In dorsal view, the boundaries in the hypoblast between the axial chorda mesoderm and paraxial segmental plate mesoderm become visible (Fig. 11I; arrows).

90%-epiboly stage (9 h). The bit of uncovered yolk cell protruding from the neighborhood of the vegetal pole may now be considered a **yolk plug** (Fig. 11I–K). The dorsal side of the blastoderm is very distinctively thicker than the ventral side (Fig. 11J). Careful inspection with the dissecting microscope reveals Brachet's cleft between epiblast and hypoblast layers, particularly near, not just at, the dorsal midline. Cells have left the ventral region by epiboly and by convergence toward the dorsal side, leaving behind an enlarged cell-depleted evacuation zone (located approximately at 10:00 o'clock in the side view shown in Fig. 11J). The dorsal epiblast thickens anteriorly to form the neural plate (at 1:00 o'clock in the same panel), representing the brain anlagen. The prechordal plate extends just past the animal pole by 90%-epiboly (Fig. 11K). Many DEL cells are in cycle 16, and the earliest postmitotic cells are present, including cells that will form the notochord, axial somite-derived muscles, and specific neurons in the hindbrain (Mendelson, 1986).

Bud stage (10 h). Epiboly comes to a close as the blastoderm completely covers the yolk plug, defining 100%-epiboly. Convergence and extension movements have spread the blastoderm across the yolk cell faster on the dorsal side than on the ventral side, and because of this asymmetry, the point at which the yolk plug disappears is not at the vegetal pole of the yolk cell, but somewhat ventral to it.

Just dorsal to the site of yolk plug closure, and usually within 10–15 minutes of the closure, the posterior or caudal end of the embryonic axis develops a distinct swelling, the **tail bud,** for which we name the bud stage (Fig. 11L, arrowhead). This region of cells may also contribute to posterior trunk, but the contribution is not a dramatic one, whereas a labeled cell in the tail bud at 10 h invariably will contribute progeny to the tail.

Along the dorsal side, anterior to the tail bud, the neural plate is now thickened along the entire embryonic axis; its more posterior cells will contribute to trunk spinal cord. The thickening is most prominent near the animal pole in the prospective head region, where the head will form, and here the surface of the

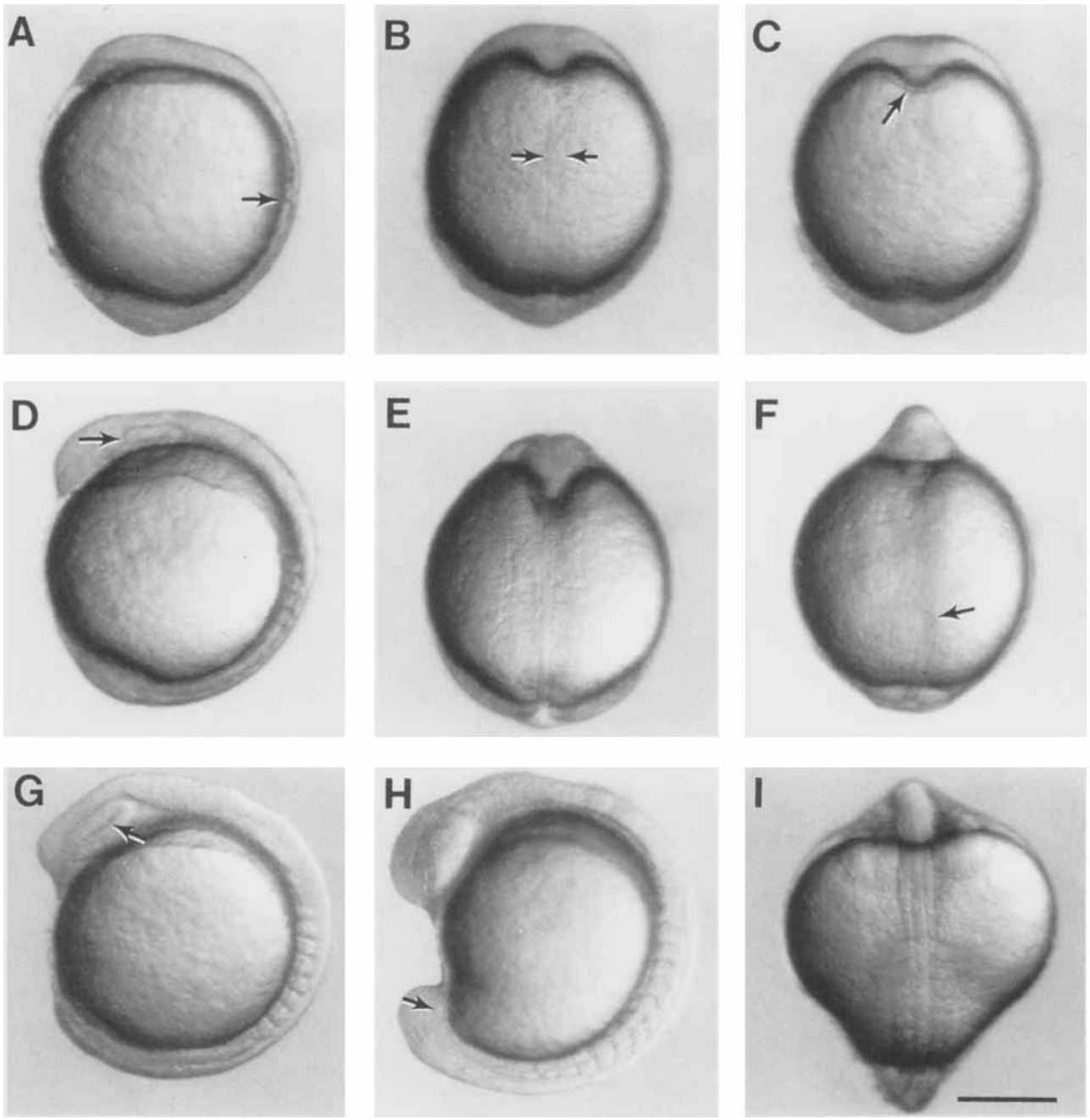

Fig. 15 A–I.

plate has a shallow midsagittal groove. Prechordal plate hypoblast accumulating deep to the anteriormost neural plate now forms a prominent bulge, or **polster** ("pillow"; arrow in Fig. 11L) of postmitotic hatching gland cells, and possibly also giving rise to other fates. The polster, along with median epiblast cells of the neural groove, begins to indent the yolk cell's surface in the embryo's midline, as can be seen by looking along the embryonic axis.

SEGMENTATION PERIOD (10–24 h)

A wonderful variety of morphogenetic movements now occur, the somites develop, the rudiments of the primary organs become visible, the tail bud becomes more prominent and the embryo elongates (Fig. 15). The AP and DV axes are unambiguous. The first cells differentiate morphologically, and the first body movements appear.

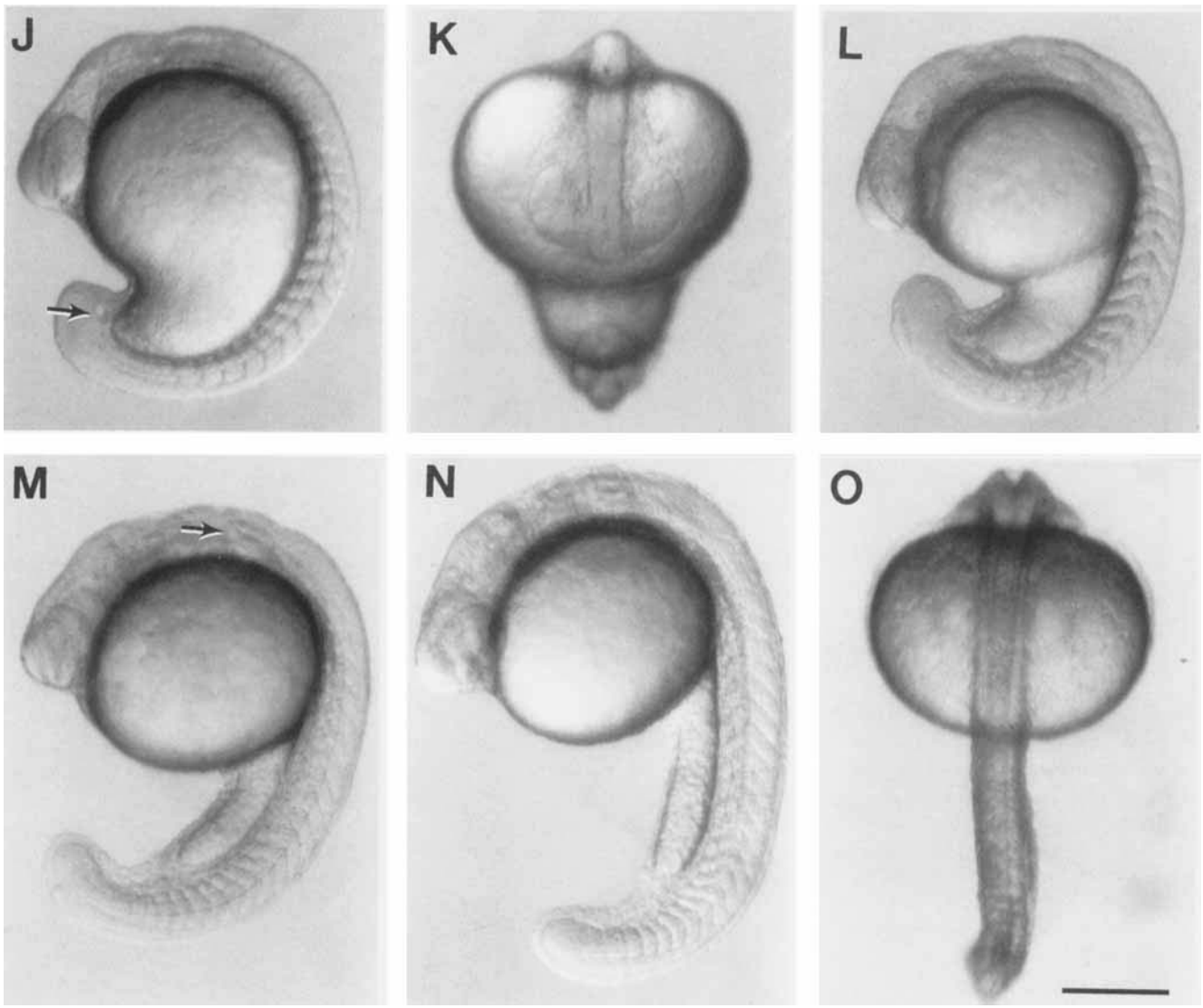

Fig. 15. Development during the segmentation period. Left side views, except where noted, with anterior up and dorsal to the left. **A:** Two-somite stage (10.7 h). Somite 2 is the only one entirely pinched off at this time, the arrow indicates its posterior boundary. Somite 1 is just developing a clear anterior boundary at this stage. **B:** Two-somite stage, dorsal view. The notochord rudiment shows between the arrows, just anterior to the level of somite 1. **C:** Two-somite stage, ventral view. The arrow indicates the polster. **D:** Four-somite stage (11.3 h). Somite 1 now has an anterior boundary. The optic primordium begins to show (arrow). **E:** Four-somite stage, dorsal view, focus is on the notochord at the level of the boundary between somites 2 and 3. Note at the top how the brain rudiment and underlying axial mesoderm prominently indent the yolk cell in the midline. **F:** Five-somite stage (11.7 h), ventral view, focus is on the newly forming Kupffer's vesicle (arrow). **G:** Eight-somite stage (13 h). The optic primordium has a prominent horizontal crease (arrow). The midbrain rudiment lies just dorsal and posterior to optic primordium. The segmental plate, developing paraxial mesoderm posterior to the somite row, is clearly delineated. **H:** Thirteen-somite stage (15.5 h). Somites begin to take on a chevron shape. The yolk cell begins to look like a kidney-bean, heralding formation of the yolk extension. The tail bud becomes more prominent and Kupffer's vesicle shows from the side (arrow). **I:** Fourteen-somite stage (16 h), dorsal view, and positioned so that the first somite pair is at the center. Note at the top the shape of the brain primordium, at the level of the midbrain. **J:** Fifteen-somite stage (16.5 h). The arrow shows Kupffer's vesicle. **K:** Fifteen-somite stage from a dorsal view to show the optic primordia. Kupffer's vesicle is also nearly in focus. **L:** Seventeen-somite stage (17.5 h). The otic placode begins to hollow. The yolk extension is now clearly delimited from the yolk ball as the tail straightens out. **M:** Twenty-somite stage (19 h). The arrow indicates the otic vesicle. **N:** Twenty-five-somite stage (21.5 h). The telencephalon is prominent dorsally, at the anterior end of the neuraxis. **O:** Twenty-five-somite stage, dorsal view. The hindbrain's fourth ventricle shows at the top. Scale bars = 250 μm.

We might have called this period the "tail bud period" because the tail bud appears at the caudal end of the lengthening axis during the whole time. Indeed, because tail morphogenesis is so prominent during this period of development, simply noting the overall shape of the embryo is a surprisingly effective way to determine its stage. Furthermore, as the tail extends, the overall body length of the embryo very rapidly in-

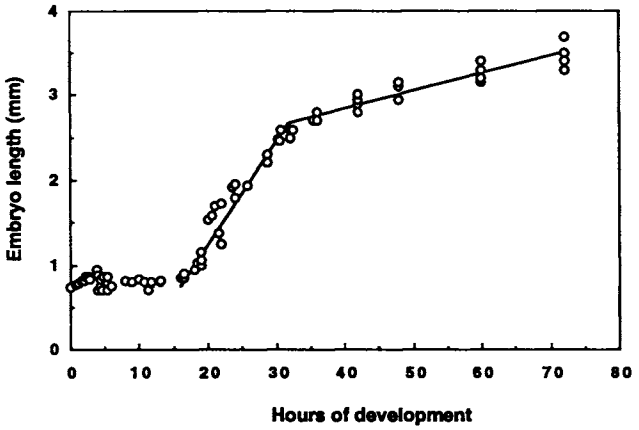

Fig. 16. Embryo length as a function of time of development (at 28.5°C). Embryo length, at any stage, refers to embryo's longest dimension. Approximately no change in length occurs during the first 16 hours (through the 14-somite stage). Tail and then head straightening produce a lengthening of about 125 μm/hr between 16 and 32 h. Then lengthening, due to growth, occurs at an approximately constant rate of about 20 μm/hr through the remainder of embryogenesis (and into the early larval period; not shown). We took the measurements with an ocular graticle, using a dissecting microscope. Each data point represents the mean length in groups of embryos (generally 5–15; not less than 3) developing together. Data from several separate experiments are included in this figure.

creases, reasonably linearly, such that length is a fairly useful staging index after about 15 h (Fig. 16). **Embryo length (EL),** at any stage, refers to the embryo's longest linear dimension. This is important to understand, for reference (to Figs. 1 and 15) will show that the tail does not extend directly opposite to the head. Rather, the extending axis (on the dorsal side) curls around the original vegetal pole, incorporating cells that were ventrally located in the gastrula, and eventually the tail bud grows toward the head. The direction reverses during the latter part of the segmentation period, for as the tail lengthens it rapidly straightens (Fig. 15L–N). Straightening of the head occurs later, for the most part during the next developmental period, the pharyngula period.

Somites appear sequentially in the trunk and tail, and provide the most useful staging index (Fig. 17). Anterior somites develop first and posterior ones last. The earliest few somites seem to form more rapidly than later ones, and we approximate the rate at 3 per hour for the first six, and 2 per hour thereafter at our standard temperature (Hanneman and Westerfield, 1989). Figure 18 shows the curve, but if one keeps in mind that 18 somites are present at 18 h and two form per hour over most of the period, then the figure is unnecessary. To accurately determine somite number use Nomarski optics, and include in the total the last (posterior-most) somite that appears to be fully segmented (see Fig. 17). The earliest furrow to form is the one posterior to the first somite, not anterior to it as as one might think. The anterior margin of the first somite becomes visible not long afterward, roughly coincidentally with the formation of somite two.

Shortly after each somite forms, its surface appears epithelial. The epithelium surrounds a more mesenchymal region (e.g., the third somite in Fig. 17A, the last two somites in Fig. 17D). The large majority of the interior cells in each somite will develop as a myotome (sometimes termed a myomere), or muscle segment (Fig. 17C; see also below, Fig. 34B). Myotomes retain the metameric arrangement of the somites, adjacent myotomes becoming definitively separated by a transverse myoseptum consisting of connective tissue.

In some vertebrates, including some teleosts, the earliest somites seem to be transient structures. However, a cell marked with lineage tracer dye in an early zebrafish somite (e.g., at the three-somite stage) produces a muscle clone in the corresponding myotome later (Fig. 19). Thus, there are no transient somites in the zebrafish; the first somite forms the first definitive myotome and so on.

The earliest cells to elongate into muscle fibers appear to derive from a part of the medial somitic epithelium, the "adaxial" region (Thisse et al., 1993) adjacent to the developing notochord, and in the middle, dorsoventrally, of each somite. The precocious subset of adaxial cells may include a special cell class, the muscle pioneers (Felsenfeld et al, 1991), recognizable by enhanced expression of specific markers (Hatta et al., 1991a). The muscle pioneers are so named because of their early development, and the name does not imply that they play any necessary morphogenetic role such as that shown for muscle pioneers in insects (Ho et al., 1984), which have many different features from the muscle pioneers in zebrafish. As the muscle pioneers elongate, the myotome takes on a chevron shape. The V points anteriorly, with the muscle pioneers present at its apex (Fig. 17C). Later a horizontal myoseptum develops at the same position.

A second derivative of the somite is the sclerotome, giving rise to vertebral cartilage. In a young somite, the sclerotome cells develop ventromedially in the somitic epithelium. Late in the segmentation period the sclerotome cells delaminate, take on a mesenchymal appearance, and migrate dorsally, along a pathway between the myotome and notochord (personal communication, B. Morin-Kensicki).

We do not know if a dermatome also develops from somitic cells.

Pronephric kidneys develop bilaterally deep to the third somite pair. They are difficult to visualize in the live preparation until later in development when they enlarge and hollow out, but their ducts, the pronephric ducts, are easy to see (Fig. 20). Each pronephric duct primordium, at first without a lumen, grows posteriorly during the early part of the period, and ventrally around the posterior end of the yolk sac extension (see below), to reach the ventral midline site near the future anus where the bilateral pair of ducts will join

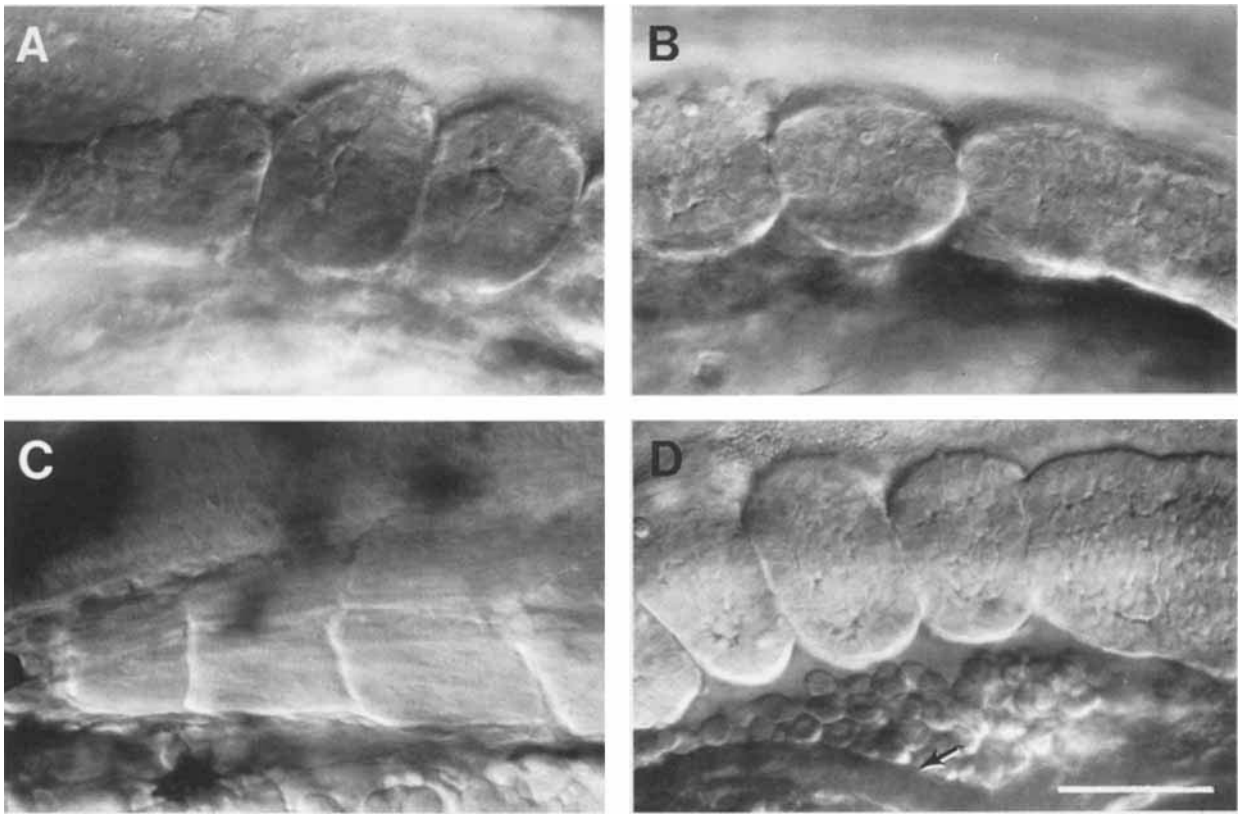

Fig. 17. Somite morphogenesis. Left-side Nomarski views, dorsal to the top, anterior to the left. **A:** The anterior-most somites (somites 1–3), at the 9-somite stage (13.5 h). **B:** The posteriormost somites, somites 8 and 9, at the same stage. The tenth somite is just beginning to form and appears as a circumscribed region, that might be called a "somitomere" (Martindale et al., 1987), within the paraxial mesodermal segmental plate. Pinching off of the posterior border of this nascent tenth somite is not yet evident; we do not count the somite for staging purposes until pinching off seems complete. **C:** Myotomes 1–3 have developed from the first three somites (compare with A) and hence we give somites and myotomes corresponding numbers. The view is of the prim-15 stage (30 h). Transverse and horizontal myosepta are prominent, and differentiated muscle fibers run obliquely through the entire length of a myotome; their cross-striations are evident. More posterior myotomes are much more prominently V-shaped (e.g., as in Fig. 34B). **D:** The last three somites at the 19-somite stage (compare with B). Somite 20 begins to pinch off; notice that the segmental plate is more epithelial-looking than earlier. The most anterior somite visible here, somite 17, is already taking on a chevron shape. The somites lie just dorsal to developing red blood cells in the blood island, which in turn is just above the rudiment of the pronephric duct at the arrow (and which does not have a lumen at this stage). The duct will open to the exterior just beneath the position that somite 19 now occupies. However, as the somites develop into myotomes they elongate considerably along the AP axis: This brings myotome 17 into the position above the end of the pronephric duct (and later the anus), by the prim-5 stage (24 h), and it brings myotome 15 to the same location by the end of embryogenesis. Scale bar = 50 μm.

together. The lumen appears, and eventually the ducts open to the outside.

The notochord differentiates, also in an AP sequence. Some of its cells vacuolate and swell to become the structural elements of this organ (Fig. 21, and compare with Fig. 34C below), and others later form a notochord sheath, an epithelial monolayer that surrounds the organ.

The endoderm becomes morphologically distinctive at about the onset of the segmentation period, as revealed in sections through the trunk (personal communication from R. Warga). At first, only a few rather disorganized-looking cells can be identified as being endodermal by their positions; they contact the YSL at or near the midline on the dorsal side of the embryo deep to the main part of the hypoblast. During this period more endodermal cells appear and form a more compact and orderly looking epithelial arrangement. Endoderm may develop on only the dorsal side of the embryo, beneath the axial and paraxial mesoderm.

The epiblast, now exclusively ectodermal, undergoes extensive morphogenesis during the segmentation period. As gastrulation ends, the primordium of the central nervous system, the neural plate, is already fairly well delineated, because of its prominent thickness. Indeed, expression of putative patterning genes, e.g., *krox20* (Oxtoby and Jowett, 1993) and *pax2* (Krauss et al., 1991) show that the neural plate is already regionalized as the segmentation period begins. The anterior region where the brain will form is particularly thick (Fig. 15B,C). Whereas the epiblast of the early and midgastrula appears several cells thick (Fig. 13), label-

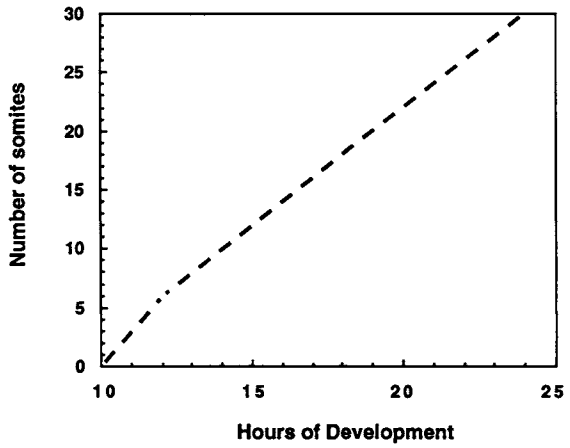

Fig. 18. Idealized rate of somitogenesis (at 28.5°C; from the data of Hanneman and Westerfield, 1989). It is useful to remember that there are 18 somites at 18 h, and the usual increase is two per hour. However, at first (between 10 and 12 h) three somites form per hour. Count only the number of fully formed somites to obtain the total.

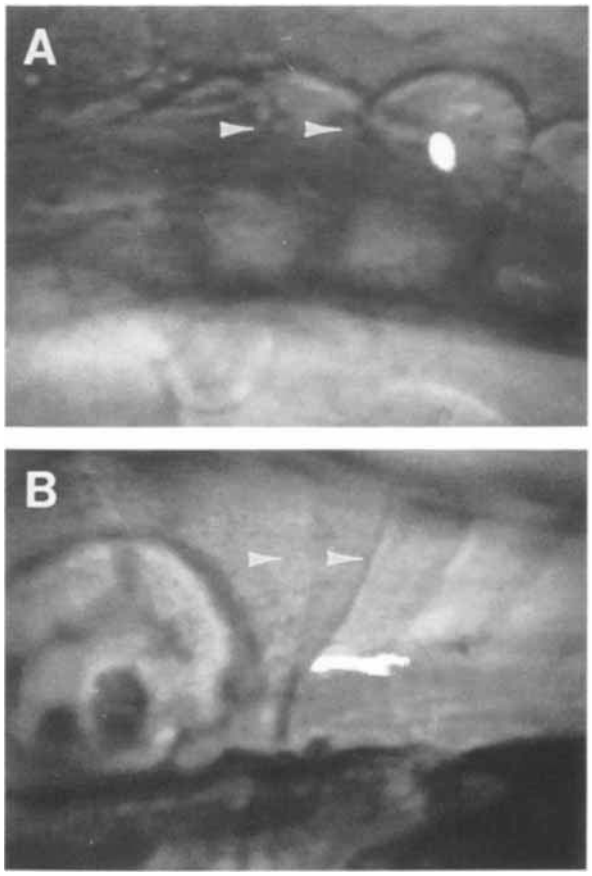

Fig. 19. Demonstration with lineage tracer that somite 3 makes myotome 3. The images combine fluorescence due to intracellularly injected rhodamine-dextran and brightfield (see Schilling and Kimmel, 1994, for method). The labeled cell in somite 3 (injected with lineage tracer at the five-somite stage in **A**) differentiates into an elongated muscle fiber spanning myotome 3 (at the protruding-mouth stage in **B**). The white arrowheads in both panels show the posterior borders of somites (myotomes) 1 and 2.

ing studies (Papan and Campos-Ortega, 1994) reveal that by the late gastrula period the epiblast becomes a monolayer, a pseudostratified epithelium. The thickness of the neural plate is due to the fact that its cells take on a columnar shape, whereas the more lateral and ventral ectodermal cells, in the epidermal primordium, remain cuboidal (diagrammed in Fig. 22A). Formation of the neural tube then occurs by a process known as "secondary neurulation," as recently studied in the zebrafish by Papan and Campos-Ortega (1994). Secondary neurulation contrasts with "primary" neurulation, the textbook version of neurulation in vertebrates where a hollow tube forms from the neural plate by an uplifting and meeting together of neural folds. In teleosts the lumen of the neural tube, the neurocoele, forms "secondarily," by a late process of cavitation. An intermediate and transient condensed primordium with no lumen, the neural keel, forms first (Fig. 15E). The neural keel rounds into a cylindrical, still solid neural rod (Figs. 15K, 21A), and only afterward hollows into the neural tube (Fig. 15O, 21B).

More covertly, primary and secondary neurulation are similar to one another (Papan and Campos-Ortega, 1994). The neural plate transforms topologically into the neural tube in fish in the same way it does in amphibians, as revealed by fate mapping in salmonids (Ballard, 1973) and zebrafish (Kimmel et al., 1990b), where it has now been studied in detail (Papan and Campos-Ortega, 1994). The medial part of the neural plate (originally from dorsal epiblast in the gastrula) forms ventral structures in the neural tube, and the lateral part of the plate (from lateral and ventral gastrula epiblast) forms dorsal tube. The similar transformation occurring in primary and secondary neurulation is due to what seems to be fundamentally similar morphogenesis; the neural keel develops by a process of epithelial infolding at the midline, equivalent to the folding of the plate in primary neurulation of amphibians (Papan and Campos-Ortega, 1994). The cells remain epithelial throughout neurulation in both types. They converge toward the midline, and then, in the zebrafish, they tip obliquely on both sides of the midline in a manner that indicates infolding (Fig. 22B), paralleling the neural folds in primary neurulation. The original outer surfaces, the apical ones, of the epithelial cells from the left and right sides of the neural plate then meet to form the midline of the developing neural keel, and subsequently the midline of the neural rod (Fig. 22C). It is then that these apical surfaces, rather late during the segmentation period, pull away from one another to form the neurocoele. This process begins at the floor plate (Fig. 21), a distinctive row of cells occupying the neural primordium's ventral midline (Hatta et al., 1991b).

Because the times of neurulation and segmentation

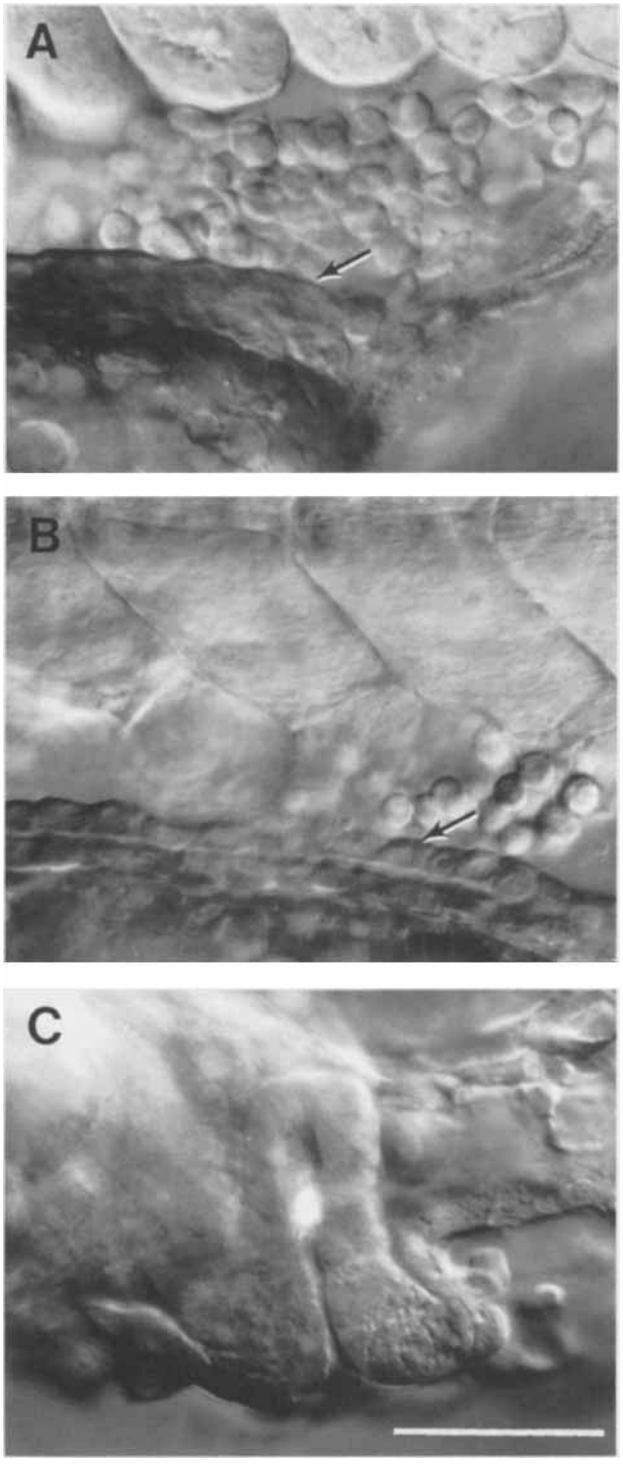

Fig. 20. Pronephric duct morphogenesis near the region where the anus forms. Left side Nomarski views, dorsal to the top, anterior to the left. **A:** At the 21-somite stage (19.5 h) the pronephric duct (arrow), not hollow at this time, courses around the posterior end of the yolk extension. The blood island, just above, is posterior to the site where the duct will open to the outside, and just ventral to the somites. **B:** By the prim-5 stage (24 h) the pronephric duct (arrow) has a lumen all along its length. **C:** The duct opens to the outside. A bright crystalline inclusion is present within it; this is not unusual to see. Scale bar = 50 μm for A,B, 39 μm for C.

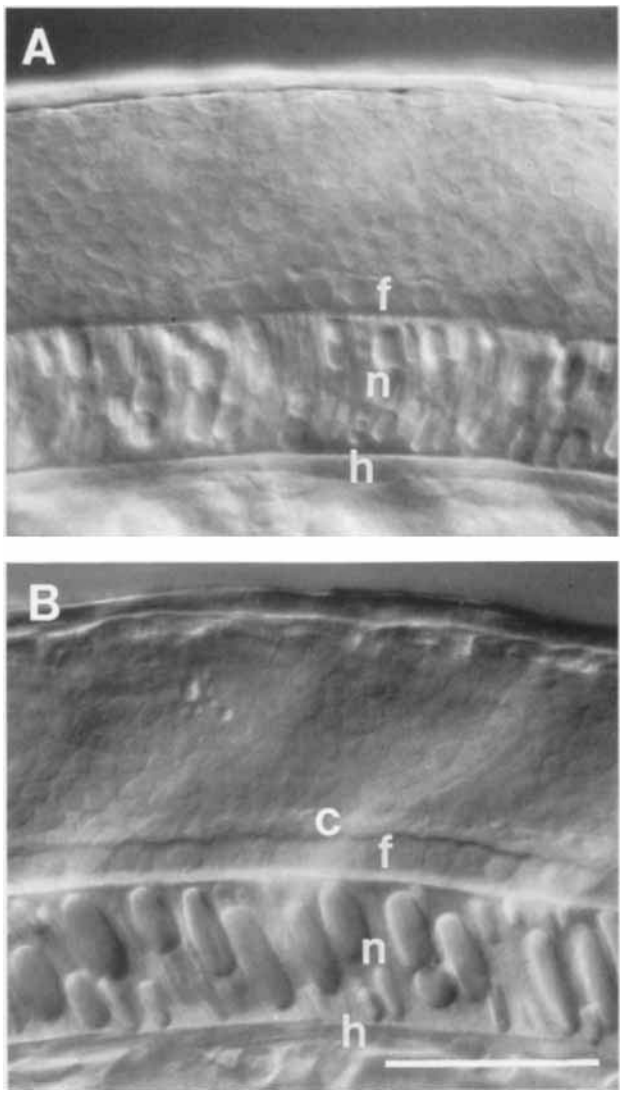

Fig. 21. The neural tube forms by cavitation. Matched left side Nomarski views (at the AP level of somite 9) focused at the midline with dorsal to the top and anterior to the left. The floor plate (f) of the developing spinal cord lies immediately dorsal to the notochord (n), which in turn is dorsal to the hypochord (h). **A:** Cavitation of the neural rod just begins at the 18-somite stage (18 h), as the floor plate develops a distinctive dorsal boundary. **B:** The central canal (c) then rapidly appears at this location. 21-somite stage (19.5 h). Notice the enlarging vacuoles within the notochord cells at the same time. Figure 34C shows a later stage in these developments. Scale bar = 50 μm.

overlap so extensively the zebrafish does not have a distinct "neurula period" of development, such as occurs largely before segmentation in amphibian embryos. Another prominent difference between zebrafish and *Xenopus,* revealed by labeling studies, is that in the amphibian one side of the neural plate forms the corresponding lateral wall of the neural tube, whereas in the zebrafish cell divisions occurring in the midline during keel formation (typically division 16; Kimmel et al., 1994) often distribute sister cells originating from

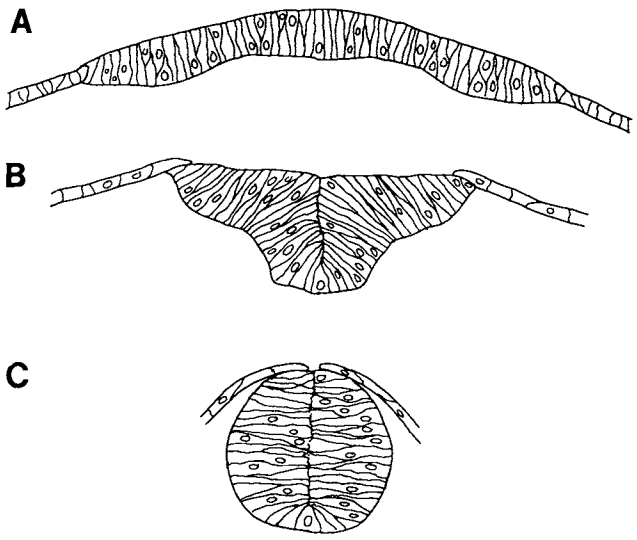

Fig. 22. Early morphogenesis of the neural primordium. Diagrammatic transverse sections, redrawn from Papan and Campos-Ortega (1994). The neural plate (**A**, ca. 10 h) develops into the neural keel (**B**, ca. 13 h) by infolding at the midline. The keel in turn rounds into the cylindrical neural rod (**C**, ca. 16 h).

one side of the neural plate to both sides of the neural tube. We presently do not understand the significance of this redistribution.

Even before cavitation, the anterior part of the neural keel that will form the brain undergoes regional morphogenesis. At the beginning of the segmentation period, the brain rudiment, although larger than the spinal cord rudiment, appears uniform along its length (Fig. 23A). Then, during the first half of the segmentation period, about ten distinctive swellings, termed neuromeres, form along it (Fig. 23B). The first three are large, and become prominently sculptured. They correspond to the two forebrain subdivisions, the diencephalon and telencephalon, and the midbrain or mesencephalon. Additionally, the rudiments of the eyes, the optic primordia, develop very early from the lateral walls of the diencephalon (Figs. 15D, 24), eventually giving a very lovely arrowhead-like shape to the brain rudiment in dorsal view (Fig. 15K). During the last part of the segmentation period the ventral diencephalon expands as the primordium of the hypothalamus, and the primordium of the epiphysis appears as a small, well-delineated swelling in the midline of the diencephalic roof (Fig. 23C). The midbrain primordium subdivides horizontally to form the dorsal midbrain (optic) tectum and the ventral midbrain tegmentum (see below, Fig. 30B).

The remaining seven neuromeres, termed rhombomeres (r1–r7), subdivide the hindbrain (Figs. 23B,C, 25). The primordium of the cerebellum forms near the end of the period as a very prominent dorsal domain in the region of the hindbrain-midbrain boundary.

Associated with the neural primordium are changes in its periphery. Neural crest, its early position indicated by expression of the homeobox gene *dlx3* (Akimenko et al., 1994), delaminates and migrates from the dorsolateral wall of both the brain (Fig. 26) and spinal cord primordia, beginning at neural keel stage, and continuing well after the tube has appeared. Just adjacent to the keel, thickened ectodermal placodes appear bilaterally at specific locations, also predicted by *dlx3* expression (Akimenko et al., 1994) within the head region, and later form sensory tissues (Figs. 26, 27). They include the olfactory placode overlying the telencephalon, the lens placode, associated with the optic primordium, and the otic (ear) placode overlying rhombomere 5 of the hindbrain (Figs. 25, 27).

Following closely upon the early morphogenesis of the neural tube, the first neurons begin to differentiate, and in comparison with what will come later the pattern of cells and axonal pathways is not overwhelmingly complicated. So far as we know all of the early developing cells, termed "primary neurons" (Grunwald et al., 1988), develop large cell bodies, and extend long axons that project between different regions of the neural tube (e.g., between the hindbrain and spinal cord), or, in the cases of sensory neurons and motoneurons, between the neural tube and the periphery. Early sensory neurons, which will mediate tactile sensibility, are located bilaterally both in a discontinuous dorsal column in the spinal cord (Rohon-Beard cells) and in a ganglion (trigeminal) in the head. Beginning at about 16 h the peripheral sensory axons extend to blanket the skin, and the central axons from the same neurons pioneer a single long tract located dorsolaterally along the wall of the neural tube (Metcalfe et al., 1990). Motoneurons differentiate in the ventral spinal cord only slightly later (Eisen et al., 1986; Myers et al., 1986). A marvelous feature of their development is that as individual motor axons grow out to meet the developing myotomal muscle cells, the axons elicit contractions in the muscle, presumably by transmitter release from the growth cones (Grunwald et al., 1988). Hence at this time an observer can very easily appreciate just where these neurons are in their development. The primary motoneurons have been particularly well studied. There are three, and sometimes four (Eisen et al., 1990), of them in each spinal hemisegment, and their axons grow without error along precise pathways to innervate restricted domains within the overlying myotome (Myers et al., 1986). By carrying out meticulously timed transplantations of single postmitotic cells to new locations in the ventral spinal cord, Eisen (1991) has shown that position of the motoneuronal cell body plays a crucial role in specification of its identity, which becomes fixed 1–2 hours before axonogenesis.

The centrally located interneurons form a relatively simple pattern at first, one that is clearly related to the neuromeric organization of the neural tube. Bilateral pairs of single interneurons or small clusters of them begin to differentiate at the centers of each of the brain neuromeres indicated in Figure 23B (reviewed in Kim-

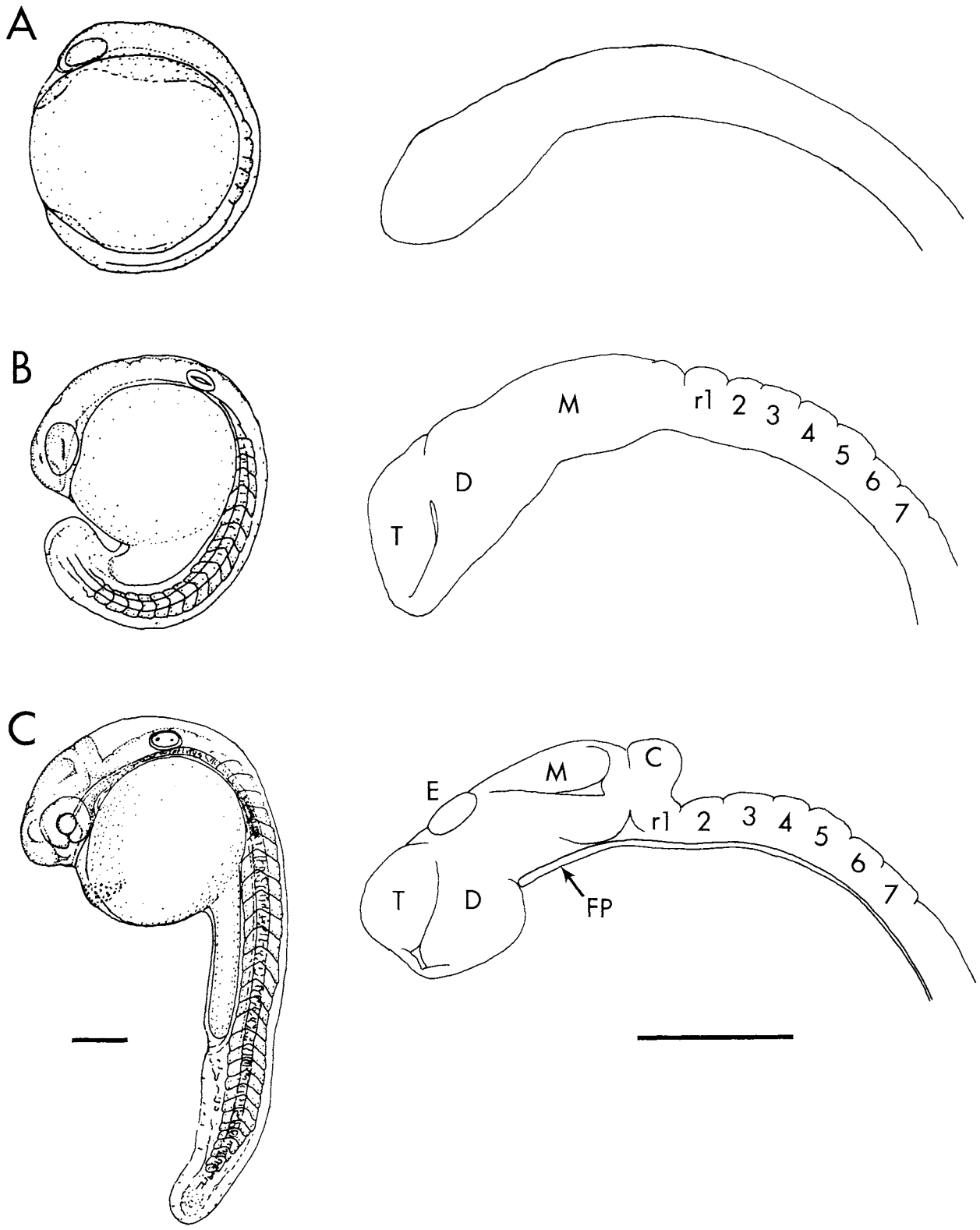

Fig. 23. Sculpturing of the brain rudiment during the segmentation period. **A:** We do not see morphological subdivisions at the six-somite stage (12 h). **B:** By the 18-somite stage (18 h) about ten neuromeres have developed—the telencephalon (T), diencephalon (D), mesencephalon (M), and about seven hindbrain rhombomeres (r1–r7). **C:** At prim-5 (24 h) the epiphysis (E) is present in the midline of diencephalic roof, and the ventral diencephalon has expanded as the rudiment of the hypothalamus. The dorsal midbrain, or tectum (M), is now partitioned from the ventral midbrain, or tegmentum. The cerebellum (C) is evident at the hindbrain/midbrain boundary region. The floor plate (FP) extends in the ventral midline up to, but not including the forebrain. Reproduced, with permission, from Kimmel (1993), © 1993, Annual Reviews Inc. Scale bars = 200 μm.

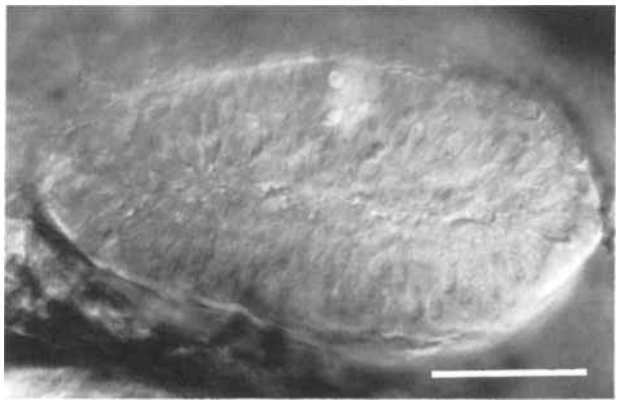

Fig. 24. The optic primordium is well formed at the nine-somite stage (13.5 h). Left-side Nomarski view, dorsal to the top, anterior to the left. In the fashion of the neural rod itself, the optic primordium is a solid tissue at this time, not a hollow vesicle. A hint of a seam runs across it that precedes development into the optic cup. Scale bar = 50 μm.

mel, 1993), and in each segment of the spinal cord (Bernhardt et al., 1990). Primary interneurons in both the spinal cord and hindbrain are individually identifiable. The timing of interneuronal development is generally not known as precisely as for the sensory neurons and motoneurons, but the earliest central axons appear at nearly the same stage as the peripheral ones. These central axons form a simple scaffold, organized orthogonally (Wilson et al., 1990; Chitnis and Kuwada, 1990; Metcalfe et al., 1990): A primary bilateral pair of ventral longitudinal tracts extend through the length of the brain and spinal cord, with the two sides connected by commissural axons crossing the midline. Each set of interneurons, or in the hindbrain and spinal cord each individual interneuron, pioneers a part of this system or joins to it in a way that is highly stereotyped (e.g., Wilson and Easter, 1991), apparently matching the precision of motor axonal pathfinding in the periphery. Notably, when and where the cells develop and where their axons extend correlate closely with the spatial domains and temporal patterns of expression of regulatory genes, including genes of the *pax, krox, eph, forkhead,* and *wnt* families (Macdonald et al., 1994; Krauss et al., 1991; Oxtoby and Jowett, 1993).

Function follows upon morphological development of the neuronal systems, and the early pattern of synaptic interconnections between the neurons seems also to be very precise. In a particularly clear example, an identified dendrite of a specific interneuron, the Mauthner neuron located in the hindbrain's fourth rhombomere, begins to extend late in the segmentation period (18 h), nearly simultaneously with the arrival to it of a set of axonal growth cones coming from trigeminal sensory neurons. As the dendrite begins its outgrowth it tightly envelops the small bundle of growing sensory axons, and at that location specifically, just at the base of a dendrite which eventually becomes quite long, synapses are made (Kimmel et al., 1990a). This connection appears to be a key one in a reflexive relay between primary sensory neurons in the head and primary motoneurons in the spinal cord, to which the axon of the Mauthner cell projects. The behavioral reflex, a motor response to a light touch to the head, becomes apparent a few hours later.

Ventrolaterally to the brain primordium, and largely posteriorly to the eye, a primordium appears that will form the series of pharyngeal or visceral arches. Including an inner epithelial lining of pharyngeal endoderm, the pharyngeal arches derive from all three germ layers, head neural crest contributing prominently to the arch mesenchyme (Schilling and Kimmel, 1994). Both morphogenesis and differentiation of the pharyngeal walls occur most dramatically later, during the hatching period.

The pharyngeal arches and rhombomeres are visible components of the head segments, as the somites are compontents of the trunk and tail segments. Early head mesoderm might also be segmentally organized, but we have no evidence for it. Head mesodermal condensations and vesicles, such as described classically as "preotic somites" from sections of embryos of sharks and other kinds of fish, have not been found in teleost embryos, as confirmed in a recent reinvestigation (Horder et al., 1993). On the other hand, head mesodermal "somitomeres" were characterized in an SEM study of the medaka, *Oryzias* (Martindale et al., 1987), a teleost fish distantly related to the zebrafish. Head mesodermal segments, if present in early zebrafish embryos, are not readily visible in live material.

Stages During the Segmentation Period

One-somite stage (10⅓ h). The first somitic furrow forms, usually, but not invariably, after both completion of epiboly and the initial appearance of the tail bud (Fig. 15A). This furrow marks the boundary between what will become the first and second somites. Viewing the embryo along the axis from the anterior pole reveals the now very prominent polster deep to the neural plate (Fig. 15C, arrow).

Five-somite stage (11⅔ h). The first five to six somites appear at the rate of about three per hour. The length of the embryo is about 0.8 mm, the same as the zygote.

The brain primordium has now distinctively thickened into the neural keel (Fig. 15E,F), and beginning at the four- or five-somite stage one can first distinguish the **optic primordium** from a side view (Figs. 15D, 24) or a dorsal view. In the trunk the neural plate is still present, and sections reveal that it has three pronounced thickenings at this stage, a bilateral pair flanking a median one. Neural keel formation occurs in the anterior trunk between the six- and ten-somite stages (Schmitz et al., 1993).

Kupffer's vesicle makes its appearance deep to the tail bud (Fig. 15F, arrow; Fig. 28B) This structure, found only in teleost embryos, is transient, and its sig-

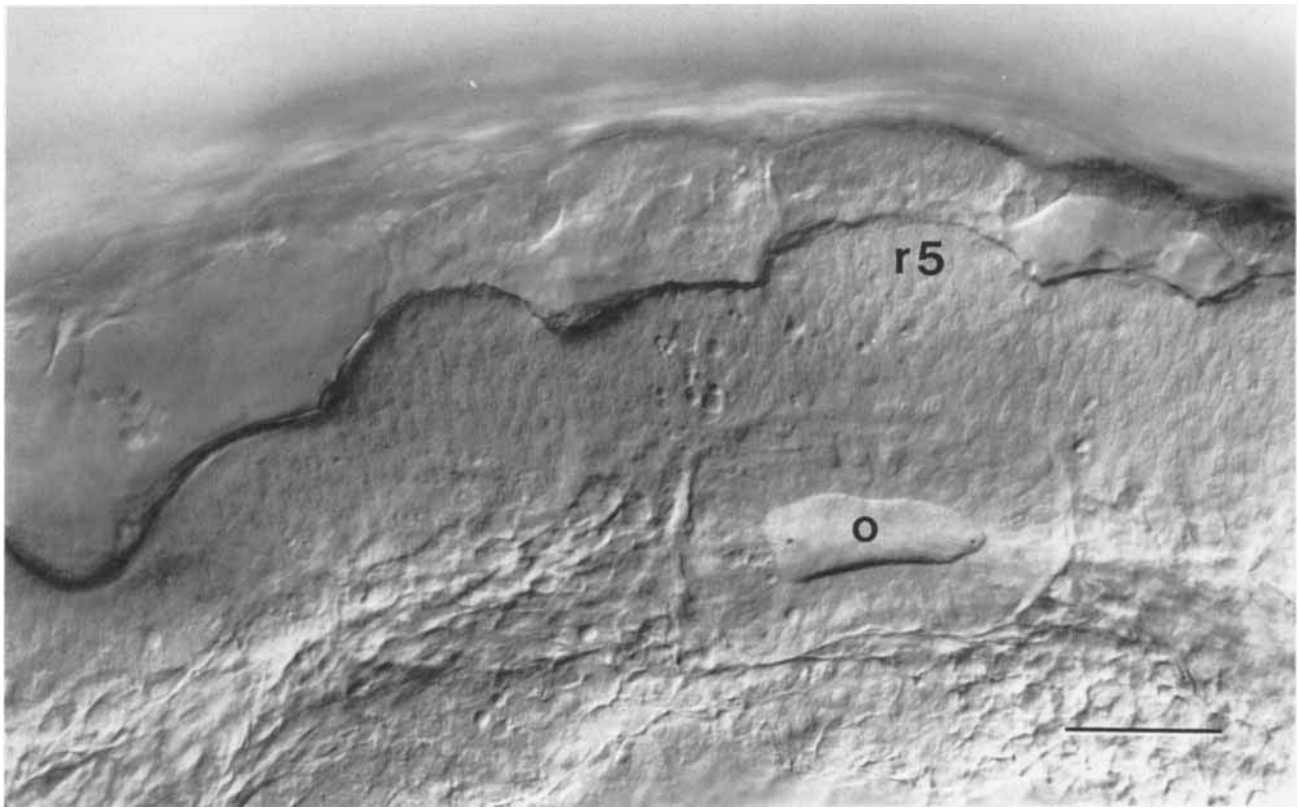

Fig. 25. Rhombomeres 2–6 at the 18-somite stage (18 h). Left-side view with dorsal to the top and anterior to the left. The odd-numbered rhombomeres, 3 and 5, are larger than the even-numbered ones, and in this embryo all of the rhombomeres are exceptionally prominent. The Nomarski view focuses on the left wall of the hindbrain, and the right wall is also visible behind it. The hindbrain roof opens just before this stage, forming the now large fourth ventricle between the two brain walls. The left hollow otic vesicle (o), containing two tiny newly forming otoliths, is visible beside the brain at the level of rhombomere 5 (r5). Mesenchyme of the pharyngeal arch primordia lies more ventrally (see Fig. 31). From Hanneman et al. (1988). Scale bar = 50 μm.

nificance has been debated in the older literature. Kupffer, who discovered it, thought it might be an allantoic rudiment (see Brummett and Dumont, 1978). Recent fate mapping studies show that the epithelial cells lining the vesicle will later form tail mesodermal derivatives, including notochord and muscle (Melby et al, 1993).

By the eight-somite stage Nomarski optics reveal the early rudiment of the pronephros, and migration of cephalic neural crest cells.

14-somite stage (16 h). Extension of the tail rudiment barely begins to elongate the embryo (Figs. 15H,I, 16); its length (EL) is about 0.9 mm. The small trigeminal placode (Fig. 26A) and more distinctive **otic placode** (Fig. 27A) are present beside the hindbrain rudiment, the latter about midway between the optic vesicle and the first somite. One can readily distinguish four prominent subdivisions of the brain, the telencephalon, diencephalon, midbrain, and hindbrain. The fourth ventricle barely begins to inflate the dorsal hindbrain, and five rhombomeres, r2–r6, become visible in a dorsolateral view (Fig. 25). Rhombomere r5 lies deep to otic placodes. In the trunk the neural keel rounds into the neural rod, still without a cavity, but now overridden by adjacent epidermis (Papan and Campos-Ortega, 1994). Neural crest migration is underway in both the head (Fig. 26; Schilling and Kimmel, 1994) and the trunk (Raible et al., 1992; Raible and Eisen, 1994).

Somites now form at a rate of about two per hour (Fig. 18), and older ones begin to develop the myotomes. They take on the V-shaped appearance that indicates the future division of the myotomes into the dorsal (epaxial) and ventral (hypaxial) muscle masses (Fig. 17C). In the center of the anterior myotomes a view with polarized light reveals early birefringence, owing to myofibrillar development, of two to six elongated differentiating muscle pioneer cells (Felsenfeld et al., 1991).

The notochord becomes more distinguishable from the ventral part of the neural keel, as can be appreciated in a dissecting microscope view along the axis. With Nomarski optics one can see that the notochord cells show a characteristic "stack-of-pennies" appearance (Fig. 21, also see Fig. 28C for the tail tip at a later developmental stage).

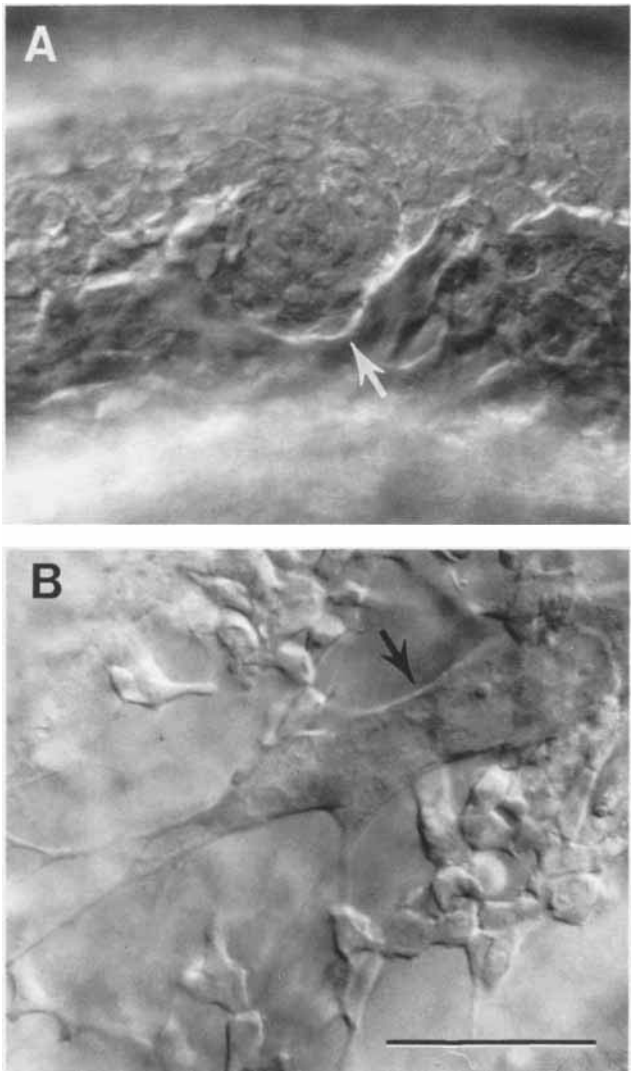

Fig. 26. Cells of the trigeminal placode (arrow in **A**, the 9-somite stage at 13.5 h) will form sensory neurons of the trigeminal ganglion (arrow in **B**, 18-somite stage at 18 h). Peripheral axons are visible to the lower left. Left-side Nomarski views, dorsal to the top, anterior to the left. The primordium is located dorsolateral to the hindbrain between the optic and otic primordia. Cranial neural crest cells are visible migrating near the trigeminal primordium at both stages. Scale bar = 50 μm.

A characteristic constriction that is important for staging appears in the posterior region of the yolk, where the tail bud ends, and gives the yolk a kidney bean shape (Fig. 15H). The constriction rapidly becomes more prominent (Fig. 15J) and squeezes progressively more anteriorwards (Fig. 15L). The constricted region develops into the thinner and cylindrically shaped posterior elongation of the yolk sac, the **yolk extension** (Milos and Dingle, 1978). The shape of the yolk extension will continue to distinguish it from the anterior region, the **yolk ball.**

The tail bud now begins to protrude away from the body of the embryo, and Kupffer's vesicle is a prominent feature at its base (Figs. 15H,J (arrow), K, 28B).

20-somite stage (19 h). Morphogenesis associated with the constriction of the yolk begins to straighten out the posterior trunk, and this, along with continued development of the tail, produces a marked increase in the length of the embryo to an EL of 1.4 mm (Fig. 15M). The length of the yolk extension is now more than half the diameter of the yolk ball. The lens placode appears and the otic placode hollows into the **otic vesicle** (Figs. 15M (arrow), 25, 27B) which contains two otoliths that are so tiny at this time that Nomarski optics must be used to see them (Fig. 25). The brain now also becomes a hollow structure, with ventricles present along its length, and with Nomarski optics one can first recognize the rudiment of the cerebellum. Seven rhombomeres are much more prominent in some embryos than others (compare Fig. 25 with Fig. 30A, below). Hollowing from the neural rod into the neural tube is also now nearly complete throughout the length of the trunk. The primordium of the postotic or posterior lateral line resides as an ectodermal placode between the otic vesicle and the first somite. A substantial part of the primordium will soon begin to migrate posteriorly, and will be important for staging, as we describe below. Neurons, including spinal primary motoneurons, trigeminal ganglion neurons (Fig. 26B), and Rohon-Beard neurons, have growing axons.

Nearly all of the trunk somites now exhibit the myotomal chevron shape, and the trunk myotomes produce weak **muscular contractions.** Nomarski reveals that anterior muscle pioneers have cross-striations. The first contractions, occurring at the 17-somite stage, involve individual (unilateral) myotomes, and, as mentioned earlier, are correlated with the ingrowth of axons from first developing primary motoneurons (Hanneman and Westerfield, 1989). Progressively the contractions begin to involve series of myotomes and become stronger, more coordinated, and more frequent.

Anterior notochord cells have vacuoles (Fig. 21). The pronephric duct extends through the whole length of the trunk and curves ventrally around the yolk extension, showing where the anus will eventually develop in the ventral midline at the level of somite 17, and serving to define the boundary between the trunk and tail. (Later, because of morphogenetic rearrangements, the position of the anus shifts to the level of somite 15.)

Just posterior and dorsal to the end of the pronephric duct in the ventral tail rudiment, mesenchyme accumulates in a so-called intermediate mass of mesoderm, the early forerunner of the hematopoietic blood island (Figs. 17D, 20A).

26-somite stage (22 h). At this stage EL = 1.6 mm. Straightening of the posterior trunk is nearly complete, but the elongating tail still curves ventrally (Fig. 15N,O). The yolk extension is now nearly the length of the yolk ball. The cerebellar primordium is prominent, and one can recognize the rudiments of both the epiphysis and hypothalamus in the diencephalon (Fig. 23C). The olfactory placodes thicken anterior and dorsal to the forebrain, and one can now easily see the two

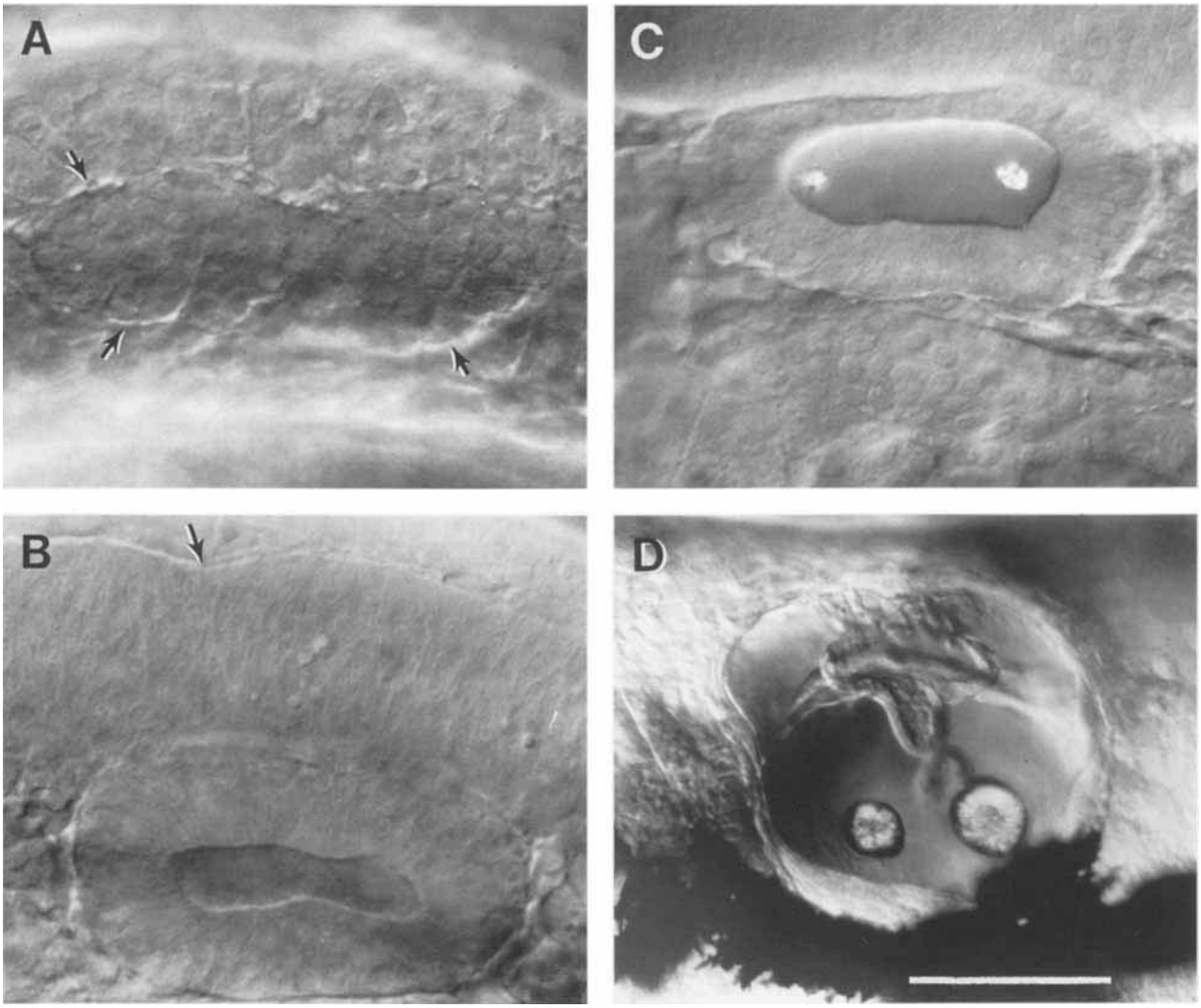

Fig. 27. Morphogenesis of the otic vesicle. Left-side Nomarski views, dorsal to the top, anterior to the left. **A:** The primordium (outlined by arrows) of the inner ear appears as a solid otic placode beside the hindbrain by the nine-somite stage (13.5 h). **B:** At the 19-somite stage (18.5 h) the placode has hollowed out into the otic vesicle. The arrow indicates the boundary between rhombomeres 4 and 5 along the dorsolateral wall of the hindbrain. **C:** Otoliths become prominent in the otic vesicle by the prim-6 stage (25 h). **D:** Pec-fin stage at 60 h. Morphogenesis of the walls of the vesicle have formed the primordia of the semicircular canals dorsally, separated from otolith-containing chambers ventrally. By this time the vesicle is becoming housed in a refractile cartilaginous capsule. The dark shadows to the bottom are out-of-focus melanophores. Scare bar = 50 μm for A–C, 100 μm for D.

otoliths in each otic vesicle with just the dissecting microscope. With Nomarski optics the early posteriorward migration of the posterior lateral line primordium is evident; the advancing tip of the primordium is located over the third somite (hence, as will be explained below, we might call this stage the prim-3 stage).

The last somites of the series form more slowly than the others (not shown in the idealized curve of Fig. 18), and the total number that eventually forms is variable, from 30 to 34 pairs. The blood island is now a distinctive nest of dividing and differentiating blood cells. The rudiment of the unpaired median finfold appears in the dorsal midline, along the length of the tail (Fig. 28C), sometimes at 22 h, but more frequently at 23 h (28-somite stage).

The spontaneous myotomal contractions now produce a lashing from side to side, and their frequency increases transiently upon dechorionation.

PHARYNGULA PERIOD (24–48 h)

Ballard (1981) coined the term "pharyngula" to refer to the embryo that has developed to the phyolotypic stage, when it possesses the classic vertebrate bauplan. According to von Baer's famous laws (discussed by Gould, 1977) this is the time of development when one can most readily compare the morphologies of embryos of diverse vertebrates, and for the zebrafish we approx-

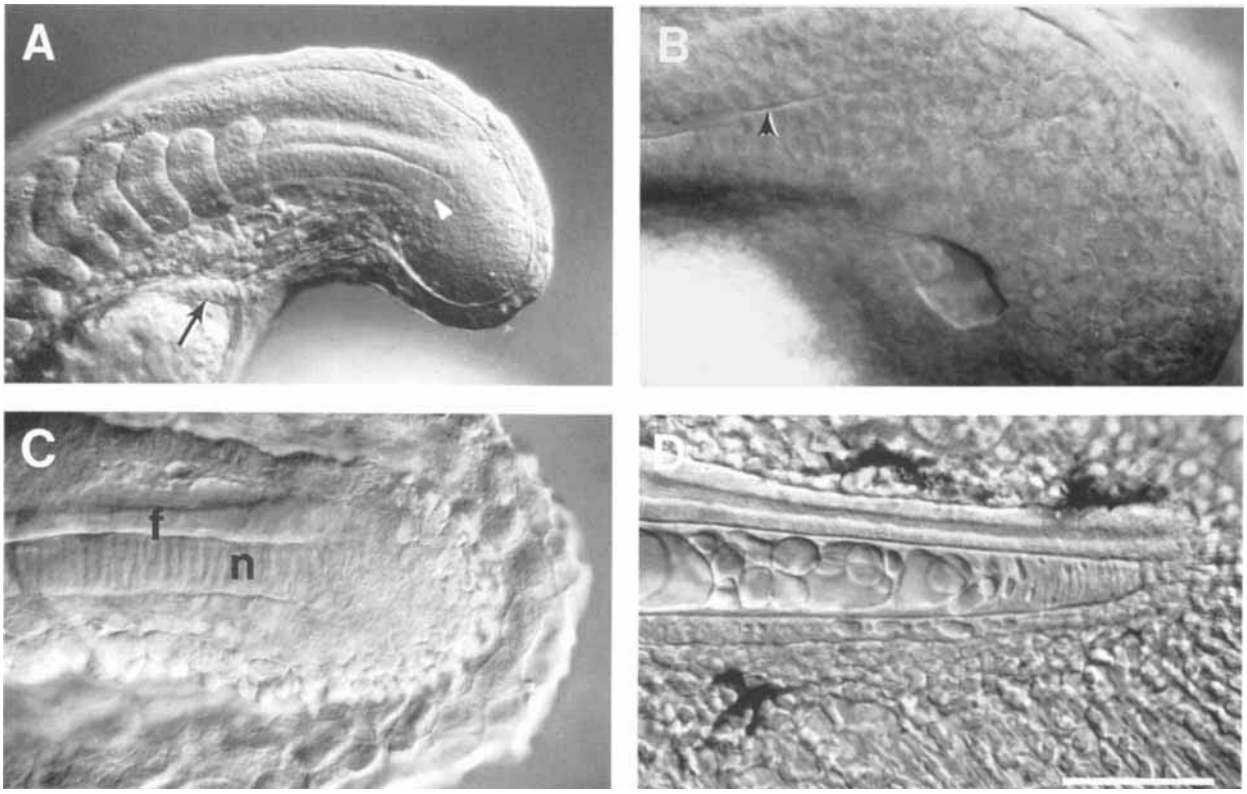

Fig. 28. Tail development. Left side Nomarski views, dorsal to the top, anterior to the left. **A:** Overview at the 21-somite stage (19.5 h). Notice how the primordia of the notochord (white arrowhead) and the spinal cord just dorsal to it spring from the tightly packed tail bud mesenchyme. These tissue primordia lie medially to the segmental plate paraxial mesoderm. The arrow shows the pronephric duct near its end, just posterior to the yolk extension. **B:** Kupffer's vesicle, in the midline at the 16-somite stage (17 h). The arrowhead shows the boundary between the primordia of the notochord (below) and spinal cord (above, not hollow at this time). **C:** By the prim-5 stage (24 h) the tail bud is very small, and is surrounded by the tail fin primordium, the median fin fold. The notochord primordium (n) has the characteristic transient "stack of pennies" appearance. The spinal cord floor plate (f) is a distinctive midline cell row sandwiched between the notochord and the neural tube lumen (the central canal). **D:** The tail bud disappears entirely (high-pec stage at 42 h). The tail spinal cord narrows to a blind-ended tube with a simple cuboidal lining. The cuboidal cells have cilia (not visible here) that are motile and protrude into the central canal. The notochord presents a neat developmental sequence of vacuolization, beginning with the stack of pennies stage at its posterior end. A distinctive midline hypochord underlies the notochord. Rays of actinotrichia are present in the fin fold that surrounds the entire structure, and melanophores (black) are differentiating. Scale bar = 125 μm for A, 50 μm for B–D.

imate the period as the 2nd of the 3 days of embryonic development (Fig. 29). The embryo is most evidently now a bilaterally organized creature, entering the pharyngula period with a well-developed notochord, and a newly completed set of somites that extend to the end of a long post-anal tail. The nervous system is hollow and expanded anteriorly. With the rapid cerebellar morphogenesis of the metencephalon (Fig. 30A), just preceding the pharyngula period, the brain is now sculptured into five lobes (Fig. 23C).

The period name focuses attention on the primordia of the pharyngeal arches, present but at early times difficult to distinguish individually. The pharyngeal arches develop rapidly during this 2nd day from a primordial region that can be visualized ventral to, and about twice as long as the otic vesicle (Fig. 31). Seven pharyngeal arches in all develop from this primordium, a prominent boundary within it (arrow in Fig. 31) occurring between pharyngeal arches 2 and 3. This boundary is important, for later the arches anterior to it (the mandibular and hyoid arches) form the jaws and the operculum, and arches (branchial arches) posterior to it will form the gills.

The cells of the hatching gland, with their brightly refractile cytoplasmic granules, are prominent features of the pericardial region throughout the pharyngula period (Fig. 32).

During the first few hours of the pharyngula period the embryo continues the rapid lengthening that started at 15 h, but then the rate of lengthening abruptly decreases. The time of the change, at 31–32 h, correlates approximately with the end of the rapid morphogenetic straightening of the tail, discussed above. The new rate of lengthening is maintained throughout the rest of embryogenesis (Fig. 16).

The head also straightens out. It lifts dorsalward fairly rapidly during the pharyngula period and then more slowly, and one can use this change to quickly

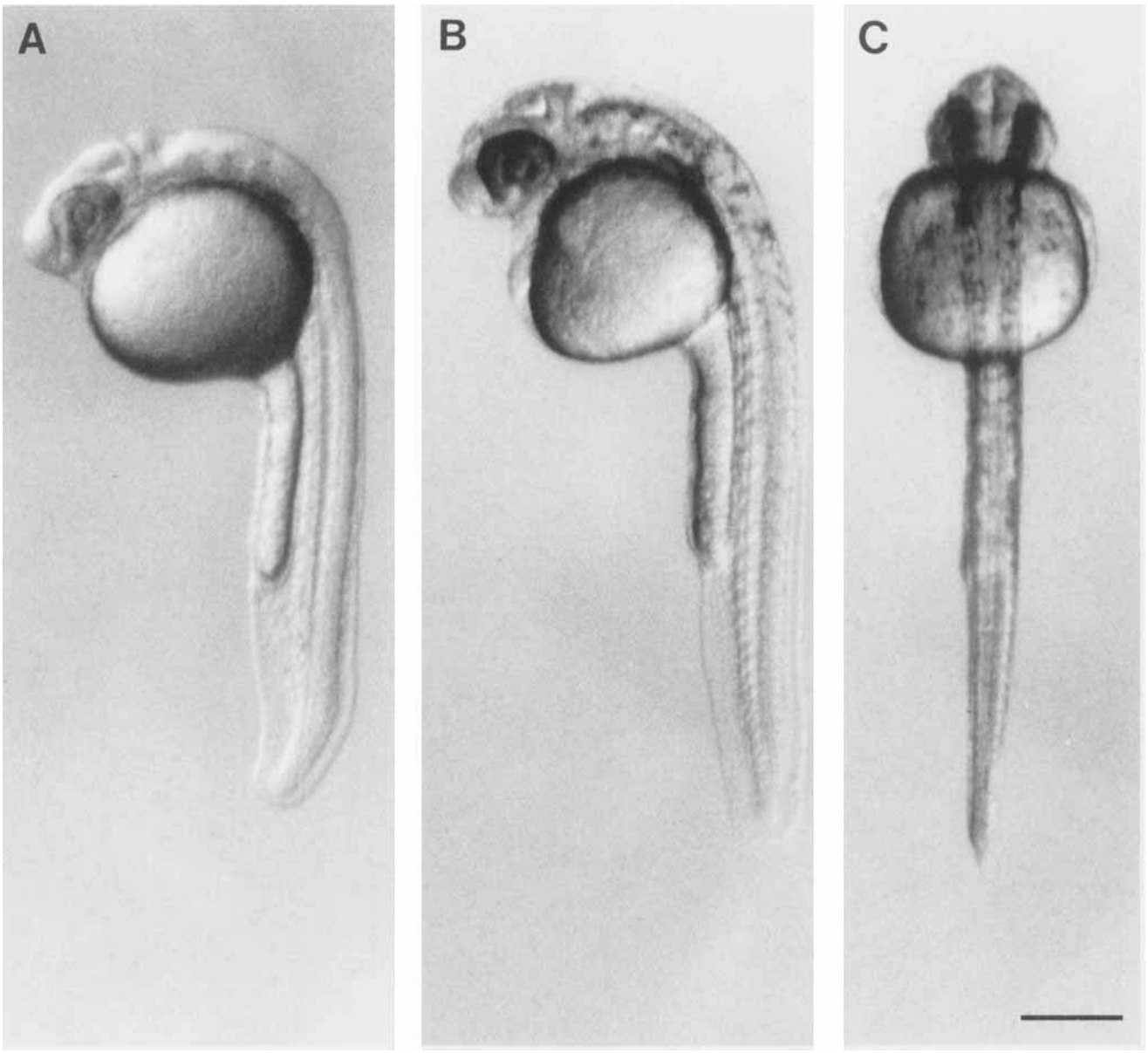

Fig. 29A–C (Legend to Fig. 29 appears on page 289).

determine the approximate stage of the embryo (Fig. 33). We imagine two lines from a side view: One, a line through the middle of the ear and eye, is the head axis. The other, along the notochord, and parallel to the horizontal myosepta at about somites 5–10, is the trunk axis. A way to estimate the angle between the two lines, the **head-trunk angle (HTA),** is to position the embryo in its dish with its tail pointing toward the observor, and mentally superimpose a clock face upon it. One of the hands of the clock, the trunk axis, points toward 6 o'clock. The position of the other hand, the head axis, changes with developmental time as as shown in Figure 33.

The morphogenesis accompanying head-straightening dramatically shortens the head, in absolute terms, making it more compact along the anterior-posterior axis. As can be seen from Figure 1, the rudiments of the eye and the ear approach one another rapidly, thus providing a second new staging index. Simply estimate the number of additional otic vesicles that could fit between the eye and the otic vesicle. We term this number "**otic vesicle length (OVL).**" It decreases from about five at the beginning of the pharyngula period to less than one at the end.

During most of the period, until about 40 h, the most precise staging method, and the most difficult, depends on using Nomarski optics to locate the leading tip of the migrating portion of the posterior lateral line primordium, as it moves steadily along the length of the trunk and tail (Fig. 34A). It leaves behind cells that

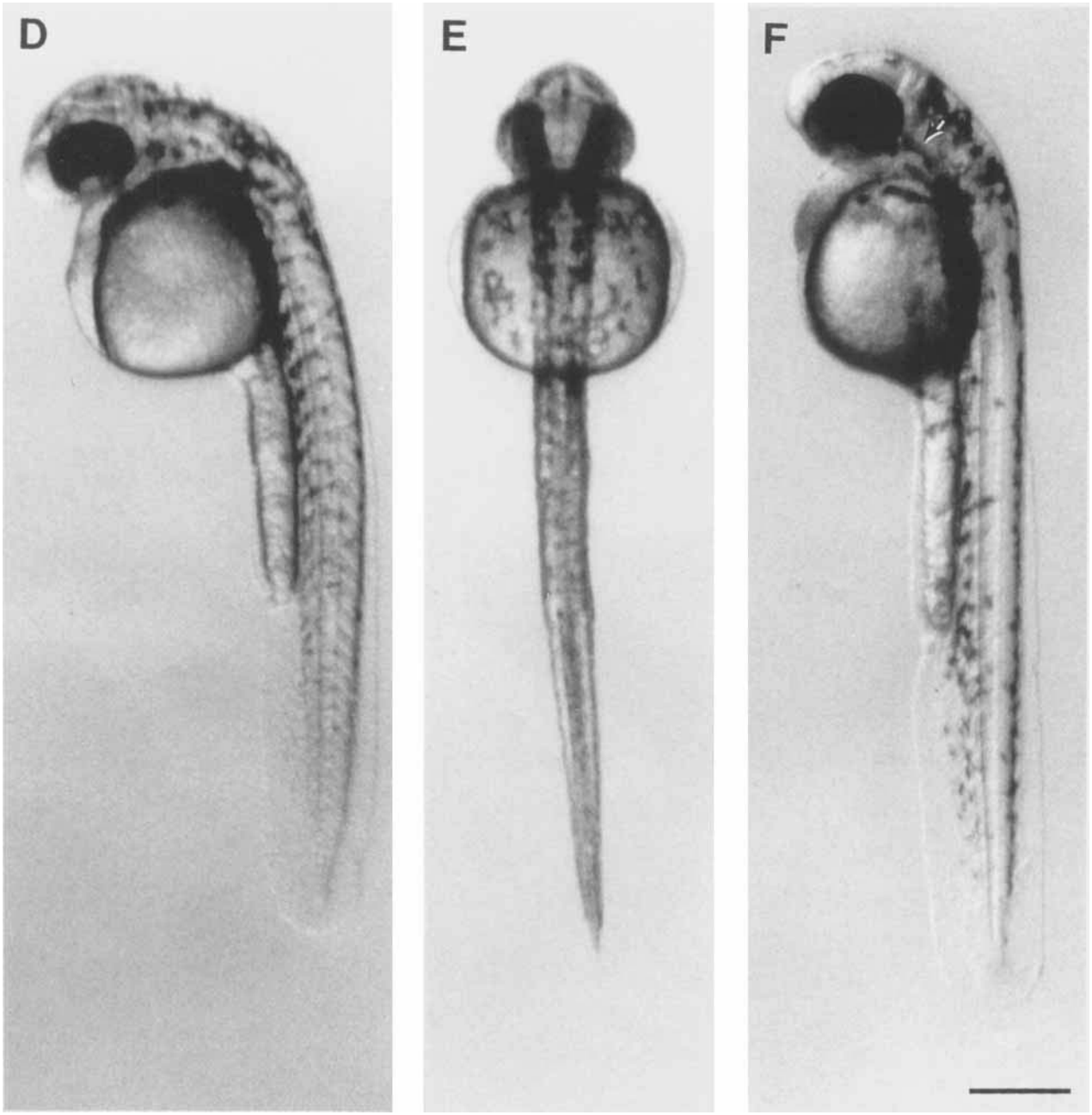

Fig. 29D–F.

form the ganglion of the lateral nerve, and as it moves it deposits cells that form the neuromasts along the nerve. The primordium migrates in the skin, superficially to the horizontal myoseptum (Fig. 34B), on each side of the body, at an approximately linear rate of 100 μm/hour (Metcalfe, 1985), or 1.7 myotomes/hour. Determine which myotome, from 1–30, the advancing (posterior) tip of the primordium overlies. We define **primordium ("prim") stages** by this index (Fig. 35). The method is tedious, and the migrations of the primordia on both sides of a single embryo are not always synchronous. After 40 h the primordium is far posterior, small, and indistinct.

In addition to these general features, and novel ones that characterize particular stages, there are several important developments during the pharyngula period that we now outline below, and then, following the same order of presentation and setting each topic off into a paragraph of its own, we add details in the stage descriptions.

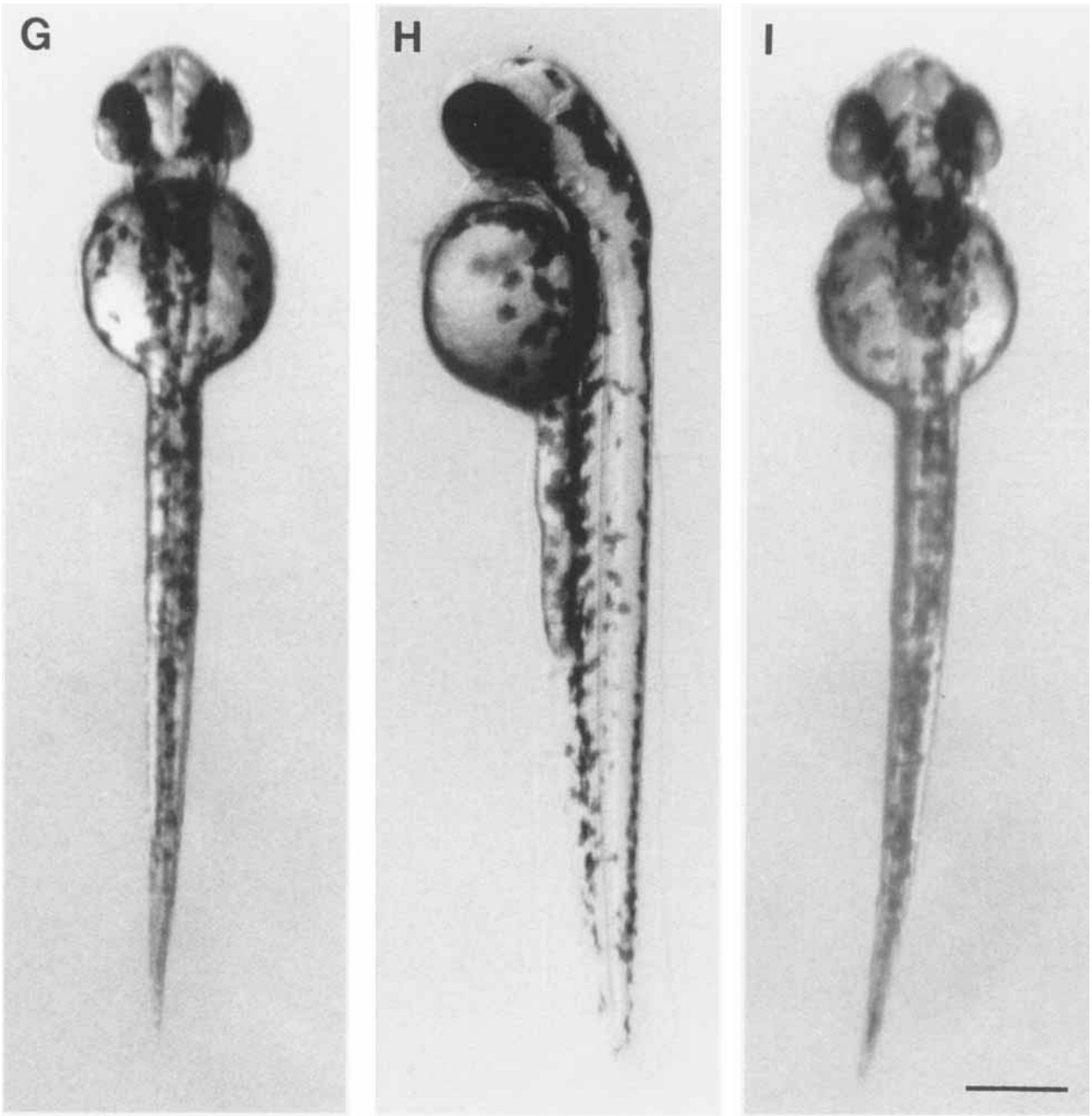

Fig. 29. Development during the pharyngula period. Left-side and dorsal views (except for the prim-5 stage) of the same embryo at the given stage. **A:** Left-side view at the prim-5 stage (24 h). The brain is prominently sculptured (see Fig. 23 for a key to the brain subdivisions). Melanogenesis has begun, but is not yet evident at this low magnification. **B,C:** The prim-12 stage (28 h). Melanophores extend from the level of the hindbrain to about the middle of the yolk ball. **D,E:** The prim-20 stage (33 h). A few pigment cells are now present along the axis dorsal to the yolk extension and on the dorsal part of the yolk ball. **F,G:** The prim-25 stage (36 h). Pigment extends almost to the end of the tail. The arrow in F indicates the ventral horn of melanophores. **H,I:** The high-pec stage (42 h). Pigment now extends the whole length of the embryo. The dorsal and ventral pigment body stripes are filled in, but not so neatly as they will be later. The lateral stripe is not yet evident. Scale bars = 250 μm.

The fins begin to form. The median fin fold, barely present at the onset of the period, becomes prominent, and forms collagenous strengthening fin rays, or actinotrichia (Fig. 28D). The rudiments of the bilaterally paired pectoral fins begin their morphogenesis: Mesenchymal cells gather together to form fin buds that serve as probably the single most useful staging feature during the second half of the pharyngula period (Figs. 36, 37). As the buds develop, an apical ectodermal ridge becomes prominent at their tips. Whether the ridge plays a morphogenetic role similar to that of the limb bud of tetrapods is unknown, but a hint that it might do

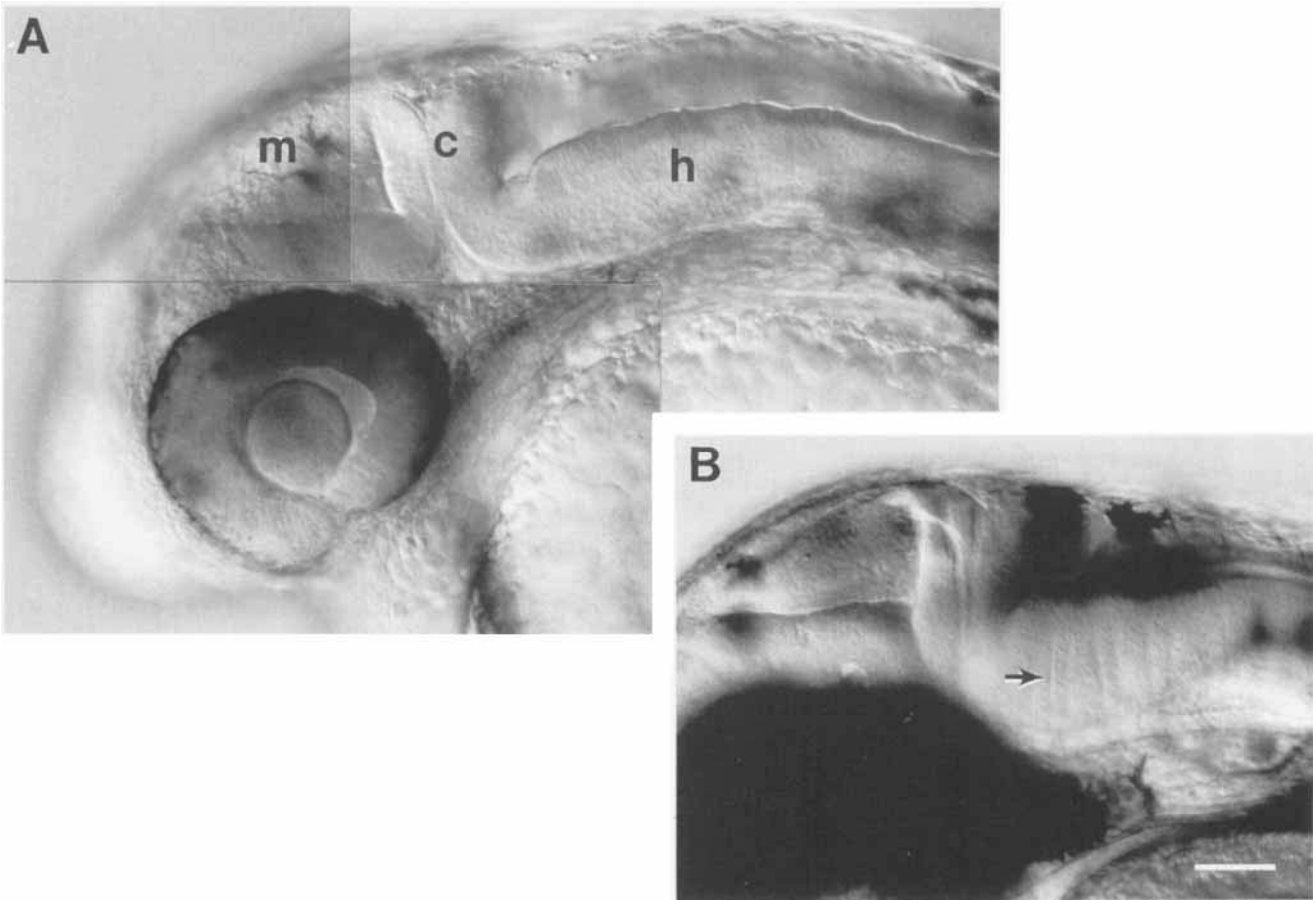

Fig. 30. Neural structures predominate in the head during the pharyngula period. Left-side Nomarski views, dorsal to the top, anterior to the left. **A:** The prominent transverse brain subdivision at the cerebellar (c) primordium shows here at the prim-13 stage (29 h), separating the midbrain (m) and the hindbrain (h). All but the posterior part of the midbrain is sculptured by a distinctive horizontal furrow that separates the midbrain (or optic) tectum (dorsal to the furrow) and the midbrain tegmentum (ventral). Rhombomeres give the dorsal surface of the thinner-looking hindbrain a lumpy appearance, although less so than at an earlier stage (see Fig. 25). The hindbrain's fourth ventricle shows above the hindbrain wall. The eye, with the retina surrounding the lens, is well shown. **B:** By the prim-25 stage (36 h) the brain walls thicken substantially, but the same subdivisions present earlier are evident. At this stage rhombomere boundaries are indicated by doubled transversely oriented stripes (arrow), formed by developing glial fibers and bundles of commissural axons (Trevarrow et al., 1990). Scale bar = 50 μm.

so comes from the fact that it is positioned at the exact boundary of the ventrally located expression domain of the *engrailed1* gene (Hatta et al., 1991a; Ekker et al., 1992). A most significant connection between the zebrafish fin bud and the tetrapod limb bud is the domain posterior mesenchymal domain of *sonic hedgehog* gene expression in both, corresponding to the zone of polarizing activity (ZPA; see Krauss et al., 1993).

Pigment cells differentiate. They are easy to see and we use them for staging landmarks. The pigmented retinal epithelium, and the neural crest-derived melanophores begin to differentiate at the onset of the period, and pigmentation gets rather far along during the period (see Fig. 29). The melanophores begin to arrange themselves in a characteristic pattern that includes a well-defined set of longitudinal body stripes (Milos and Dingle, 1978).

The circulatory system forms (Reib, 1973). The heart begins to beat just at the onset of the period, and forms well-delineated chambers. Blood begins to circulate though a closed set of channels. A bilateral pair of aortic arches appears just at the outset of the pharyngula period: This is aortic arch 1, the earliest and most anterior arch of the eventual serial set of six. The others develop rapidly near the end of the period. The blood flows into each side of the head from the anterior two arches via the carotid artery and returns via the anterior cardinal veins. The more posterior aortic arches (arches 3–6) also connect to the left and right radices (roots) of the dorsal aortae, which anastomose in the trunk to form an unpaired midline vessel lying just ventral to the notochord. The dorsal aorta is renamed the caudal artery as it enters the tail (Reib, 1973). At a point along the tail the channel makes a smooth ven-

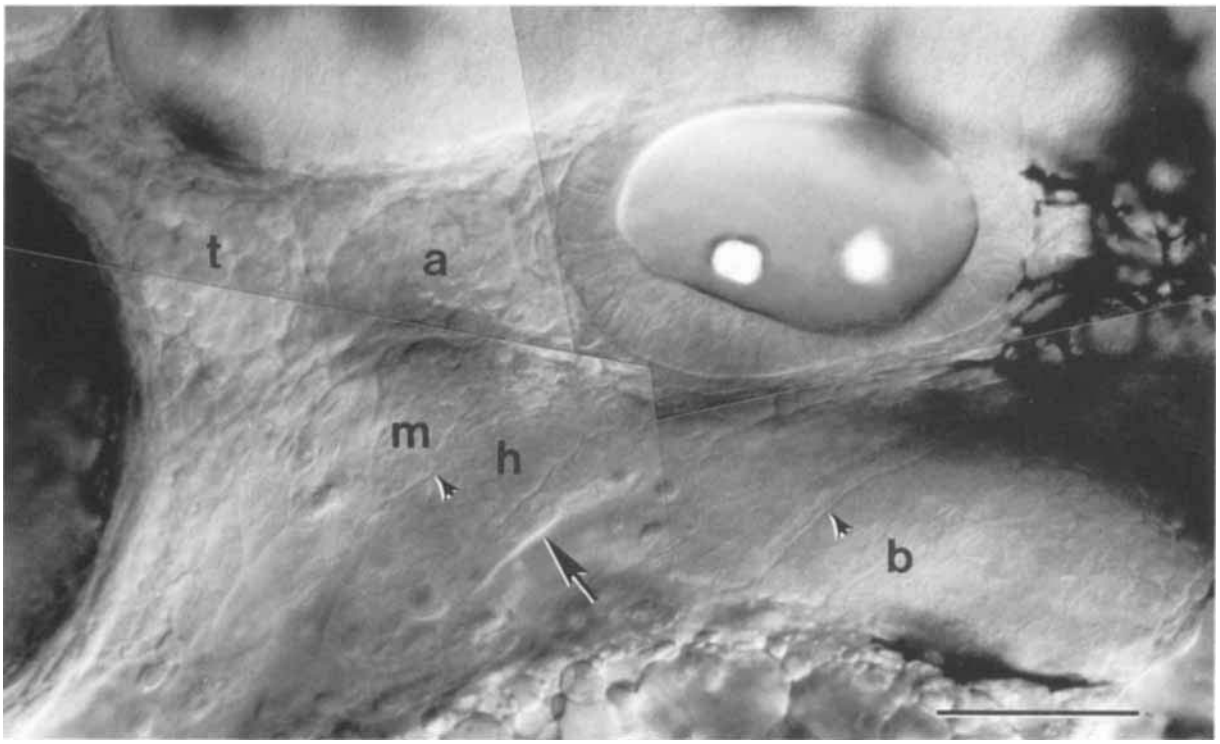

Fig. 31. The pharyngeal arch primordial region at the prim-25 stage (36 h). Left-side Nomarski view, dorsal to the top, anterior to the left. The plane of focus is more lateral than for Figure 30, to show the mesenchyme of the pharyngeal arch primordial region that fills most of the field of view between the otic vesicle (to the upper right) and the yolk sac (at the bottom right). Transversely oriented grooves (arrowheads) cut the mesenchymal mound into separate fields for the individual pharyngeal arches: The most prominent groove, at the arrow, subdivides the whole region into the anterior jaw-forming mandibular (m) and hyoid (h) arches, and the posterior set of five branchial (b) arches. Pigmented melanophores show on the right, posterior to the otic vesicle, and on the left the posteriormost part of the darkly pigmented eye is included. The brain is at the top; the ventral part of the boundary between the midbrain and hindbrain lies just at the upper left. Two cranial sensory neuronal ganglia, the trigeminal ganglion (t) and the anterior lateral line ganglion (a), show between the eye and the ear. Scale bar = 50 μm.

trally directed 180° turn to form the caudal vein, returning the blood to the trunk. The vein continues in the posterior trunk as the unpaired median axial vein, lying just ventral to the dorsal aorta. Just posterior to the heart, the vein then splits into the paired left and right posterior cardinal veins. In turn, each posterior cardinal joins with the anterior cardinal to form the common cardinal vein (or duct of Cuvier) that leads directly to the heart's sinus venosus. The name sometimes used for the common cardinal as it crosses the yolk sac, the vitelline vein, is not very appropriate, because the vessels named vitelline veins in other fish have different connections (see Reib, 1973). The common cardinal veins, at first very broad and not very well defined, carry the blood ventrally across the yolk. As development continues the common cardinals become narrower channels, and relocate to the anterior side of the yolk.

Finally, there is marked behavioral development. Tactile sensitivity appears, and the flexions that occurred in uncoordinated individual myotomes during the late segmentation period become orchestrated into rhythmic bouts of swimming.

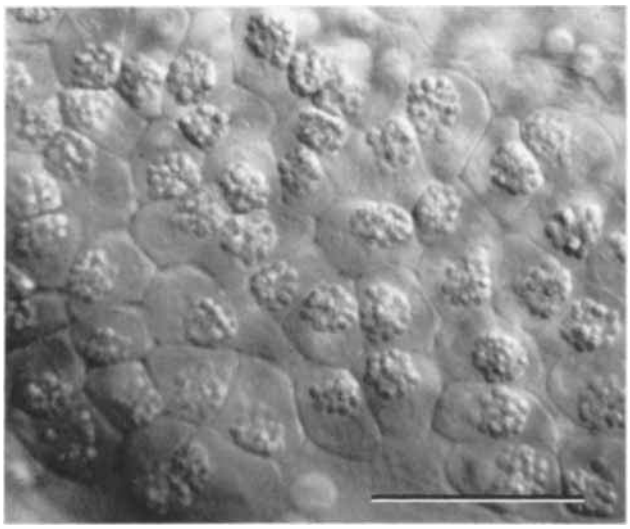

Fig. 32. Cells of the hatching gland, present on the pericardium over the anterior yolk sac, have prominent granules during the pharyngula period. Later they lose the granules, presumably due to the release of hatching enzymes. Nomarski view at the prim-15 stage (30 h). Scale bar = 50 μm.

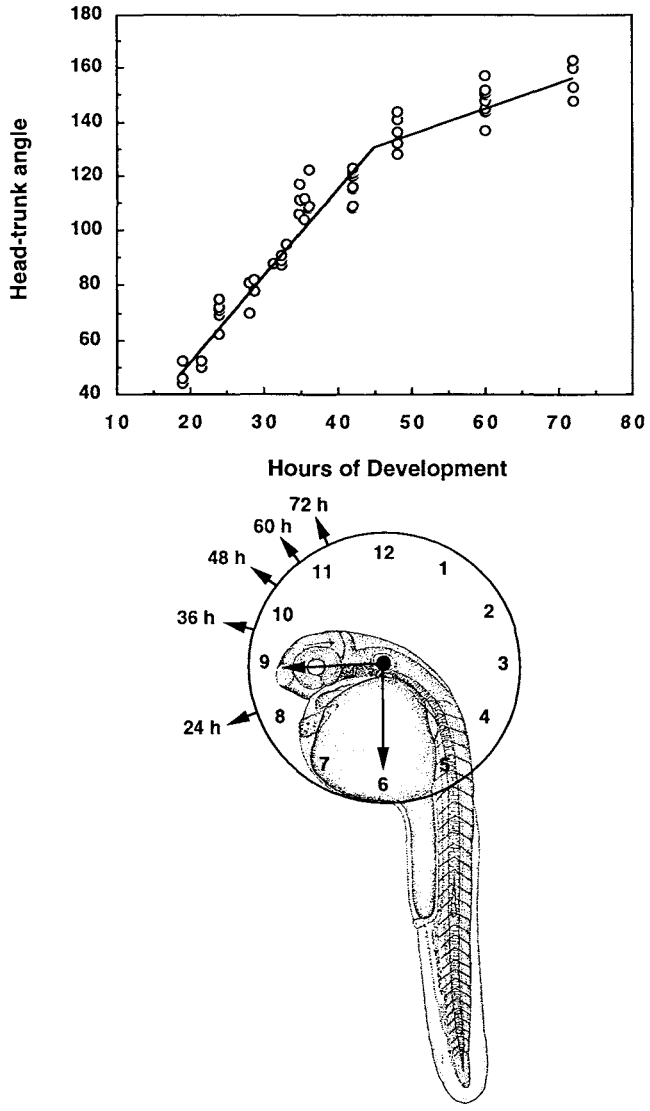

Fig. 33. Head-trunk angle as a function of hours of development (at 28.5°C). The head-trunk angle is the angle between a line drawn through the middle of the ear and eye, and a second line parallel to the notochord in the midtrunk region (myotomes 5–10). The head-trunk angle increases between 20 h and 70 h, as a consequence of straightening of the embryo. Mentally superimposing the embryo upon a clock face, as shown in the lower drawing, is a convenient way to estimate the head-trunk angle. Set the trunk axis to 6 o'clock, and the head axis changes with developmental stage. The head axis of the embryo in the drawing (at the prim-17 stage corresponding to 31 h) points to about 9 o'clock.

Stages During the Pharyngula Period

Prim-5 stage (24 h). At this stage, EL = 1.9 mm, HTA = 120°, and OVL = 5. The advancing end of the lateral line primordium overlies myotome (somite) 5. There are about 30 somites, 13 of them in the tail. The length of the yolk extension just equals the greatest diameter of the yolk ball.

The median fin fold is easily recognized (Fig. 28C). By 26 h (prim-8), mesenchyme gathers specially at the paired locations where the pectoral fin buds will form, lateral to the third somites. The buds first appear as mounds by 28–29 h.

Pigment formation begins in cells of the pigmented retinal epithelium and then in melanophores dorsolaterally in the skin. Melanophores appear in an approximate AP gradient, first just posterior to the otic vesicle. At the prim-5 stage the pigmentation is so light that a compound microscope may be required to see it. Use brightfield, not Nomarski, transmitted illumination so that background contrast will be minimal. The pigment cells develop rapidly, such that within a few hours they are a prominent feature of the embryo (Fig. 30A); readily apparent at low magnification by the prim-12 stage (28 h; Fig. 29B). From a dorsal view at the same stage (Fig. 29C) one can see that melanophores now migrate to reach the dorsal and more anterior part of the yolk sac.

The heart is first visible as a cone-shaped tube deep to the brain, seemingly more dorsal than its later location, and prominently occupying a pericardial sac on the anteriormost region of the yolk. The heart begins to beat just prior to this stage, at first with no apparent direction to the beat, and the rhythm may be interrupted. By 26 h (prim-7), the heart tube is elongated and the contraction occurs as an AP-going wave. Most blood cells are in the blood island (Fig. 17D, 20A), and by 24–25 h some of them move more anteriorly and dorsally, into the region between the yolk and notochord, where the major vessels supplying the trunk and tail are forming. Blood cells also occupy the yolk ball, over very ill-defined and broad regions that herald the development of the common cardinal veins. The blood cells will begin circulation very soon after the stage when they first appear on the yolk ball.

The prim-5 embryo continues to exhibit spontaneous side-to-side contractions involving the trunk and tail. The contractions often occur in bursts, at a rate of about eight episodes per minute (Grunwald et al., 1988). Sensory-motor reflexive circuits are becoming functional. At the prim-5 stage one cannot clearly distinguish responsiveness to light touches to the head or body of the dechorionated embryo, possibly because of a fairly high background level of spontaneous contractions. However, by 27 h (prim-10), this background lowers (it remains transiently high just after dechorionationation), and the first consistent tactile responses appear. The reflexive movements have approximately the same nature as the spontaneously occurring ones.

Prim-15 stage (30 h). At this stage EL = 2.5 mm, HTA = 95°, OVL = 3. The yolk extension is just longer than the yolk ball. In dorsal view the yolk ball appears about twice as wide as the head.

The ventral portion of the median fin fold extends anteriorly, to underlie the yolk extension. The pectoral fin buds have the form of shallow domes, each with a height less than one-third of the diameter at its base.

The embryo now begins to slow its overall rate of lengthening as tail morphogenesis comes to an end. A

distinctive tail bud is no longer present; rather, some degenerating cells, evident by their bright appearance with Nomarski optics, occupy its position. The cell death may represent a natural process of elimination of the excess cells remaining in the bud after tail somitogenesis is complete (Kimmel et al., 1989).

Cells throughout the pigmented layer of the retina develop visible pigment granules. One can now very readily distinguish many of these pigmented epithelial cells, as well as the mesenchymal-looking melanophores in the skin by their dark pigmentation. A distinctive dorsal clustering of melanophores presages the formation of the median **dorsal stripe,** lengthwise and overlying the tops of the myotomes, and at this stage extending posteriorly to about somite 12. Other melanophores have appeared anteriorly in the head; a few of them are present overlying the dorsal midbrain and occasionally the forebrain. Yet others have migrated ventrally and begin to fill in a **ventral stripe** of pigmentation that underlies the myotomes bilaterally, but still is dorsal to the yolk. This ventral stripe is now very ill defined and incomplete, particularly in the tail. Other melanophores migrate superficially to the myotomes but are not yet organized into a lateral stripe that will eventually overlie the horizontal myosepta. Melanophores also continue to accumulate on the dorsal yolk sac. Migration proceeds faster anteriorly than

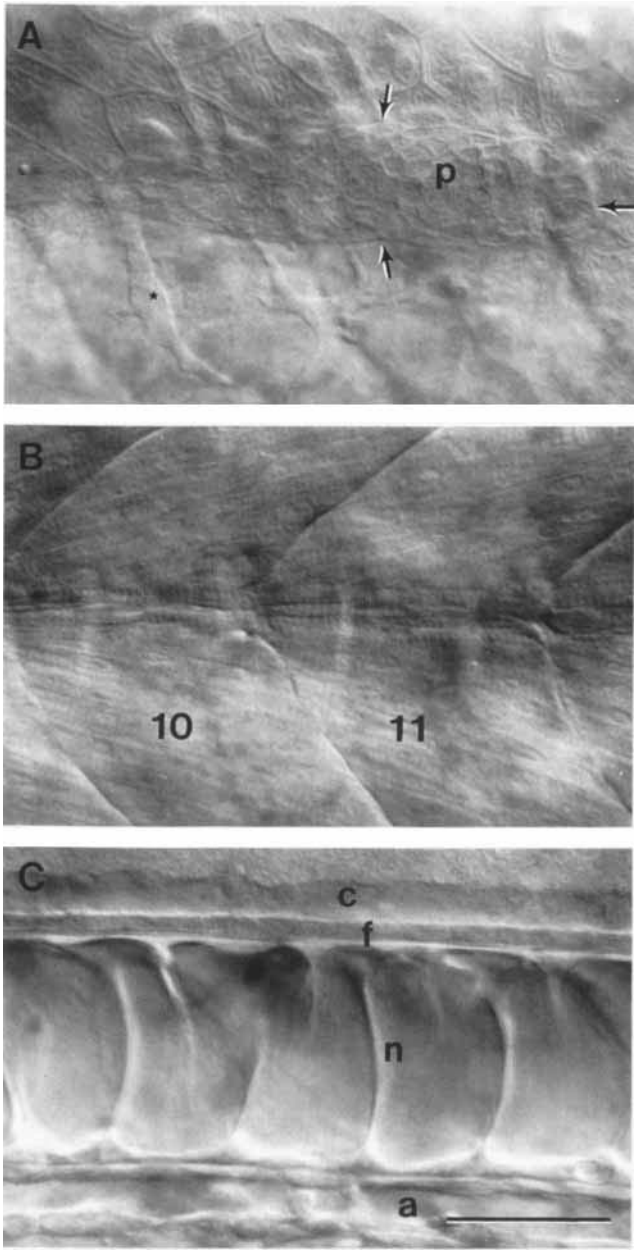

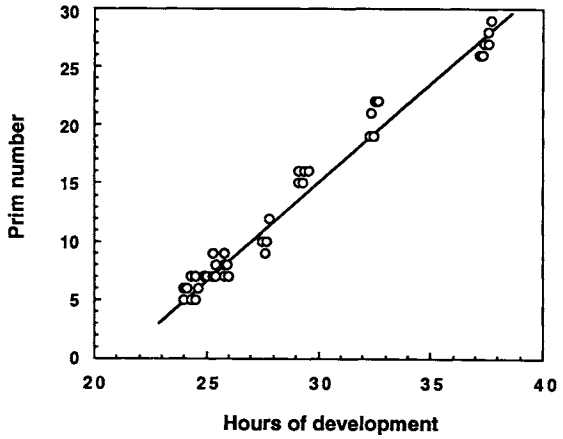

Fig. 35. Prim number as a function of hours of development (at 28.5°C). Prim number is the number of the myotome (equivalent to somite) that the leading, posterior end (see Fig. 34) of the posterior lateral line primordium has reached during its migration from the head to the tip of the tail. The rate of migration is roughly linear. Points represent measurements from individual embryos; data are pooled from different experiments.

Fig. 34 (left). The posterior lateral line primordium, and underlying structures along the flank of the pharyngula. Left-side Nomarski views, dorsal to the top, anterior to the left. Three focal planes at the same position are shown. **A:** The lateral line primordium (p), outlined by arrows, is in focus most superficially. The rightmost arrow shows its posterior, leading, boundary that we use to obtain the prim stage. Out-of-focus transverse myosepta are visible (compare with B, where they are in sharp focus). They mark off myotomes 10 and 11, which fill most of the field, and the anteriormost part of myotome 12, present to the far right. Myotome 12 underlies the leading edge of the lateral line primordium, hence the embryo is at the prim-12 stage (28 h). The embryo is slightly tipped so that the focus at the top of the field is more superficial, and the focal plane to the bottom is deeper. At the top, periderm cells are present. These flattened cells, developing from the EVL, have a characteristic cobblestone appearance, with their most superficial face uplifted into fine folds or rugae. The star shows one of two mesenchymal cells present in the ventral part of the field. They lie deep to the periderm, as does the primordium itself. **B:** Myotomes (10 and 11) are in focus. Cross-striations are apparent. The horizontal myoseptum crosses the field of view at the center; the muscle cells at this location, muscle pioneers, are horizontally flattened such that they look thinner from this viewpoint. Other fibers, those more dorsally and ventrally, run obliquely across the myotome, pointing toward the chevron apex. **C:** The focus is at the midline, deep to the myotomes. From top to bottom the following structures are visible: the spinal cord's central canal (c) and floor plate (f), the notochord (n), and the dorsal aorta (a). Scale bar = 50 μm.

Fig. 36. Condensing mesenchyme of the early pectoral fin bud. The view is along the proximal-distal axis of the bud, at the dorsolateral aspect of the embryo's left side. Dorsal is to the top and anterior is to the left. Nomarski optics at the prim-15 stage (30 h). The bud is outlined by melanophores anteriorly and ventrally, and by arrowheads dorsally. The posterior lateral line nerve runs superficial to the horizontal myoseptum in the upper part of the field (arrow). Cross-striations of muscle fibers (in myotomes 2 and 3) are in focus above the nerve, and a mesenchymal cell, present just deep to the epidermis, is in focus between the nerve and the bud (star). Refractile yolk granules are at the bottom of the field. Scale bar = 50 μm.

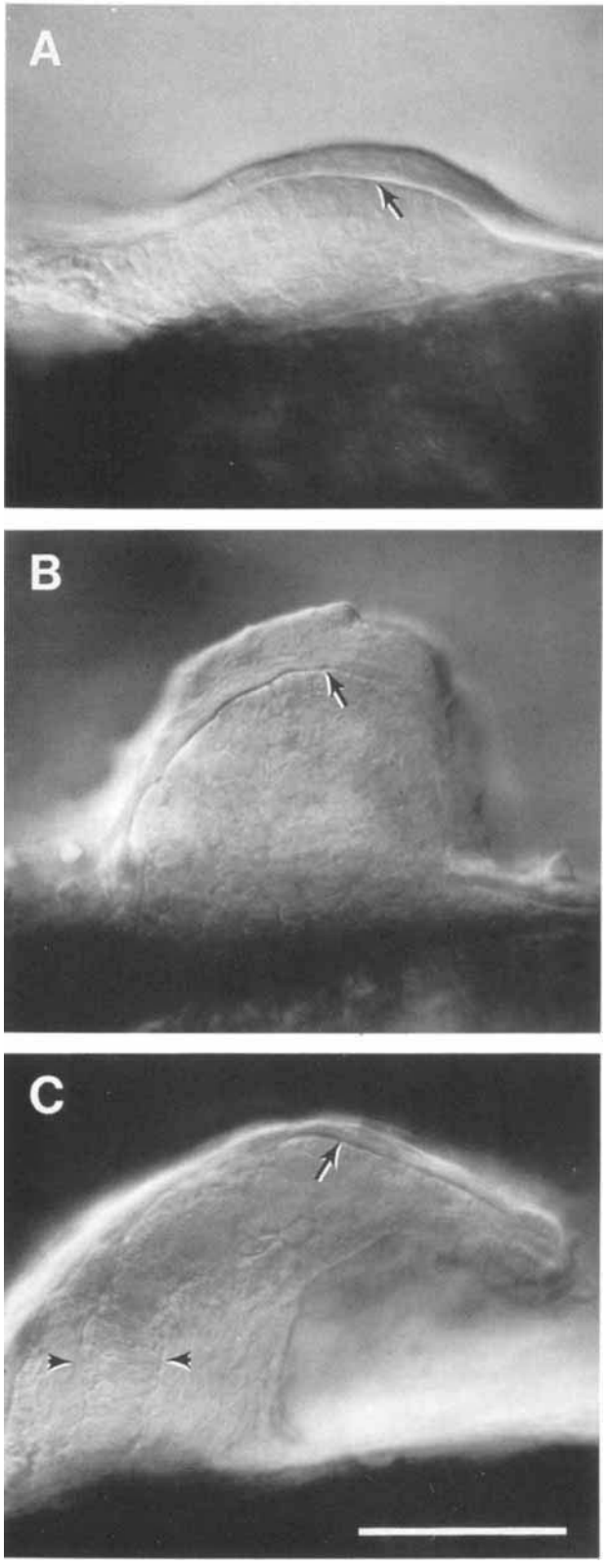

Fig. 37. Morphogenesis of the pectoral bud during the late pharyngula period. Left-side Nomarski views from the ventrolateral aspect of the embryo to show the bud in relief. Dorsal is to the top, anterior is to the left. Arrows indicate the boundary between the bud's surface epithelium and inner mesenchyme. **A:** Prim-18 stage (32 h). The bud is now symmetrical in outline, a shallow dome with a height less than one-third of its width. The common cardinal vein passes just anteriorly, beneath the epithelium. **B:** Prim-25 stage (36 h). The bud's height is now about three quarters its width. Its posterior face (to the right) is relatively steeply angled. The focus is along the prominent apical ectodermal ridge, crossing the bud distally. **C:** Long-pec stage (48 h). The bud curves posteriorly and tapers, to give a pointed appearance from this viewpoint; its length along the proximal-distal axis is about twice the width of its base. An innermost precartilage core has now begun to differentiate within the mesenchyme (arrowheads). Scale bar = 50 μm.

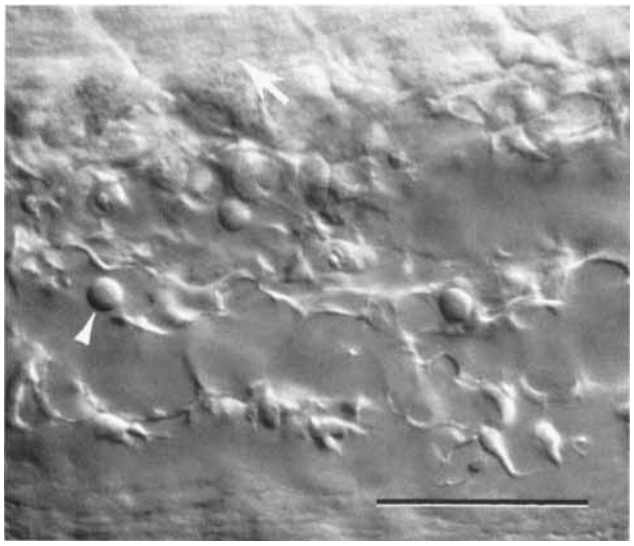

Fig. 38. Refractile tail reticular cells line sinusoids that make up the wall of the developing caudal vein. Left-side Nomarski view, dorsal to the top, anterior to the left at the prim-15 stage (30 h). The tail reticular cells have a specialized branching morphology and also appear functionally specialized, relative to other endothelial cells, in their ability to rapidly clear particulate material from the circulating blood by phagocytosis. Three red blood cells (one indicated by the arrowhead) are in view in the sinusoids and can be distinguished from the reticular cells by their spherical shapes. The ventral parts of tail myotomes are visible just at the top of the field (arrow). Scale bar = 50 μm.

in more posterior regions, and results in a ventrally projecting **anterior horn** subregion of the ventral stripe containing broad, smoothly outlined melanophores extending to the bases of the eyes on each side of the midline (Fig. 29E, arrow in F).

The heart is still a straight tube, and its beat is becoming more prominent. Each heartbeat is in two parts, the first indication of development of chambers. There is a single aortic arch and complete arterial system between the pharynx and the tail, through which blood slowly circulates. A bit more than half-way along the tail a labyrinth-like network of channels connect between the caudal artery and vein. An apparently specialized set of very refractile cells line these particular channels (Fig. 38). We term the elements the tail reticular cells, because they very rapidly take up latex beads injected into the circulatory system (unpublished observations of C.B. Kimmel and B. Ullmann), in the manner of reticulo-endothelial elements of the adult blood vascular system.

The frequency of spontaneous body contractions now diminishes to one to two episodes per minute. A light touch placed anywhere on the body or head usually elicits a robust reflexive side-to-side bout of wriggles. However, the embryo cannot yet effectively move its body through the water.

Prim-25 stage (36 h). At this stage EL = 2.7 mm, HTA = 75°, OVL = 1. The length of yolk extension now markedly surpasses the diameter of the yolk ball. In dorsal view, the width of the yolk ball exceeds that of the head by a factor of about 1.3.

Actinotrichia develop posteriorly in the median fin fold where they can be revealed by Nomarski optics (Fig. 28D). Each pectoral fin bud is a dome-shaped mound raised about three-fourths as high as its width. As the bud grows outward it loses the symmetrical appearance it had earlier, beginning to form an apical tip posterior to the center of the bud (Fig. 37B). The apical ectodermal ridge is now present at the tip, and easily visible with Nomarski optics if the orientation is correct, because the ridge runs obliquely across the bud, in a ventroposterior to dorsoanterior direction (Hatta et al., 1991a).

Pigmentation is prominent in the eye, but is still light enough so that one can readily visualize the unpigmented cell nuclei in this retinal epithelium. Melanophores on the body elaborate a bolder and longer (but still not sharply defined) dorsal stripe, now usually extending from the diencephalic region of the head to the tip of the tail, excluding the fin fold. There are still gaps along this dorsal stripe. Melanophores also appear laterally on the trunk and tail, some of them lodged in the region of the horizontal myoseptum where the lateral stripe will form. Others fill in the ventral stripe, making its anterior horn more readily apparent (Fig. 29H,I), and extending the ventral stripe posteriorly to about halfway to the tip of the tail. Melanophores are also present on the dorsal and lateral surfaces of the yolk sac. Beginning at this time it is useful to examine the embryo with epi-illumination, using either the dissecting or compound microscope, not just with transmitted light. This is because the first reflective pigment cells, iridophores, soon appear on the eye. However, one cannot identify them at 36 h.

The pericardial cavity is not yet prominently inflated. Blood circulation is strong. The heart, previously a straight tube, now bends slightly. There is still but a single pair of aortic arches. The circulatory loop connecting the caudal artery and vein has moved to about three-quarters of the way to the end of the tail. Returning blood through the trunk and across the yolk, the pathway that includes the axial vein, the posterior cardinal vein and common cardinal vein are well-defined channels.

Spontaneous episodes of lashing activity of the embryo are now infrequent, occurring at less than one episode per minute. The reflexive escape response to a touch lasts longer than before, and now effectively serves to displace the embryo, usually up to several body-lengths. The wriggles still occur slowly enough that one can easily resolve their rhythm; later the reflex is snappier and individual swimming beats occur so quickly that they simply cannot be resolved by eye.

High-pec stage (42 h). At this stage EL = 2.9 mm, HTA = 55°, OVL = 3/4. The name for this stage, as well as for the next two, draws attention to the appearance of the rudiments of the pectoral fins. Now, at the high-pec stage, the fin bud's height is about equal to

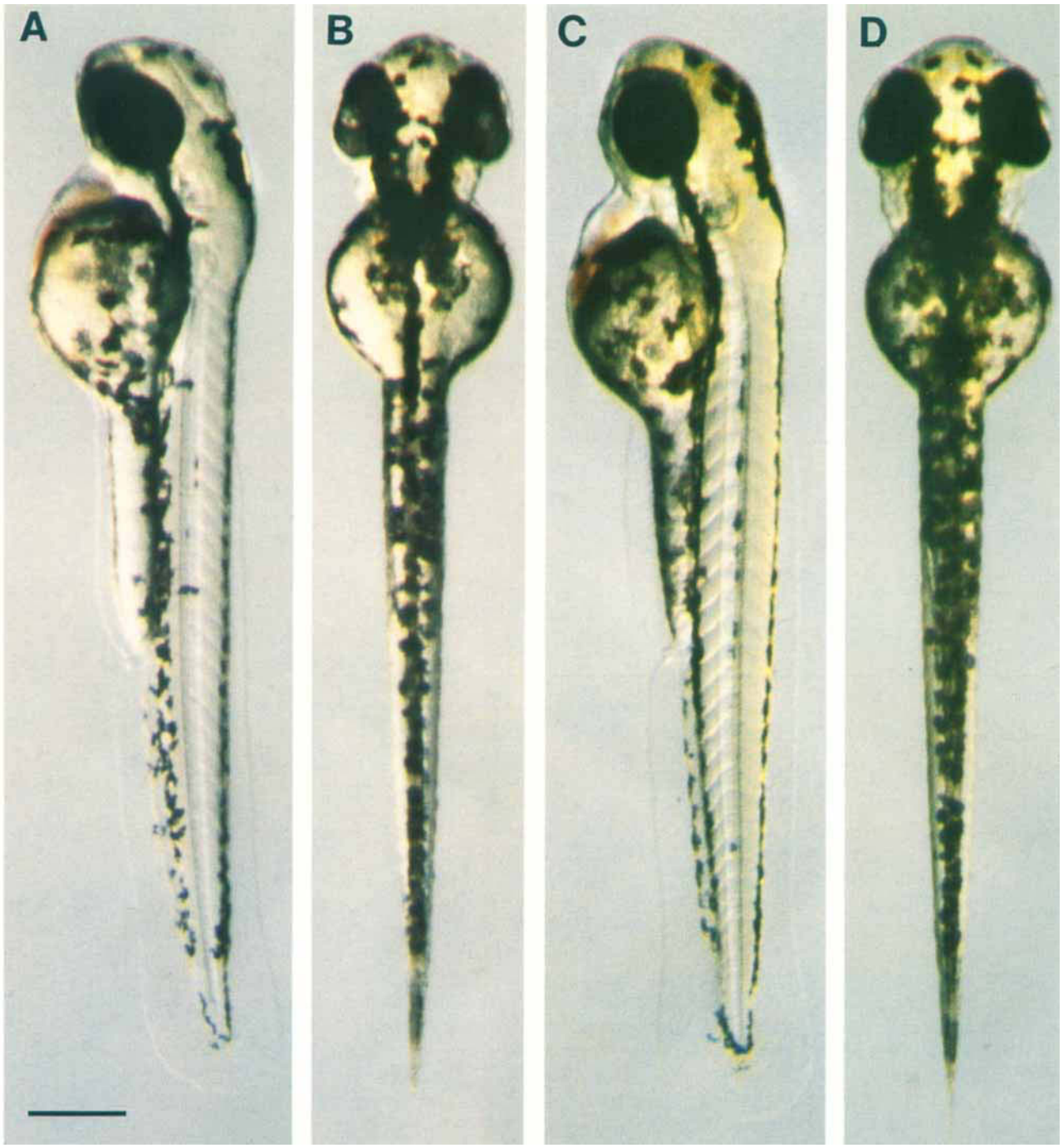

Fig. 39. Development during the hatching period of embryogenesis (**A–F**), and the early larva (**G,H**). Left-side and dorsal views of the same embryo are paired for each time point. A,B: Long-pec stage (48 h). C,D: Pec-fin stage (60 h). E,F: Protruding-mouth stage (72 h). Note the progressive increase dorsally in yellow pigmentation owing to xanthophore development, and the progressive filling of melanophores into the lateral stripe. G,H: The early larva (120 h) is photographed with a combination of transmitted and incident illumination, the latter revealing reflective iridophores. The swim bladder is inflated at this stage. Continued development of the lower jaw, protruding it more anteriorly, brings the lower and upper jaws close together in front of the eyes. Scale bars = 250 μm.

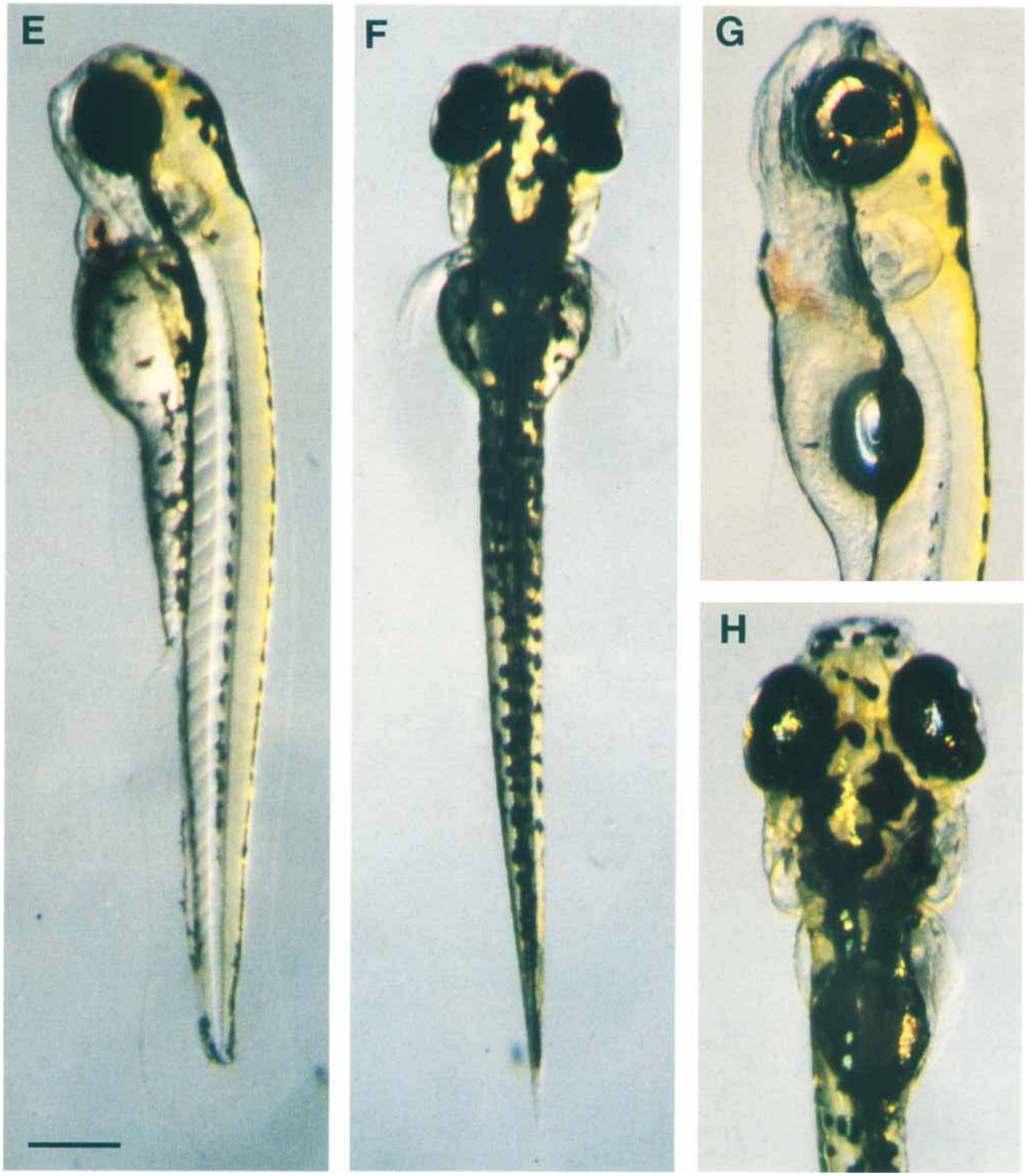

Fig. 39E–H.

the width of its base. The apical ridge is readily visible using just the dissecting microscope. The ridge has increased prominence because it now incorporates, in addition to ectodermal epithelium, an underlying loose mesenchyme that will participate in development of the blade of the fin.

The yolk extension retains a distinctly cylindrical shape along most of its length, but its posterior end begins to taper, to take on a more conical appearance. Its length is about 1.5 times the diameter of the yolk ball. A dorsal view reveals that the yolk ball is about 1.3 times wider than the head.

The migrating primordium of the posterior lateral line gets smaller as it migrates, making it harder to identify (its identification never was particularly easy), and by 42 h it has reached the posterior end of the axis, so that its position can no longer be used as a staging index. The mandibular and hyoid arches (the first and second pharyngeal arches) are well defined. Inspection of the olfactory pits with Nomarski optics reveals the first formation of cilia by the epithelial cells. There is little or no ciliary beat. The same method also reveals a thickening in a dorsolateral region along the inner side of the otic vesicle's epithelial wall that preludes development of the semicircular canals.

The primordia of the liver and probably the swim bladder make their appearances along the gut tract, posterior to the pharynx in the region of the anterior yolk ball. However, they are rather hidden by the dorsal part of the yolk ball; sectioned material reveals endodermal morphogenesis much more readily rather than do views of the living embryo. Hindgut endoderm is now recognizeable (first at the prim-28 stage at 39 h) as a solid plug (not a hollow tube) of midline cells in the anal region, thicker than the adjacent pronephric ducts.

The dorsal stripe of melanophores now is very well filled out to the end of the tail. The ventral stripe, now filled out anteriorly from the eye, also may contain pigment cells to the end of the tail. However, gaps along it in the tail region are conspicuous, one of these persisting at its posterior end. At this stage the dorsal and ventral stripes come together at the end of the tail to make an incompletely pigmented posteriorly pointed V. Melanophores along the lateral aspect of the myotomes now begin to organize distinctively along the horizontal myosepta as the **lateral stripe** (Fig. 29H). Only a very few cells are in it, three or so on each side of the body. The first few melanophores also reach the ventral surfaces of both the yolk ball and yolk extension, and will later organize into a yolk stripe that joins the ventral stripe at the level of the anus. Very bright illumination will for the first time reveal that the head has a very pale yellow cast, marking the first appearance of **xanthophores.** Also for the first time, bright incident illumination occasionally reveals a very few faintly reflective pigment spots, **iridophores,** scattered in a disorganized fashion on the eye. Iridophores are not yet apparent elsewhere on the body. Both xanthophores and iridophores will be much more easily and consistently recognized at the long-pec stage (48 h).

The bend in the heart is now prominent and marks the division between the atrium and ventricle, and Nomarski optics reveal an endothelial cushion between them. The heart beats (about 180 per minute) with the atrial beat preceding the ventricular one. There is still only one pair of aortic arches. The common cardinal vein on the yolk sac is very broad and prominent. Segmental arteries and veins are present along the trunk and tail. These vessels are deep to the myotomes and are most easily recognized overlying the spinal cord near each transverse myoseptum. Those in the anterior tail begin to carry circulating blood.

Dechorionated embryos lie on their sides when at rest, yolk sac obliquely upward. A touch elicits a vigorous and rapid response, with a wriggling rhythm just slow enough that its beat is still barely discernable. The response propels the embryo from a few body lengths in many cases, or up to the whole width of a 5 cm dish in others. At the end of the bout of swimming the embryo comes to rest on its side, not dorsal-up.

HATCHING PERIOD (48–72 h)

The time of hatching is not useful as a staging index for the zebrafish, in contrast to some other types of embryos, because individuals within a single developing clutch hatch sporadically during the whole 3rd day of development (at standard temperature), and occasionally later. Whether or not an embryo has hatched, its development progresses, hour by hour, and generally individuals that have spontaneously hatched are not more developmentally advanced than ones remaining in their chorions. We arbitrarily call the creatures "embryos" until the end of the 3rd day, and afterward, "larvae," whether they have hatched or not (Fig. 39).

During the hatching period the embryo continues to grow at about the same rate as earlier (Fig. 16). Morphogenesis of many of the organ rudiments is now rather complete and slows down considerably, with some notable exceptions including the gut and its associated organs. However, these endodermal structures are difficult to visualize in the living embryo because of their deep positions, and we do not consider them completely here. Much easier to see are the rapidly developing rudiments of the pectoral fins, the jaws, and the gills.

Pectoral fin development continues to be a useful feature for staging, especially during the early part of the hatching period. At the onset of the period the paired fin rudiments are elongated buds, each already containing centrally located mesenchymal condensations that will form the girdle cartilages (arrowheads in Fig. 37C). The distal epithelial fold capping the bud, which developed from the apical ectodermal ridge, now expands into the blade of the fin proper, and strengthening actinotrichia appear. At the same time a circulatory channel appears as a continuous loop at the base

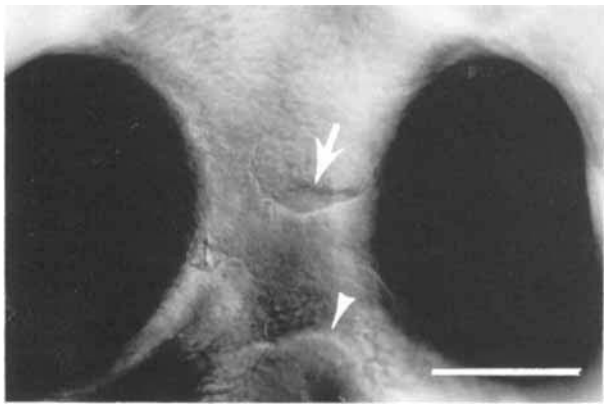

Fig. 40. The embryo's small open mouth (arrow) lies between the two eyes at the pec-fin stage (60 h). Ventral Nomarski view with anterior to the top. The midline bulge at the bottom of the field (arrowhead) is the developing ventral part of the hyoid arch (pharyngeal arch 2). The mandibular arch (pharyngeal arch 1), forming the lower jaw, is faintly outlined between the hyoid arch and the mouth. Scale bar = 50 μm.

of the enlarging fin, i.e., its position is proximal to the actinotrichia but distal to the cartilage. This channel will develop both as artery and vein. The subclavian artery takes the blood outward into the fin from the paired portion of the dorsal aorta posterior to the last aortic arch. The subclavian vein returns the blood again, connecting proximally near the origin of the common cardinal.

Prominent changes occur in the pharyngeal region. During the early part of the hatching period the small open **mouth** can be located with Nomarski optics in a midventral position, between the eyes (Fig. 40), a position that seems surprising, at first, because it is so far posterior in the head. Then, especially during the last 12 hours of embryogenesis, a dramatic repositioning of the mouth occurs. Jaw morphogenesis moves the position of the mouth anteriorward, and just at the end of the hatching period the mouth protrudes beyond the eye, where it gapes wide open. Rapid jaw and mouth morphogenesis will continue in the early larva.

Examining cartilage development in the **jaw** primordia is also useful for staging, especially during the last part of the hatching period. As noted above, the two anteriormost pharyngeal arches (the mandibular and hyoid arches) that form the jaw and associated supportive apparatus are always distinctive from the more posterior arches, collectively termed branchial arches. Cartilage development in the jaws lags behind cartilage development in the pectoral fin and behind formation of the first cartilages of the chondrocranium (the latter, basal cartilages located deep beneath the brain, are rather difficult to see in the living preparation, and we do not describe them here). On the other hand the jaw cartilages develop ahead of the branchial cartilages. Mesenchymal precartilage condensations appear in both the mandibular and hyoid arches near the beginning of the hatching period and distinctive cartilages, ventral and dorsal elements, develop in each arch by the end of this period (Fig. 41). The ventral cartilage of the mandibular arch (the mandibular or Meckel's cartilage) and the ventral element of the hyoid arch (the ceratohyal cartilage), are large supportive structures of the lower jaw, beneath the pharyngeal or oral cavity. The dorsal elements, the quadrate of the first arch and the hyosymplectic (also called the hyomandibular) of the second, are more delicate and more elaborate in their shapes. A complex set of jaw muscles accompanies development of the cartilages (e.g., the adductor of the mandible in Fig. 41).

Earlier, during the pharyngula period, a single bilateral pair of aortic arches formed, and they occupied the jaw primordial region. Now, when the hatching period begins, a second aortic arch has joined the first one on each side of the embryo in the region of the jaw. The first aortic arch passes dorsally just anterior to the prominent ceratohyal cartilage, and the second aortic arch passes just posterior to the same cartilage (Fig. 41). The two vessels join together beneath the eye to form a single artery that dives into the interior of the head as the internal carotid artery.

The next four pharyngeal arches, **branchial arches 1–4** (corresponding to pharyngeal arches 3–6), will bear gills. These house prominent aortic arches 3–6, such that the whole series of six pairs of aortic arches is present and carries circulating blood early in the hatching period. A gill slit forms posterior to the hyoid arch and between each branchial arch, making five in all. The rudiments of gill filaments develop late in the hatching period as buds along the posterior walls of the four branchial arches facing the slits (Fig. 42A).

The last arch of the pharyngeal series (branchial arch 5 or pharyngeal arch 7) does not develop gills. There is no gill slit behind it, nor does there appear an aortic arch within it. However, in the fashion of the other branchial arches it does make a supportive cartilage. Pharyngeal teeth develop in association with this particular cartilage, the only teeth in fact that the zebrafish will ever have.

The cartilages of the branchial arches begin to develop morphologically about a half day after the jaw cartilages. Each branchial arch initially develops a single simple linear element, a ceratobranchial cartilage, not dorsal and ventral elements developing nearly together as discussed above for the jaw arches. Moreover, the series of ceratobranchial cartilages does not develop synchronously; the first cartilages (ceratobranchials 1 and 5) develop ahead of the others (Fig. 42B,C). The cartilages of middle branchial arches in the series, particularly ceratobranchials 3 and 4, are still undifferentiated by the end of the 3rd day.

Stages During the Hatching Period

Long-pec stage (48 h). At this stage EL = 3.1 mm, HTA = 45°, OVL = 1/2. The OVL changes only little hereafter, so this value of 1/2 is a good initial indication

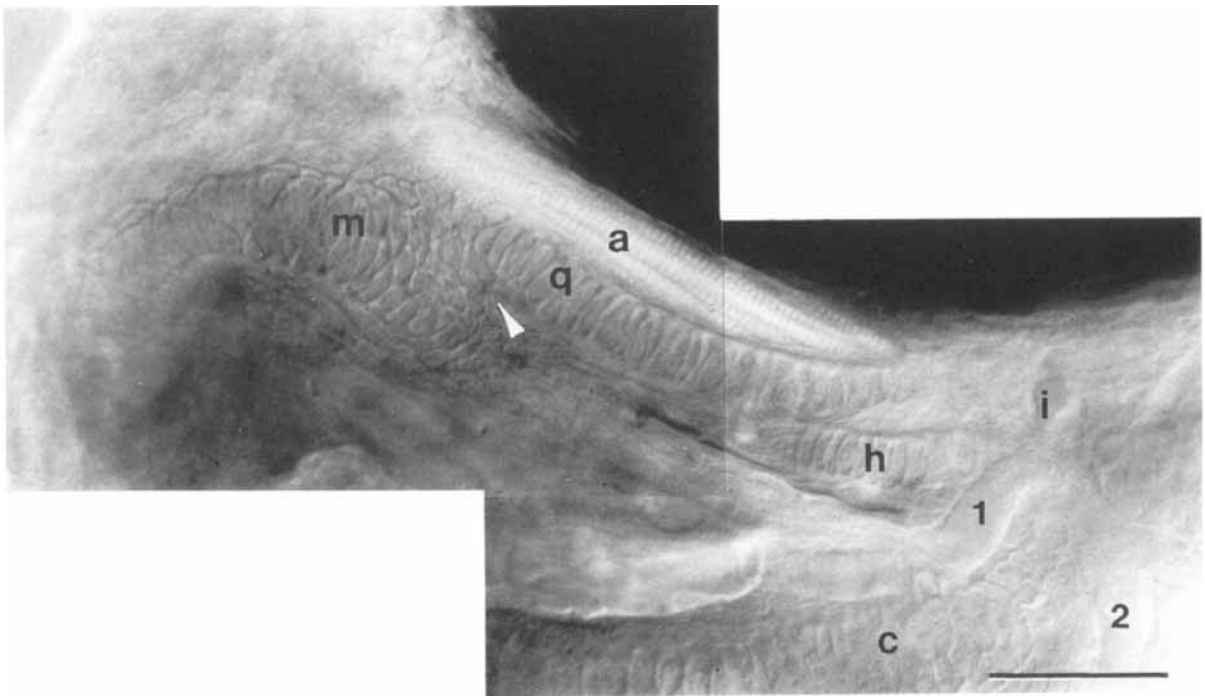

Fig. 41. Jaw cartilage and muscle formation is well underway by the end of the hatching period. Left-side Nomarski view, dorsal to the top, anterior to the left, at the protruding-mouth stage (72 h). The quadrate (q) and more ventral and anterior Meckel's (m) cartilages of the mandibular arch meet at the arrowhead, the primary jaw articulation. The adductor mandibulae muscle (a), that closes the mouth, runs ventral to the eye. It inserts on both of these mandibular arch cartilages. The posterior end of the quadrate overlaps with the anterior end of the dorsal cartilage of the hyoid arch, the hyosymplectic (h). The field of view includes only a small portion of the ventral cartilage of the hyoid arch, the ceratohyal (c). The ceratohyal is the thickest cartilage present in the embryo; at first one might mistake it for Meckel's cartilage. The first aortic arch (1) passes just anterior to the ceratohyal. The second aortic arch (2) passes just posterior to it. Dorsal to the same cartilage these two arteries join together to form the internal carotid artery (i). Scale bar = 50 μm.

that the embryo has reached some stage during the hatching period, vs. some earlier stage.

As the stage name indicates, the pectoral fin buds now are quite elongated, stretching to a height-to-width ratio of about 2 (Fig. 37C). The buds curve posteriorly and have a prominently pointed shape, with the apical ectodermal ridge at the point. They still do not look fin-like, and the apical ridge is yet more prominent than earlier, its expansion accounting for a considerable portion of the lengthening of the bud. More proximally, the central region of the bud forms forms a compact mesenchymal condensation, visible in Figure 37C, that heralds development of the supportive girdle of the fin. Here, the first cartilage in the embryo begins to differentiate morphologically at this stage, and with Nomarski optics the chondrocytes may be recognized by their cobblestone arrangement and bright appearance.

Because of both yolk depletion and growth of the head, now, as viewed from the side, the yolk ball approximately equals the size of the head. However, in a dorsal view the yolk ball is slightly wider than the head; the widths become about equal at 51 h. The yolk extension has a taper along nearly its whole length, giving it a shallow conical rather than a cylindrical shape.

The olfactory placodes are at the anterior borders of the eyes, and Nomarski reveals that they have beating cilia. Morphogenesis in the dorsal part of the otic vesicle produces the rudiments of the semicircular canals. Hair cells have differentiated in the sensory maculae of the otic vesicle, and neuromasts, complete with protruding sensory hairs, have differentiated in the head (a prominent one is positioned between the ear and the eye), and along the posterior lateral line. The notochord has vacuolated differentiating cells to its caudal tip. With some difficulty one can visualize early precartilage condensations in the developing mandibular and hyoid arches, but not in the branchial arches.

The dorsal stripe of melanophores is now very well defined and densely populated, present along the midline of the anterior trunk and tail, but as bilateral rows of cells in the posterior trunk. In the head the dorsal stripe also avoids the midline, where over the brain a dorsal view reveals that it takes the form of an open posteriorly pointing V. A side view reveals that the dorsal and ventral stripes join together at the tail tip into another posterior-pointing V that is rather completely filled with pigment, save for a small ventral gap. Further, a second component of the ventral stripe now forms in the tail medially to the earlier stripe, and associated with the caudal (and the axial) vein. At this

stage melanophores only sparsely populate this median ventral stripe, but by the early larval period the two parts of the ventral stripe will neatly frame the vein. Over the yolk ball, the bilateral ventral melanophore rows join in the midline as a distinctive patch at the location of the developing swim bladder. The lateral stripe along the horizontal myoseptum is now quite clear, and contains a small and variable number of melanophores (as described in detail by Milos and Dingle, 1978). Xanthophore differentiation gives the head a very distinct but still very pale yellow cast (Fig. 39A). The dorsal aspect of the trunk and tail is a fainter yellow. The iridophores are scattered over the retina, as earlier, but now many more appear, some arranged in a discontinuous ring of individual cells or small reflective cell groups around the lens, where the iris will develop. Most long-pec embryos have other iridophores associated with the dorsal stripe in the tail, and occasional feebly reflective ones that appear on the dorsolateral yolk sac. These foreshadow development of distinctive iridophore patches ("lateral patches") that flank the position where the swim bladder forms.

The shrinking yolk sac makes the pericardial cavity conspicuous. The vigorous beat of the heart easily shows that the heart tube is bending to bring the atrium to a position dorsal to the ventricle. Nomarski optics reveal that the definitive six pairs of aortic arches are now all present, but typically at the long-pec stage not all of them are carrying circulating blood. Generally, the more anterior arches, especially aortic arches 1–3, join the circulation earlier, but participation varies. Circulation is now strong in most segmental vessels along the trunk and tail. There is a single channel associated with each segment, but, as can be determined by following the course of the blood flow, an artery in one segment leading from the dorsal aorta alternates with veins in the adjacent segments leading to the axial vein. There is no blood circulation in the pectoral fin bud until about 52 h, more consistently at 54 h. At this point one can find the **subclavian** vessel looping around the bud at the base of the ridge, and without a clear distinction between the arterial and venous side of the loop. The common cardinal vein on the yolk ball is fan-shaped, narrower at its origin and broadening more ventrally.

When at rest, dechorionated embryos are beginning to assume a dorsal-up body position. Some come to rest dorsal-up upon completion of a swimming episode.

Pec-fin stage (60 h). At this stage EL = 3.3 mm, HTA = 55°. The pectoral fin now has a flat flange or blade. The blade is confined to the distal part, where the ridge was earlier, and now it makes the distal part of the rudiment considerably wider than the base, op-

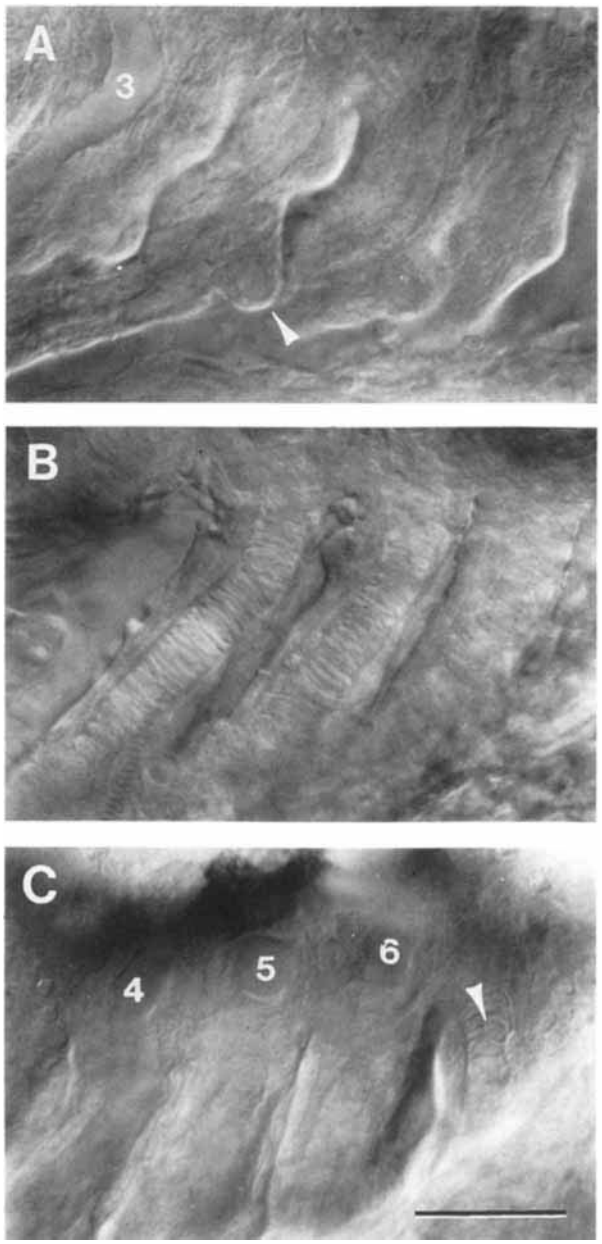

Fig. 42. Branchial arches develop late in embryogenesis. Left-side Nomarski views, dorsal to the top, anterior to the left, at the protruding-mouth stage (72 h). To avoid confusion, keep in mind that in fish (but not necessarily in tetrapod species that do not develop gills) branchial arch and pharyngeal arch numbering systems differ. By convention, branchial arch 1 is the same as pharyngeal arch 3 and contains ceratobranchial cartilage 1 and aortic arch 3. **A:** A superficial view of the four gill-bearing branchial arches (branchials 1–4) to show the clefts between them and developing buds of gill filaments (the arrowhead indicates a bud emerging from the posterior surface of branchial arch 2). The third aortic arch (3) is in focus within the first branchial arch. **B:** A deeper plane of focus reveals a gradient of cartilage development in branchial arches 1–3. To the left, branchial arch 1 includes a long stretch of differentiated cartilage (this cartilage being ceratobranchial 1). In the next arch, ceratobranchial 2 is less differentiated, and in branchial arch 3, to the right, the ceratobranchial is represented by only a row of precartilaginous mesenchymal cells. **C:** The posteriormost branchial does not follow the same gradient rule; ceratobranchial cartilage 5 (arrowhead), the last cartilage of the series, is further developed than the third or fourth ceratobranchials at the same stage. Aortic arches (numbered 4–6 in the figure) are in focus dorsally above the precartilage masses. The fifth branchial arch does not possess an aortic arch (that would be numbered aortic arch 7, were it to exist). Neither will the fifth branchial arch bear gills. Scale bar = 50 μm.

posite to the situation at the long-pec stage. The fin is held back along the side of the body, and extends posteriorly to cover more than half of the yolk ball. Nomarski optics reveals the presence of actinotrichia in the pectoral fin, as well as continued differentiation of cartilage in the proximal part of the rudiment.

A dorsal view reveals that the width of the head at the eyes, but not the ears, now exceeds the width of the yolk ball. The taper of the yolk extension is more prominent and meets the yolk ball without a sharp angle being present where the two regions of the yolk cell join, such as was present at earlier times.

A ventral view shows that the mouth is open to the exterior (Fig. 40), but not gaping. It lies entirely behind the anterior limit of the eye at this stage. Precartilage condensations are distinctive in the mandibular and hyoid arches, and short stretches of differentiating cartilage cells can be identified in these arches as well, particularly in Meckel's cartilage and the ceratohyal cartilage. Jaws muscles are also differentiating. The earliest mesenchymal precartilage condensations now appear in the first one or two branchial arches (pharyngeal arches 3 and 4), but probably distinctive cartilage cells are not yet present in this region. The rudiments of the gill filaments now appear as shallow buds along the posterior surfaces of the anterior gill arches.

A partition is forming in the otic vesicle that will separate two otolith-containing chambers, ventral to the more well-formed semicircular canals. In a side view with the dissecting microscope the gut tract can now be visualized along part, but typically not all, of its length. A lumen appears within the hindgut.

Pigmentation of the retina is now so dense that, using transmitted illumination, its opacity nearly hides the lens. Iridophores in the eye fill out a rather complete brightly reflective ring around the lens (e.g., Fig. 39G). Other reflective regions occur outside of the ring, mostly as contiguous patches of cells rather than as scattered individual cells.

On the trunk and tail, up to about ten melanophores occupy each lateral stripe (Fig. 39C). Where the dorsal stripe is bilateral, in the posterior trunk and anterior tail, the melanophores now neatly flank reflective iridophores present in the midline. Bilateral patches of reflectivity, the **lateral patches,** also have formed on the dorsal yolk sac, just to either side of the median black patch marking the location of the developing swim bladder. A few scattered iridophores appear elsewhere on the yolk sac, but only variably in a distinctive ventral median row that accompanies the melanophore **yolk stripe** at the same location. Xanthophore development continues, producing a rich yellow color on the head, and a still somewhat paler yellow cast to the dorsal trunk and tail (Fig. 39C).

The heart is prominent, beating strongly, and full of circulating blood. Blood flows in all of the aortic arches and through the subclavian loop. The common cardinal vein no longer has a fan-shape, but remains narrow along its length, as it takes a direct course, anterior to most of the yolk, toward the heart.

Fig. 43. The appearance of the cleithrum, the first easily visible bone, marks the end of embryogenesis. Left-side Nomarski view, dorsal to the top, anterior to the left at the protruding-mouth stage (72 h). The cleithrum, forming as a transversely oriented rod of dermal acellular bone, is homogeneous in structure and refractile in appearance. The granular pronephric kidney is also in the field of view to the right, posterior to the cleithrum and dorsal to the yolk sac. Scale bar = 50 μm.

Most dechorionated embryos now rest in a dorsal-up attitude and nearly always finish a bout of swimming in this attitude. The contractions during the escape response occur so rapidly that one cannot resolve them by eye.

Protruding-mouth stage (72 h). At this stage EL = 3.5 mm, HTA = 25°. The mouth is wide open and it protrudes anteriorly just beyond the eye.

The blade of the pectoral fin continues to expand, now extending posteriorly over most of the length of the diminishing yolk ball (Fig. 39F).

With Nomarski optics one can see gill slits and prominent buds of developing gill filaments (Fig. 42A), sometimes including a blood vessel that carries circulating blood. Cartilage cells are distinctive in branchial arches 1, 2 (Fig. 42B) and 5 (Fig. 42C) but not in branchial arches 3 and 4. The primordium of the operculum

extends posteriorly to cover the first or even the second branchial arch. The first visible bone in the zebrafish, the transversely oriented **cleithrum** (Fig. 43) now appears, superficial to, and at the boundary between the first two myotomes. At this location, posterior to the otic vesicle and last pharyngeal arch, it extends ventrally into the pectoral region, where it serves as an anchor of the pectoral fin girdle. Nomarski optics are required to see it at this stage; in the young larva it becomes more prominent. Histological sectioning shows that the cleithrum is lined with osteoblasts, but these bone-forming cells are not easily visualized in the living embryo.

A side view with the dissecting microscope now reveals the whole length of the gut tract behind the pharynx.

Melanin accumulates in the patch overlying the swim bladder rudiment, making this region very distinctively darkened. Iridophore coverage of the eye has expanded to more than half its surface, except for radial stripes, where black melanin shows between the golden patches. Iridophores accompany each of the melanophore stripes, including the yolk stripe. Shortly, the latter will become a rather solid reflective band. The yellow cast of the whole dorsal aspect of the body has increased, so that the hue of the trunk now matches that of the head.

Circulation in the pharyngeal arch region is becoming more complex with the advent of gill filament development. A subintestinal vein (Reib, 1973) is variably present, ventral to the gut tract.

EARLY LARVAL PERIOD

By day 3 the hatched larva has completed most of its morphogenesis, and it continues to grow rapidly. Prominent changes during the next day include the inflation of the swim bladder and the continued anterior-dorsal protrusion of the mouth (Fig. 39G,H). During the same time the reflective strips of iridophores brighten and lengthen, the ventral yolk band extending in both directions. The gut tube drops more ventrally, where it can be seen more easily, and the yolk extension nearly empties. Whereas during the hatching period the embryo is usually at rest, the early larva gradually begins to swim about actively, and moves its jaws, opercular flaps, pectoral fins, and eyes. These developments produce swift escape responses and herald respiration, the seeking of prey, and feeding.

ACKNOWLEDGMENTS

During the past 20 years a very large number of our colleagues at the University of Oregon have been most generous in sharing their findings and insights that have helped immeasurably in our being able to assemble this series. Walter K. Metcalf, Eric Hanneman, and Rachel Warga did the first staging work at Oregon at particular periods of embryogenesis. Many others, including Cosima Fabian, Robert Kelsh, Beth Morin-Kensicki, Mark Fishman, Beatte Schmitz, J.P. Trinkaus, and Rachel Warga have shared unpublished information, and Monte Westerfield criticized several versions of the text. Jerry Gleason and Greg Kruse helped technically, and Pat Edwards located many of, and entered all of the references. Reida Kimmel made the photographic prints, and helped in multitudinous other ways including giving her unfailing encouragement throughout the project. The more recent work and the writing were supported by NIH grants HD22486 and 5T32 HD07348.

GLOSSARY

actinotrichia unsegmented collagenous fin rays of the embryo and early larva, replaced later by the lepidotrichia, the definitive segmented bony fin rays

adaxial paraxial mesoderm subregion developing just adjacent to the chorda mesoderm

animal pole location on the egg where the polar bodies emerge, corresponding to the point of fertilization in fish like zebrafish, just below where the sperm penetrates the chorion through the micropile (passageway)

animal-vegetal axis a line passing through the animal and vegetal poles of the embryo before the end of epiboly

anterior toward the front (or head)

anterior horn the distinctive anterior region of the ventral stripe of melanophores, developing between the ear and eye

anterior-posterior (AP) axis the principal axis of the embryo, here synonymous with rostrocaudal axis and embryonic axis

anterior posterior cardinal vein see cardinal vein

aorta see dorsal aorta

aortic arch artery leading from the ventral aorta to the paired radix (root) of the dorsal aorta, or, for the first two arches, to the internal carotid artery; an aortic arch develops in all but the most posterior of the seven pharyngeal arches, and the last four will carry the blood supply to and from the gills

AP anterior-posterior

atrium heart chamber collecting venous blood from the sinus venosus and delivering it to the ventricle; generates the first of each (doubled) heartbeat

axial hypoblast hypoblast that consists of mesodermal and probably endodermal precursor cells developing in the dorsal midline; includes prechordal plate and chorda mesoderm

axial vein unpaired vein in the caudal trunk leading from the caudal vein and to the left and right posterior cardinal veins

axis a line, or alternatively shorthand for the anterior-posterior or embryonic axis

bauplan hypothetical basic or ancestral blueprint for developmental patterning, most often used with reference to the whole embryo pattern at the phylotypic stage

blastoderm cellular part of the embryo, excluding

the yolk cell, derived from the blastodisc by early morphogenesis; refers particularly to the time when the cell array is sheet-like, between 30%-epiboly and the end of gastrulation

blastodisc (-disk) dome of cytoplasm (disk-like in the case of larger teleost eggs such as *Fundulus* and *Salmo*) that segregates from the yolk toward the animal pole during and after the one cell-stage, and which undergoes cleavage

blastomere a cell arising during cleavage; the term encompasses the partially cleaved, incomplete "cells" at the blastodisc margin before they collectively form the yolk syncytial layer in the midblastula

blastula classically the single-layered hollow ball of cells formed by cleavage in organisms that show this developmental style; here used to mean a stereoblastula, not hollowed-out, and as a descriptor for the period of development when the blastodisc begins to look ball-like, at the 128-cell stage through the time of onset of gastrulation

blood island nest of developing blood cells arising late in the segmentation period from the intermediate mass, and located in the anterior-ventral tail, just posterior to the yolk extension

Brachet's cleft the visible division between epiblast and hypoblast in the gastrula

branchial arch gill arch; the last five of the set of seven pharyngeal arches; the numbering system can be confusing; generally branchial arch 1 is the first gill arch, or the third pharyngeal arch, but some authors do not follow this convention

cardinal vein bilaterally paired longitudinial vein; the anterior cardinal returns blood from the head, and the posterior cardinal returns it from the trunk; these two vessels join together on each side as the common cardinal vein (duct of Cuvier; misnamed the vitelline vein) that leads across the yolk cell to the heart's sinus venosus

carotid artery see internal carotid artery

caudal pertaining to the tail, or the posterior direction

caudal artery extension of the dorsal aorta in the tail

caudal vein vein in the tail returning blood from the trunk and tail to the heart, leads directly into the axial vein in the posterior trunk

central canal fluid-filled narrow cavity in the spinal cord

central nervous system the brain and spinal cord

ceratobranchial cartilage cartilaginous element present in a branchial arch at the end of embryogenesis; other cartilages will form in these arches later in the young larva

ceratohyal cartilage massive ventral cartilage of the hyoid arch, generally supposed to be serially homologous to the ceratobranchial cartilages, and perhaps to Meckel's cartilage

cerebellum specialized brain region derived from the dorsal metencephalon (anterior hindbrain, and perhaps including posterior midbrain) and becoming distinctive late in the segmentation period

chondrocranium the initially cartilaginous region of the skull that eventually surrounds the brain and forms capsules over the sensory organs, including the olfactory organ, eye, and ear; distinct from the dermatocranium (skull bones forming without cartilage models, and mostly after embryogenesis) and the splanchnocranium (the portion of the head skeleton developing from the pharyngeal arches)

chorda mesoderm the notochord rudiment

chorion the egg shell

cleavage an early mitotic cell division occurring in the blastodisc, special in that the cell cycles are short in length, are not accompanied by cell growth during interphase, and occur synchronously or metasynchronously with other cleavages of the same number; in the staging series, the cleavage period refers to the period of development encompassing the first six zygotic cell cycles

cleithrum transversely oriented bone connecting the occipital region of the skull dorsally and pectoral girdle ventrally; appears near the end of embryogenesis

coelom (coelomic cavity) fluid-filled mesodermally lined cavity separating visceral organs including the heart from the body wall

common cardinal vein see cardinal vein

conus (bulbus) arteriosus muscular heart region leading blood out of the heart to the ventral aorta

convergence deep cell movement toward the dorsal side of the embryo during the gastrula and early segmentation periods

deep cell a cell in the the blastodisc (first at the 64-cell stage) or blastoderm that is completely covered over by other cells, the outermost being cells of the enveloping layer

deep cell layer (DEL) a multilayer of deep cells of fairly uniform thickness that forms during early epiboly (at dome stage; upon conversion of the blastodisc to the blastoderm); during gastrulation the DEL gives rise to the epiblast and hypoblast

DEL deep cell layer

diencephalon the more posterior and ventral of two forebrain neuromeres, the other being the telencephalon; major derivatives are the eye cups, the brain pretectal region, the thalamus, hypothalamus, and epithalamus (including the habenula and epiphysis)

dorsal toward the back (the side opposite to the belly)

dorsal aorta principal unpaired, median artery of the trunk, leading from the paired roots (radices) of the dorsal aorta to the caudal artery

dorsal stripe longitudinal arrangement of melanophores along the dorsal side of the embryo, underlying the median fin fold; the cells lie in the midline

in the anterior trunk and tail, and are present bilaterally in the head and posterior trunk

dorsal-ventral (dorsoventral) axis passing from the back to the belly; within a sagittal plane and at right angles to the anterior-posterior axis

duct of Cuvier see cardinal vein

EL embryo length

embryo length (EL) at any stage the embryo's longest linear dimension

embryonic axis see anterior-posterior axis

endothelium epithelial lining of any blood vessel including the heart

enveloping layer (EVL) outermost monolayer of cells surrounding the embryo that become very flattened in the blastula and give rise to the periderm

epaxial muscle somite-derived body wall muscle present dorsal to the horizontal myoseptum

epiblast the outer of the two layers of the blastoderm that form during gastrulation, corresponding to primitive ectoderm during gastrulation and to the definitive ectoderm after gastrulation

epiboly the thinning and spreading of both the YSL and the blastoderm over and across the yolk cell, eventually encompassing the yolk cell completely; epiboly begins at dome stage, converts the blastodisc to the blastoderm, and is considered to be over when the yolk plug closes over (at 100%-epiboly)

epiphysis a circumscribed swelling, includes the pineal primordium that appears late in the segmentation period in the dorsal midline of the diencephalon

epithelium a compact and sheet-like arrangement of cells, polarized with the apical surface to one side (primitively the outside) and the basal surface to the other

evacuation zone the anterior-ventral region of the mid and late gastrula that becomes cell-poor, as cells leave by both epiboly and convergence

EVL enveloping layer

extension lengthening of the embryonic axis, principally by deep cell repacking (by intercalations), and occurring during the gastrula and early segmentation periods

external yolk syncytial layer (E-YSL) portion of the YSL that is outside of the blastoderm margin during epiboly

extraembryonic making no direct cellular contribution to the body of the embryo

E-YSL external yolk syncytial layer

face view side view along the odd-numbered cleavage planes during the cleavage or blastula periods

fate map map at a early developmental stage (here at gastrula onset) of what cells normally will become

fin fold the rudiment of the median unpaired fins, appearing in the late segmentation period, prominent throughout the rest of embryogenesis

forebrain the most anterior region in the brain including both the telencephalon and diencephalon; we have not observed an early transient stage when the forebrain is distinguished from the midbrain but has not subdivided that would correspond to the prosencephalon in tetrapods

gastrula classically a postblastula stage in which an archenteron (primitive gut or gastrocoele) forms by invagination or involution of cells through a blastopore and when the germ layers and embryonic axis appear; the zebrafish forms neither an archenteron nor a blastopore, and here the term refers to the roughly equivalent period of development, beginning at the onset of involution (at the 50%-epiboly stage) that produces the two primary germ layers, the epiblast and hypoblast, and during which the definitive embryonic axis forms by convergence and extension movements

gastrulation morphogenesis during the gastrula period

gill arch one of the subset of pharyngeal arches (pharyngeal arches 3–6, or branchial arches 1–4) that will develop gills

gill filament branched region of the gill where respiratory exchange takes place

hair cell specialized neuronal receptor cell of the lateral line and acoustico-vestibular systems

hatching gland a transversely oriented set of cells located deep to the EVL on the pericardial membrane, especially prominent during pharyngula period because of the brightly refractile cytoplasmic granules (containing hatching enzymes) of the principal cells of the gland

head-trunk angle (HTA) in side view, the smaller angle between the head axis (a line through the middle of the ear and eye) and the trunk axis (a line parallel to the long axis of the notochord at about somites 5–10

hindbrain the most posterior of the three principle regions of the brain, forming the rhombencephalon and all or most of the metencephalon

horizontal during cleavage and blastula periods a plane perpendicular to the animal-vegetal axis; later a longitudinal plane parallel to the embryonic axis and perpendicular to the dorsal-ventral axis, i.e., at right angles to both transverse and sagittal planes

horizontal myoseptum a connective tissue partition developing at the apex of the chevron-shaped myotome and separating dorsal (epaxial) and ventral (hypaxial) body wall muscle masses

HTA head-trunk angle

hyoid arch the second pharyngeal arch, forming the operculum and secondary supportive elements of the jaw

hyosymplectic (hyomandibular, epihyal) cartilage the dorsal cartilage forming in the hyoid arch

hypaxial muscle somite-derived body wall muscle present ventral to the horizontal myoseptum

hypoblast (mesendoderm) the inner of the two layers of the blastoderm that forms during gastrula-

tion and gives rise to the definitive mesoderm and endoderm

hypothalamus a specialized brain region of the ventral diencephalon arising near the end of the segmentation period; the embryonic hypothalamic region will give rise to the posterior pituitary gland as well as a number of brain nuclei

incomplete cleavage see meroblastic cleavage

intermediate mass the very early blood rudiment located deep to the somites in the posterior trunk at a stage before the blood cells collect into the (more prominent) blood island

internal carotid artery artery originating at the junction of the first two aortic arches and supplying the anterior brain

internal yolk syncytial layer (I-YSL) the portion of the YSL that lies deep to the blastoderm during epiboly

involution deep cell movement at the blastoderm margin in which the DEL folds inward and back upon itself, producing the germ ring and its two primary germ layers, the epiblast and hypoblast

iridophore reflective pigment cell

I-YSL internal yolk syncytial layer

keel see neural keel

Kupffer's vesicle small but distinctive epithelial sac containing fluid, located midventrally posterior to the yolk cell or its extension, and transiently present during most of the segmentation period

lateral away from the midline

lateral patch a prominent collection of iridophores on the dorsolateral yolk sac flanking the position of the developing swim bladder

lateral stripe melanophore stripe along the horizontal myosepta

lens placode ectodermal primordium of the lens of the eye

mandibular arch first (most anterior) pharyngeal arch, forming the principal elements of the jaw of the early larva

mandibular cartilage see Meckel's cartilage

marginal blastomere cell (incompletely cleaved before the YSL forms), located in the surface layer (EVL) just at the rim of the blastodisc

MBT midblastula transition

Meckel's (mandibular) cartilage ventral cartilage of the mandibular arch forming the principal support of the (lower) jaw

medial toward the midline

median at the midline

mediolateral horizontal axis oriented perpendicular to both the anterior-posterior and dorsal-ventral axes

mediolateral intercalation ordered cellular repacking along the mediolateral axis brought about by interdigitations of deep cells during the gastrula and early segmentation periods; produces convergence and extension

melanophore (melanocyte) a neural crest-derived cell containing black melanin pigment

meroblastic (incomplete) cleavage cell division in which sister cells are only partially separated from one another by cytokinesis; includes all of the early cleavages, and also occurs along the blastodisc margin in the late cleavage and early blastula periods

mesencephalon see midbrain

mesenchyme a mesh-like cell arrangement, less compact than an epithelium

mesendoderm see hypoblast

metasynchronous occurring in a nearly synchronous wave

metencephalon brain region in the neighborhood of the first rhombomere; gives rise to structures including the fourth cranial (troclear) motor nucleus, the cerebellum dorsally, and the interpeduncular nucleus ventrally

midblastula transition (MBT) the time of increase in cell cycle length above the rapid rate characterizing the cleavage period, beginning at the tenth zygotic cycle; at the MBT cells also begin to divide less synchronously, and motility and zygotic transcription are first observed

midbrain (mesencephalon) the brain region between the forebrain anteriorly and the hindbrain posteriorly, including the tectum dorsally and the midbrain tegmentum ventrally

midsagittal plane the plane of bilateral symmetry, located at the midline

myomere see myotome

myotome portion of the somite giving rise to body wall muscle masses

neural crest a cell population arising from the dorsolateral aspect of the central nervous system primordium during the segmentation period, and later migrating along stereotyped pathways to give rise to a diverse and well-defined set of cell types including pigment cells, peripheral neurons and glia, and head cartilage

neural groove a midsagittal depression on the surface of the anterior neural plate present during the early segmentation period

neural keel an intermediate stage (between the neural plate and neural rod) during the early segmentation period in the morphogenesis of the central nervous system primordium; the keel is roughly triangular shaped in cross section

neural plate the earliest recognizeable dorsal ectodermal primordium of the central nervous system present near the end of gastrulation before infolding to form the neural keel; consists of a thickened pseudostratified epithelium

neural retina the sensory retinal epithelium, developing from the inner layer of the optic cup; the neural retina forms prominent sublayers during the hatching period, including the inner ganglion cell

layer, interneuronal layers, and the outer layer of photoreceptor cells just deep to the retinal pigment layer

neural rod an intermediate stage in the development of the central nervous system present during the segmentation period; the neural rod is roughly cylindrical in shape, forms from the neural keel, and is not yet hollowed out into the neural tube

neural tube cavity-containing primordium of the central nervous system, developing from the neural rod in the late segmentation period

neuromast volcano-shaped lateral line sensory organ located in characteristic positions within the skin epithelium and containing hair cells and their support elements

neuromere a brain subdivision recognized morphologically as a swelling bounded by constrictions

notochord rod-like principal supportive element of the embryo and larva, present in the midline just ventral to the neural tube, and differentiating during the segmentation period to form large vacuolated principal cells and a surrounding thin epithelial notochord sheath

optic cup two-layered stage of eye development arising from the seemingly unlayered optic primordium; the inner layer develops as the neural retina, and the outer layer forms the pigmented retina

optic primordium lateral outgrowth from the forebrain that will form the eyeball (excluding the lens); equivalent to the optic vesicle of tetrapods, but apparently not a hollow structure; develops into the two-layered optic cup

optic tectum the roof of the midbrain, morphologically visible by the end of the segmentation period

otic capsule region of the chondrocranium surrounding otic vesicle

otic placode primordium of the ear epithelium before it hollows into the otic vesicle, present beside the hindbrain rudiment in the midsegmentation period

otic vesicle epithelial sac present beside the fifth rhombomere; forms the semicircular canals dorsally and the otolith organs ventrally, and houses the acoustico-vestibular sensory epithelia (maculae) of hair cells

otic vesicle length (OVL) a staging device or index defined as the number of additional otic vesicles that could be fit in between the otic vesicle and the eye

otolith brightly refractile stone-like organ within the otic vesicle and positioned over a sensory macula; two form in each vesicle during the late segmentation period

OVL otic vesicle length

palatoquadrate see quadrate

paraxial hypoblast hypoblast that is mainly or entirely mesodermal, positioned laterally to the axial hypoblast; forms somites and their derivatives in the trunk and muscles and endothelium in the head

periblast archaic term for the YSL

pericardium portion of the coelomic cavity present as a distinctive chamber surrounding the heart

periderm flattened tightly sealed epithelial monolayer of specialized impermeable cells covering the entire embryo after epiboly ends, and representing the sole derivative of the EVL

peripheral nervous system nervous structures including ganglia outside of the central nervous system

pharyngeal (visceral) arch a segment of the lateral wall of the pharynx that will form jaw structures (anterior two arches) or gill structures (posterior five arches); an arch includes a compact mesenchyme lined by inner endoderm and outer epidermis; each arch is separated from neighboring arches by an endodermal outpocketing (a pharyngeal pouch) meeting a slight ectodermal inpocketing (a pharyngeal cleft) where a gill slit develops during the hatching period (except between the first and second arches)

pharyngula generally, a vertebrate embryo that has developed to the phylotypic stage; in the series used as a period name to describe the 2nd of the 3 days of embryonic development

pharynx swollen region of the anterior foregut, posterior to the mouth and anterior to the liver; its walls form the jaws and gills

phylotypic stage the stage at which the embryo develops features defining it as a vertebrate or chordate, including the notochord, neural tube, pharyngeal arches, somites and postanal tail

pillow see polster

placode a thickened or plate-like region within an epithelium

polster (pillow) the hatching gland rudiment at the time it underlies the forebrain during the early segmentation period

posterior toward the rear (or tail—not meaning toward the dorsal side)

posterior cardinal vein see cardinal vein

prechordal plate axial hypoblast located anterior to the chorda mesoderm; the polster is its most anterior region

prim see primordium of the lateral line

primary motoneuron one of a subset of spinal motoneurons innervating body wall muscle that develop early and achieve large size; present in three or four identifiable pairs per spinal segment

primordium of the lateral line placodally derived rudiment of the posterior lateral line that during the pharyngula period migrates posteriorly through the skin overlying the horizontal myosepta and deposits neuromast primordia along the way; its progress is used as a staging index during the pharyngula period to define "prim" stages

pronephric duct duct of the embryonic kidney, present bilaterally ventral to the somites and lead-

ing to the anal region where it empties separately from, and just posterior to the anus

pronephros embryonic kidney, present at the level of the third somite

prosencephalon see forebrain

quadrate (palatoquadrate) the dorsal cartilage (later ossifying) of the first pharyngeal arch forming the main part of the upper jaw skeleton and lateral part of the larval palate

radial intercalation ordered cellular repacking among deep cells of the deep and shallow regions of the blastodisc, effecting epiboly and producing a uniformly thin blastoderm; begins during the late blastula period, and perhaps continues during gastrulation

reticular cell see tail reticular cell

retina the portion of the eye developing from the optic primordium and including the neural retina and the retinal pigment layer

retinal pigment layer (tapetum) a monolayer of pigmented epithelium covering the neural retina; develops from the outer of the two layers of the optic cup

rhombencephalon hindbrain, or the division of the hindbrain posterior to the metencephalon and anterior to the spinal cord

rhombomere hindbrain segment or neuromere

Rohon-Beard neuron a primary sensory neuron present in the dorsal spinal cord of the embryo and early larva

rostral toward the head, for the zebrafish embryo synonymous with anterior

rostral-caudal (rostrocaudal) axis here synonymous with anterior-posterior axis

sagittal a plane parallel to the plane of bilateral symmetry

sclerotome medial ventral region of the somite that will form vertebral cartilages

segmental artery artery leading from the dorsal aorta or caudal artery to the spinal cord; the arteries alternate in adjacent segments with segmental veins

segmental plate unsegmented field of paraxial mesoderm present posterior to the somite file, from which somites will form

segmental vein vein leading from the spinal cord to the caudal vein, axial vein, or posterior cardinal vein

segmentation a repetition of elements, particularly along the AP axis; used in the series to define the period of development between the gastrula and pharyngula

sinus venosus heart region collecting blood from the paired common cardinal veins and delivering to the atrium

somite undifferentiated mesodermal component of an early trunk or tail segment or metamere, derived from paraxial mesoderm; forms the myotome, sclerotome, and perhaps dermatome

stereoblastula see blastula

subclavian artery artery supplying the pectoral fin

subclavian vein vein returning blood from the pectoral fin to the cardinal system

tail reticular cell cell lining the vascular channel network in the posterior and ventral tail that connects between the caudal artery and vein, apparently specialized for phagocytic clearing of the blood

tectum see optic tectum

telencephalon the anterior and dorsal forebrain neuromere, includes the olfactory bulb

tier arrangement of blastomeres horizontal rows of blastomeres as seen in a face view of the embryo during the cleavage and blastula periods; tiers are counted between the blastodisc margin and the animal pole as a staging aid

trigeminal ganglion a prominent collection of touch-sensory neurons of the trigeminal or fifth cranial nerve, positioned beside the brain between the eye and the ear

trigeminal placode the ectodermal rudiment of the trigeminal ganglion, distinguishable during much of the segmentation period

vegetal pole location on the egg opposite to the animal pole, corresponding later to the point on the yolk cell furthest from the developing blastodisc

ventral toward the belly (or yolk)

ventral aorta outflow artery from the heart to the aortic arches

ventral stripe melanophore stripe just ventral to the myotomes

ventricle fluid-filled brain cavity; alternatively a heart chamber collecting venous blood from the atrium and delivering it to the conus arteriosus; the ventricle mediates the second and major component of each (doubled) heartbeat

vertical here meaning a plane parallel to the animal-vegetal axis during the cleavage and blastula periods

visceral pertaining to the gut or endoderm or splanchnic mesoderm associated with endoderm

visceral arch see pharyngeal arch

vitelline vein see cardinal vein

xanthophore a neural crest-derived cell pigmented yellow

yolk nutrient store for embryonic development in the form of semicrystalline phospholipoprotein and contained within yolk granules

yolk ball the anterior round region of the yolk cell present after the yolk extension forms during the segmentation period

yolk cell giant syncytial uncleaved cell containing the yolk; underlies the blastodisc early, and becomes enveloped by the blastoderm during epiboly

yolk extension the posterior elongated region of the yolk cell that forms during the segmentation period

yolk granule membrane-bounded sac, of the order of 50 μm in diameter, containing yolk; yolk granules

are packed densely in the interior of the yolk cell, deep to its syncytial layer, and make up the great bulk of its total volume

yolk plug the bit of yolk cell protruding beyond the blastoderm margin in the late gastrula before epiboly is complete

yolk stripe a late-forming melanophore stripe along the median ventral aspect of the yolk ball and particularly the yolk extension

yolk syncytial layer (YSL) peripheral layer of the yolk cell including nuclei and nonyolky cytoplasm

YSL yolk syncytial layer

zygote the fertilized egg, defining in the series the period between fertilization and the end of the first cleavage

REFERENCES

Abdelilah, S., Solnica-Krezel, L., Stainier, D.Y.R., and Driever, W. (1994) The zebrafish mutation *janus:* implications for dorsoventral axis determination. Nature 370:468–471.

Akimenko, M.-A., Ekker, M, Wegner, J., and Westerfield, M., (1994) Combinatorial expression of three zebrafish genes related to *distal-less:* part of a homeobox gene code for the head. J. Neurosci. 14: 3475–3486.

Ballard, W.W. (1973) Morphogenetic movements in *Salmo gairdneri* Richardson. J. Exp. Zool. 184:28–48.

Ballard, W.W. (1981) Morphogenetic movements and fate maps of vertebrates. Am. Zool. 21:391–399.

Ballard, W.W., and Ginsberg, A.S (1980) Morphogenetic movements in acipenserid embryos. J. Exp. Zool. 213:69–116.

Bennett, M.V.L., and Trinkaus, J.P. (1970) Electrical coupling between embryonic cells by way of extracellular space and specialized junctions. J. Cell Biol. 44:592–610.

Bernhardt, R.R., Chitnis, A.B., Lindamer, L., and Kuwada, J.Y. (1990) Identification of spinal neurons in the embryonic and larval zebrafish. J. Comp. Neurol. 302:603–616.

Betchaku, T., and Trinkaus, J.P. (1978) Contact relations, surface activity, and cortical microfilaments of marginal cells of the enveloping layer of the yolk syncytial and yolk cytoplasmic layers of *Fundulus* before and during epiboly. J. Exp. Zool. 207:381–426.

Brummet, A.R., and Dumont, J.N. (1978) Kupffer's vescicle in *Fundulus heteroclitus*. A scanning and transmission electron microscope study. Tissue Cell 10:11–22.

Chitnis, A.B., and Kuwada J.Y. (1990) Axonogenesis in the brain of zebrafish embryos. J. Neurosci. 10:1892–1905.

Dale, L. and Slack, J.M.W. (1987) Fate map for the 32-cell stage of *Xenopus laevis*. Development 99:527–551.

Eisen, J.S. (1991) Determination of primary motoneuron identity in developing zebrafish embryos. Science 252:569–572.

Eisen, J.S., Myers, P.Z., and Westerfield, M. (1986) Pathway selection by growth cones of identified motoneurons in live zebrafish embryos. Nature 320:269–271.

Eisen, J.S., Pike, S.H., and Romancier, B. (1990) An identified neuron with variable fates in embryonic zebrafish. J. Neurosci. 10:34–43.

Ekker, M., Wegner, J., Akimenko, M.-A., and Westerfield, M. (1992) Coordinate embryonic expression of three zebrafish engrailed genes. Development 116:1001–1010.

Felsenfeld, A.L., Curry, M., and Kimmel, C.B. (1991) The *fub-1* mutation blocks initial myofibril formation in zebrafish muscle pioneer cells. Dev. Biol. 148:23–30.

Gould, S.J. (1977) "Ontogeny and Phylogeny." Cambridge: Harvard Univ. Press.

Grunwald, D.J., Kimmel, C.B., Westerfield, M., and Streisinger, G. (1988) A neural degeneration mutation that spares primary neurons in the zebrafish. Dev. Biol. 126:115–128.

Halpern, M.E., Ho, R.K., Walker, C., and Kimmel, C.B. (1993) Induction of muscle pioneers and floor plate is distinguished by the zebrafish *no tail* mutation. Cell 75:99–111.

Hanneman, E., and Westerfield, M. (1989) Early expression of acetylcholine-sterase activity in functionally distinct neurons of the zebrafish. J. Comp. Neurol. 284:350–361.

Hanneman, E., Trevarrow, B., Metcalfe, W.K., Kimmel, C.B., and Westerfield, M. (1988) Segmental pattern of development of the hindbrain and spinal cord of the zebrafish embryo. Development 103:49–58.

Hatada, Y., and Stern, C.D. (1994) A fate map of the epiblast of the early chick embryo. Development 120:2879–2889.

Hatta, K., BreMiller, R.A., Westerfield, M., and Kimmel, C.B. (1991a) Diversity of expression of *engrailed* homeoproteins in zebrafish. Development 112:821–832.

Hatta K., Kimmel, C.B., Ho, R.K., and Walker, C. (1991b) The cyclops mutation blocks specification of the floor plate of the zebrafish CNS. Nature 350:339–341.

Helde, K.A., Wilson, E.T., Cretekos, C.J., and Grunwald, D.J. (1994) Contribution of early cells to the fate map of the zebrafish gastrula. Science 265:517–520.

Hisaoka, K.K., and Battle H.I. (1958) The normal developmental stages of the zebrafish, *Brachydanio rerio* (Hamilton-Buchanan). J. Morphol. 102:311–323.

Hisaoka, K.K., and Firlit, C.F. (1960) Further studies on the embryonic development of the zebrafish, *Brachydanio rerio* (Hamilton-Buchanan). J. Morphol. 107:205–225.

Ho, R.K. (1992a) Cell movements and cell fate during zebrafish gastrulation. Development [Suppl]:65–73.

Ho, R.K. (1992b) Axis formation in the embryo of the zebrafish, *Brachydanio rerio*. Semin. Dev. Biol. 3:53–64.

Ho, R.K., and Kimmel, C.B. (1993) Commitment of cell fate in the early zebrafish embryo. Science 261:109–111.

Ho, R.K., Ball, E.E., and Goodman, C.S. (1984) Muscle pioneers: large mesodermal cells that erect a scaffold for developing muscles and motoneurones in grasshopper embryos. Nature 301:66–69.

Horder, T.J., Presley, R., and Slípka, J. (1993) The segmental bauplan of the rostral zone of the head in vertebrates. Funct. Dev. Morphol. 3:79–89.

Kane, D.A. (1991) Zebrafish midblastula transition: the onset of zygotic control during development. Ph.D. Dissertation, Univ. of Oregon.

Kane, D.A., and Kimmel, C.B. (1993) The zebrafish midblastula transition. Development 119:447–456.

Kane, D.A., Warga, R.A., and Kimmel, C.B. (1992) Mitotic domains in the early embryo of the zebrafish. Nature 360:735–737.

Keller, R.E. (1975) Vital dye mapping of the gastrula and neurula of *Xenopus laevis*. I. Prospective areas and morphogenetic movements of the superficial layer. Dev. Biol. 42:222–241.

Keller, R.E. (1976) Vital dye mapping of the gastrula and neurula of *Xenopus laevis*. II. Prospective areas and morphogenetic movements in the deep region. Dev. Biol. 51:118–137.

Keller, R.E. (1980) The cellular basis of epiboly: an SEM study of deep cell rearrangement during gastrulation in *Xenopus laevis*. J. Embryol. Exp. Morphol. 60:201–234.

Keller, R.E., and Tibbets, P. (1989) Mediolateral cell intercalation is a property of the dorsal, axial mesoderm of *Xenopus laevis*. Dev. Biol. 131:539–549.

Kimmel, C.B. (1993) Patterning the brain of the zebrafish embryo. Annu. Rev. Neurosci. 16:707–732.

Kimmel, C.B., and Law, R.D. (1985a) Cell lineage of zebrafish blastomeres. I. Cleavage pattern and cytoplasmic bridges between cells. Dev. Biol. 108:78–85.

Kimmel, C.B., and Law, R.D. (1985b) Cell lineage of zebrafish blastomeres. II. Formation of the yolk syncytial layer. Dev. Biol. 108: 86–93.

Kimmel, C.B., and Warga, R.M. (1987) Indeterminate cell lineage of the zebrafish embryo. Dev. Biol. 124:269–280.

Kimmel, C.B., Kane, D.A., Walker, C., Warga, R.M., and Rothman, M.B. (1989) A mutation that changes cell movement and cell fate in the zebrafish embryo. Nature 337:358–362.

Kimmel, C.B., Hatta, K., and Metcalfe, W.K. (1990a) Early axonal contacts during development of an identified dendrite in the brain of the zebrafish. Neuron 4:535–545.

Kimmel, C.B., Warga, R.M., and Schilling, T.F. (1990b) Origin and organization of the zebrafish fate map. Development 108:581–594.

Kimmel, C.B., Kane, D.A., and Ho, R.K. (1991) Lineage specification during early embryonic development of the zebrafish. In: "Cell-Cell Interactions in Early Development," Gerhart, J. (ed). New York: Wiley-Liss, Inc., pp 203–225.

Kimmel, C.B., Warga, R.M., and Kane, D.A. (1994) Cell cycles and clonal strings during formation of the zebrafish central nervous system. Development 120:265–276.

Krauss, S., Johansen, T., Korzh, V., and Fjose, A. (1991) Expression pattern of zebrafish *pax* genes suggest a role in early brain regionalization. Nature 353:267–270.

Krauss, S., Concordet, J.-P., and Ingham, P.W. (1993) A functionally conserved homolog of the Drosophila segment polarity gene *hh* is expressed in tissues with polarizing activity in zebrafish embryos. Cell 75:1431–1444.

Lawson, K.A., Meneses, J.J., and Pedersen, R.A. (1991) Clonal analysis of epiblast fate during germ layer formation in the mouse embryo. Development 113:891–911.

Macdonald, R., Xu, Q., Barth, K.A., Mikkola, I., Holder, N., Fjose, A., Krauss, S., and Wilson, S.W. (1994) Regulatory gene expression boundaries demarcate sites of neuronal differentiation in the embryonic zebrafish forebrain. Neuron 13:1–20.

Martindale, M.Q., Meier, S., and Jacobson, A.G. (1987) Mesodermal metamerism in the teleost, *Oryzias latipes* (the Medaka). J. Morphol. 193:241–252.

Melby, A.E., Ho, R.K., and Kimmel, C.B. (1993) An identifiable domain of tail-forming cells in the zebrafish gastrula. Soc. Neurosci. Abstr. 19:445.

Mendelson, B. (1986) Development of reticulospinal neurons of the zebrafish. I. Time of origin. J. Comp. Neurol. 251:160–171.

Metcalfe, W.K. (1985) Sensory neuronal growth cones comigrate with posterior lateral line primordial cells in zebrafish. J. Comp. Neurol. 238:218–224.

Metcalfe, W.K., Myers, P.Z., Trevarrow, B., Bass, M., and Kimmel, C.B. (1990) Primary neurons that express the L2/HNK-1 carbohydrate during early development in the zebrafish. Development 110: 491–504.

Milos, N., and Dingle, A.D. (1978) Dynamics of pigment formation in the zebrafish, *Brachydanio rerio*. I. Establishment and regulation of the lateral line melanophore stripe during the first eight days of development. J. Exp. Zool. 205:205–216.

Myers, P.Z., Eisen, J.S., and Westerfield, M. (1986) Development and axonal outgrowth of identified motoneurons in the zebrafish. J. Neurosci. 6:2278–2289.

Newport, J., and Kirshner, M. (1982a) A major developmental transition in early *Xenopus* embryos: I. Characterization and timing of cellular changes at the midblastula stage. Cell 30:675–686.

Newport, J., and Kirshner, M. (1982b) A major developmental transition in early *Xenopus* embryos: II. Control of the onset of transcription. Cell 30:687–696.

Oxtoby, E., and Jowett, T. (1993) Cloning of the zebrafish *krox*-20 gene (*krx*-20) and its expression during hindbrain development. Nucleic Acid Res. 21:1087–1095.

Papan, C., and Campos-Ortega, J. (1994) On the formation of the neural keel and neural tube in the zebrafish *Danio (Brachydanio) rerio*. Rouxs Arch. Dev. Biol. 203:178–186.

Raible, D.W., and Eisen, J.S. (1994) Restriction of neural crest cell fate in the trunk of the embryonic zebrafish. Development 120:495–503.

Raible, D.W., Wood, A., Hodsdon, W., Henion, P.D., Weston, J.A., and Eisen, J.S. (1992) Segregation and early dispersal of neural crest cells in the embryonic zebrafish. Dev. Dyn. 195:29–42.

Reib, J.P. (1973) La circulation sanguine chez l'embryon de *Brachydanio rerio*. Ann. Embryol. Morphol. 6:43–54.

Schilling, T.F., and Kimmel, C.B. (1994) Segment and cell type lineage restrictions during pharyngeal arch development in the zebrafish embryo. Development 120:483–494.

Schirone, R.C., and Gross, L. (1968) Effect of temperature on early embryological development of the zebra fish, *Brachydanio rerio*. J. Exp. Zool. 169:43–52.

Schmitz, B., and J.A. Campos-Ortega (1994) Dorso-ventral polarity of the zebrafish embryo is distinguishable prior to the onset of gastrulation. Rouxs Arch. Dev. Biol. 203:374–380.

Schmitz, B., Papan, C., and Campos-Ortega, J.A. (1993) Neurulation in the anterior trunk region of the zebrafish *Brachydanio rerio*. Rouxs Arch. Dev. Biol. 202:250–259.

Schulte-Merker, S., Ho, R.K., Herrmann, B.G., and Nüsslein-Volhard, C. (1992) The protein product of the zebrafish homologue of the mouse *T* gene is expressed in nuclei of the germ ring and the notochord of the early embryo. Development 116:1021–1032.

Schulte-Merker, S., van Eeden, F.J.M., Halpern, M.E., Kimmel, C.B., and Nüsslein-Volhard, C. (1994) *no tail (ntl)* is the zebrafish homologue of the mouse *T (Brachyury)* gene. Development 120:1009–1015.

Solnica-Krezel, L., and Driever, W. (1994) Microtubule arrays of the zebrafish yolk cell: organization and function during epiboly. Development 120:2443–2455.

Stachel, S.E., Grunwald, D.J., and Myers, P.Z. (1993) Lithium perturbation and *goosecoid* expression identify a dorsal specification pathway in the pregastrula zebrafish. Development 117:1261–1274.

Stainier, D.Y.R., Lee, R.K., and Fishman, M.C. (1993) Cardiovascular development in the zebrafish. I. Myocardial fate map and heart tube formation. Development 119:31–40.

Strähle, U., and Jesuthasan, S. (1993) Ultraviolet irradiation impairs epiboly in zebrafish embryos: evidence for a microtubule-dependent mechanism of epiboly. Development 119:909–919.

Strehlow, D., and Gilbert, W. (1993) A fate map for the first cleavages of the zebrafish. Nature 361:451–453.

Strehlow, D., Heinrich, G., and Gilbert, W. (1994) The fates of the blastomeres of the 16-cell zebrafish embryo. Development 120: 1791–1798.

Streisinger, G., Walker, C., Dower, N., Knauber, D., and Singer, F. (1981) Production of clones of homozygous diploid zebra fish (*Brachydanio rerio*). Nature 291:293–296.

Thisse, C., Thisse, B., Schilling, T.F., and Postlethwait, J.H. (1993) Structure of the zebrafish *snail1* gene and its expression in wild-type, *spadetail* and *no tail* mutant embryos. Development 119: 1203–1215.

Trevarrow, B., Marks, D.L., and Kimmel, C.B. (1990) Organization of hindbrain segments in the zebrafish embryo. Neuron 4:669–679.

Trinkaus, J.P. (1984) Mechanism of *Fundulus* epiboly—a current view. Am. Zool. 24:673–688.

Trinkaus, J.P. (1992) The midblastula transition, the YSL transition and the onset of gastrulation in *Fundulus*. Development [Suppl]: 75–80.

Warga, R.M., and Kimmel, C.B. (1990) Cell movements during epiboly and gastrulation in zebrafish. Development 108:569–580.

Westerfield, M. (1994) "The Zebrafish Book," Edition 2.1. Eugene, OR: Univ. Oregon Press.

Wilson, H.V. (1889) The embryology of the sea bass. Bull. U.S. Fish Comm. 9:209–277.

Wilson, S.W., and Easter, S.S., Jr. (1991) Sterotyped pathway selection by growth cones of early epiphysial neurons in the embryonic zebrafish. Development 112:723–746.

Wilson, S.W., Ross, L.S., Parrett, T., and Easter, S.S., Jr. (1990) The development of a simple scaffold of axon tracts in the brain of the embryonic zebrafish, *Brachydanio rerio*. Development 108:121–145.

Wilson, E.T., Helde, K.A., and Grunwald, D.J. (1993) Something's fishy here—rethinking cell movements and cell fate in the zebrafish embryo. TIG 9:348–352.

Wood, A., and Timmermans, L.P.M. (1988) Teleost epiboly: reassessment of deep cell movement in the germ ring. Development 102: 575–585.